Nonresonant central exclusive production of charged-hadron pairs in proton-proton collisions at $\sqrt{s} = 13$ TeV

A. Hayrapetyan *et al.*[*]
(CMS and TOTEM Collaborations)

(Received 25 January 2024; accepted 21 March 2024; published 11 June 2024)

The central exclusive production of charged-hadron pairs in pp collisions at a center-of-mass energy of 13 TeV is examined, based on data collected in a special high-β^* run of the LHC. The nonresonant continuum processes are studied with the invariant mass of the centrally produced two-pion system in the resonance-free region, $m_{\pi^+\pi^-} < 0.7$ or $m_{\pi^+\pi^-} > 1.8$ GeV. Differential cross sections as functions of the azimuthal angle between the surviving protons, squared exchanged four-momenta, and $m_{\pi^+\pi^-}$ are measured in a wide region of scattered proton transverse momenta, between 0.2 and 0.8 GeV, and for pion rapidities $|y| < 2$. A rich structure of interactions related to double-pomeron exchange is observed. A parabolic minimum in the distribution of the two-proton azimuthal angle is observed for the first time. It can be interpreted as an effect of additional pomeron exchanges between the protons from the interference between the bare and the rescattered amplitudes. After model tuning, various physical quantities are determined that are related to the pomeron cross section, proton-pomeron and meson-pomeron form factors, pomeron trajectory and intercept, and coefficients of diffractive eigenstates of the proton.

DOI: 10.1103/PhysRevD.109.112013

I. INTRODUCTION

The cross sections of proton-proton (pp) and proton-antiproton ($p\bar{p}$) interactions steadily rise with the center-of-mass energy and approach each other at high energies [1]. This observation was initially explained assuming the exchange of a family of particles [2] with the vacuum quantum numbers of the pomeron [3]. This pomeron is now interpreted in terms of the sum of ladder-type diagrams (multiperipheral model [4]) composed of gluons. Pomeron physics, its nonperturbative characteristics, and its relations with the theory of the strong interaction (quantum chromodynamics, QCD) are a topic of ongoing research both experimentally and theoretically [3,5,6].

In pp collisions, the central exclusive production of a few particles (Fig. 1) offers a clean laboratory for the study of various phenomena [7,8] and is often seen as a discovery channel for new physics coupled to quarks and gluons. At energies above 20 GeV, the exchange of hadrons is suppressed [9] and, for proton transfer momenta above 0.2 GeV, these central exclusive processes are dominated by double-pomeron exchange. They provide a gluon-rich environment, which may lead to the creation of hadrons free of valence quarks, collectively called glueballs [10], whose existence is yet to be experimentally demonstrated.

Double-pomeron exchange processes in pp collisions were intensively studied at CERN in the 1990s [11,12] at $\sqrt{s} = 12.7$, 23.8, and 29 GeV, with the most significant results published by the WA102 Collaboration [13–16], which concluded that the pomeron has a vectorlike behavior. With the advent of high-energy collider experiments, there is a renewed interest in the study of central exclusive production, especially in double-pomeron exchange processes. Measurements in $p\bar{p}$ collisions at $\sqrt{s} = 0.9$ and 1.96 TeV were performed by the CDF Collaboration [17] at the Fermilab Tevatron and in pp collisions by the STAR Collaboration [18] at $\sqrt{s} = 0.2$ TeV at the BNL RHIC. Recent measurements in pp collisions at $\sqrt{s} = 7$ TeV were reported by the ATLAS Collaboration [19] at the LHC.

The CMS Collaboration at the LHC has recently published a study of central exclusive $\pi^+\pi^-$ production at $\sqrt{s} = 5.02$ and 13 TeV [20] exploiting the presence of rapidity (y) gaps between the $\pi^+\pi^-$ system and the outgoing (untagged) protons. The present study at $\sqrt{s} = 13$ TeV is based on data with an integrated luminosity, 4.7 pb^{-1}, that is more than 4 orders of magnitude higher, where the kinematic variables of both the forward-scattered

[*]Full author list given at the end of the article.

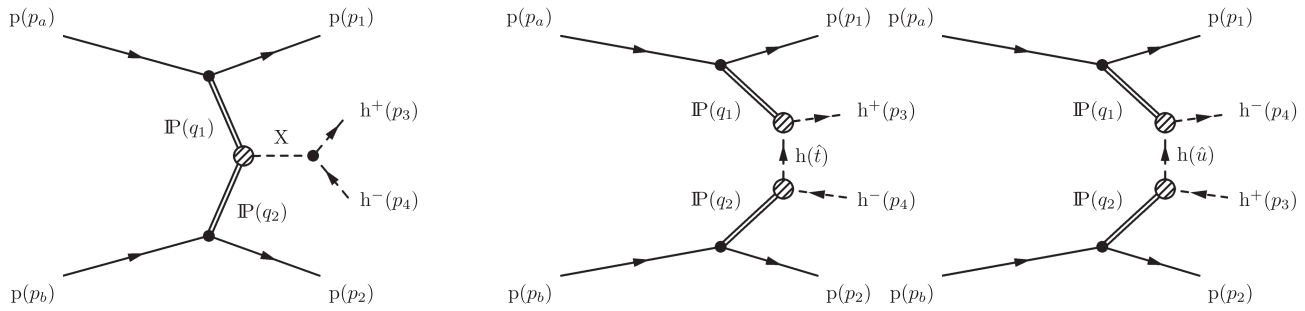

FIG. 1. Born-level Feynman diagrams for central exclusive production of hadron pairs via double-pomeron exchange, depicting resonant (left) and nonresonant continuum (center, t-channel; right, u-channel) contributions.

protons and the centrally produced charged-hadron pair are measured with high precision.

Central exclusive production of hadron pairs is an active area of theoretical study, and several groups are investigating the scalar, vector, or tensor nature of the pomeron [9,21], producing detailed predictions for $\pi^+\pi^-$ [22,23], K^+K^- [24], and $p\bar{p}$ production [25,26], and studying various absorptive effects and properties of diffractive eigenstates [27–29]. Monte Carlo (MC) event generators [30] that describe these processes are available with empirical parametrizations [31,32].

In this paper, after a theoretical introduction, details of the CMS and TOTEM detectors and the outline of the analysis are presented in Sec. I. The conditions of data taking are discussed in Sec. II, with the reconstruction and corrections of scattered protons in the Roman pots (Sec. III) and those of produced particles in the central region (Sec. IV). Event classification is described in Sec. V. Results, model tuning, and data-model comparisons are shown next (Sec. VI), and the paper ends with a summary in Sec. VII.

A. Theoretical background

Proton-proton collisions can be either elastic or inelastic. The latter include double-pomeron exchange, single- and double-diffractive, as well as nondiffractive and photon fusion processes. The elastic scattering of protons is essentially understood through the exchange of pomerons and also odderons [33]. Born-level Feynman diagrams of processes playing a role in central exclusive production of charged-hadron pairs via double-pomeron exchange are shown in Fig. 1. We distinguish two main processes. The two pomerons may fuse through a short-lived resonance (X), which in turn decays into a pair of oppositely charged hadrons. Alternatively, the two pomerons may interact via the exchange of a virtual hadron (h), leading to the production of a pair of oppositely charged hadrons in a nonresonant process, the topic of the present study. Both t-channel and u-channel graphs must be included. The variables of the outgoing protons are labeled with subscripts 1 and 2, and the produced hadron ones with subscripts 3 and 4.

Such a simple picture becomes more complicated when the effects of suppression, absorption, and other corrections are properly included. Here we follow the notations of Ref. [9]. The matrix element for the nonresonant continuum process is

$$\mathcal{M} = M_{13}(t_1, s_{13})\frac{F_m^2(\hat{t})}{\hat{t}-m^2}M_{24}(t_2, s_{24}) + M_{14}(t_1, s_{14})\frac{F_m^2(\hat{u})}{\hat{u}-m^2}M_{23}(t_2, s_{23}), \quad (1)$$

where p_a and p_b are the momenta of the incoming protons, $t_1 = (p_1 - p_a)^2$, $t_2 = (p_2 - p_b)^2$, M_{ik} denotes the "interaction" between one of the scattered protons and one of the created hadrons, $s_{ik} = (p_i + p_k)^2$, $\hat{t} = (p_3 - q_1)^2 = (p_4 - q_2)^2$, and $\hat{u} = (p_4 - q_1)^2 = (p_3 - q_2)^2$. The meson-pomeron form factor $F_m(\hat{t})$ is included twice, once for each vertex connected to the meson. The propagator $(\hat{t} - m^2)^{-1}$ of the virtual hadron is also present, where m is the mass of the exchanged meson. At high meson-proton center-of-mass energies ($\sqrt{s_{ik}} > 20$ GeV) the double-pomeron exchange contribution dominates,

$$M_{ik}(t_i, s_{ik}) = is_{ik}\sigma_0\left(\frac{s_{ik}}{s_0}\right)^{\alpha_{\mathbb{P}}(t_i)-1}F_p(t_i), \quad (2)$$

which is the product of the proton-hadron cross section term $s^{\alpha_{\mathbb{P}}}$ and the exponential proton-pomeron form factor $F_p(t) = \exp(B_{\mathbb{P}}/2t)$. From a fit to the energy dependence of the measured cross sections [34], the strength parameter is $\sigma_0 \approx 13.63$ mb ($\pi^+\pi^-$ production) or 11.82 mb (K^+K^- production), $s_0 = 1$ GeV^2 is a dimensional constant, $B_{\mathbb{P}}$ is related to the proton-pomeron vertex (usually $B_{\mathbb{P}} =$ 5.5–6.0 GeV^2 is assumed), and the soft-pomeron trajectory is $\alpha_{\mathbb{P}}(t) = 1.0808 + 0.25\ \text{GeV}^{-2}t = \alpha_{\mathbb{P}}(0) + \alpha'_{\mathbb{P}}(0)t$. The cross section is proportional to $|\mathcal{M}|^2/s^2$. The strength parameter (referred to as σ_0 in the following), the intercept $\alpha_{\mathbb{P}}(0)$, and the slope $\alpha'_{\mathbb{P}}(0)$ of the pomeron trajectory are usually taken from the Donnachie-Landshoff model [34], based on a fit to the $\sqrt{s}$ dependence of the total cross

sections. A more complete analysis was performed by the COMPETE Collaboration [35].

The meson-pomeron form factor takes into account that the virtual meson is off shell. There are several parametrizations [9,30] available for $F_m(\hat{t})$,

$$\begin{cases} \exp\left(b_{\text{exp}}(\hat{t}-m^2)\right) & \text{(exponential)}, \\ \exp\left(b_{\text{ore}}\left[a_{\text{ore}}-\sqrt{a_{\text{ore}}^2-(\hat{t}-m^2)}\right]\right) & \text{(Orear)}, \\ 1/\left(1-b_{\text{pow}}(\hat{t}-m^2)\right) & \text{(power law)}. \end{cases} \tag{3}$$

The Orear-type parametrization is given in Ref. [36]. They are equal to unity if the hadron is on shell, $F_m(m^2)=1$. The parameters b_{exp}, b_{pow}, a_{ore}, and b_{ore} are determined from measurement. To account for the low-mass diffractive dissociation of the proton, a multichannel framework is needed, where the incoming proton is a coherent superposition of diffractive eigenstates with amplitudes a_i and coupling factors γ_i. A two-channel model is considered here, including a ground state p and its first excitation N^*. The coupling of the pomeron to the diffractive eigenstates is parametrized as in Ref. [30],

$$F_i(t)=\exp\left[-(b_i(c_i-t))^{d_i}+(b_i c_i)^{d_i}\right], \tag{4}$$

where b_i, c_i, and d_i are parameters. This factor is unity at $t=0$ with $F_i(0)=1$ and is a more complex version of the simple $F_p(t)=\exp(B_{\mathbb{P}}/2t)$ form displayed in Eq. (2).

Additional pomeron exchanges between the incoming (and outgoing) protons cause interference between the bare $\mathcal{M}$ [Eq. (1)] and the rescattered $\mathcal{M}_{\text{res}}$ amplitudes (Fig. 2). The resulting quantity is often referred to as the eikonal survival factor. The interference is expected to lead to dips in the angular distributions [30]. The rescattered amplitude is obtained through a loop integral over $\vec{k}_{\text{T}}$ as

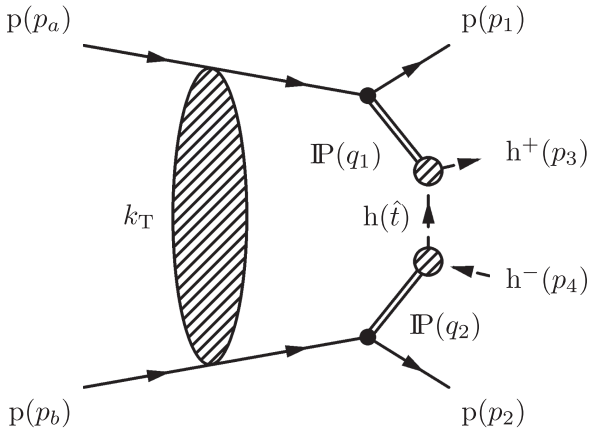

FIG. 2. Feynman diagram for the nonresonant continuum of central exclusive production of hadron pairs via double-pomeron exchange, including the rescattering correction.

$$\mathcal{M}_{\text{res}}=\int \mathrm{d}^2\vec{k}_{\text{T}}\mathcal{M}(\vec{p}_1-\vec{k}_{\text{T}},\vec{p}_2+\vec{k}_{\text{T}}) \times\sum_{i,j}\gamma_i|a_i|^2F_i(t_1)\gamma_j|a_j|^2F_j(t_2)S_{ij}(k_{\text{T}}), \tag{5}$$

where t_1 and t_2 implicitly depend on $\vec{k}_{\text{T}}$. The screening amplitude S can come either from a calculation or from an empirical parametrization of a direct measurement of the elastic differential pp cross section. In the calculation of the cross section, the bare amplitude $\mathcal{M}$ is replaced by the sum of the bare and rescattered amplitudes, $\mathcal{M}+\mathcal{M}_{\text{res}}$.

B. The CMS and TOTEM detectors

The central feature of the CMS apparatus is a superconducting solenoid of 6 m internal diameter, providing a magnetic field of 3.8 T. Within the magnetic volume are a silicon pixel and strip tracker, a lead tungstate crystal electromagnetic calorimeter, and a brass and scintillator hadron calorimeter, each composed of a barrel and two end cap sections. Forward calorimeters extend the coverage provided by the barrel and end cap detectors. Muons are detected in gas-ionization chambers embedded in the steel flux-return yoke outside the solenoid. The silicon tracker measures charged particles within the pseudorapidity range $|\eta|<2.5$. During the LHC running period when these measurements were performed, the silicon tracker consisted of 1856 silicon pixel and 15 148 silicon strip detector modules. For nonisolated particles with transverse momentum $1<p_{\text{T}}<10$ GeV, the track resolutions are typically 1.5% in p_{T} and 20–75 μm in the transverse impact parameter [37]. A more detailed description of the CMS detector is reported in Ref. [38].

The proton spectrometer of the TOTEM experiment consists of two telescope arms, referred to as "arm 1" and "arm 2" for positive and negative η, respectively. The spectrometer is used to detect protons scattered at very small angles. In each arm, there are two detector "stations" located at about ±213 and ±220 m relative to the nominal interaction point. Each station consists of two units. Each unit has two vertical Roman pots (RPs), one located above and one below the LHC beam. An RP contains ten layers of silicon strip detectors, placed alternately in two orthogonal orientations (u and v). They approach the beam to a distance of a few millimeters without affecting the LHC operation (they are retracted for injection). The RPs are used to detect protons deflected by only a few microradians relative to the beam, through reconstruction of their short track segments ("tracklets"). The kinematic variables of the scattered protons are reconstructed by modeling the transport of the protons from the interaction point to the RP location, through the inhomogeneous magnetic fields of several quadrupole and dipole magnets. The TOTEM detector is described in Refs. [39,40].

We use a right-handed coordinate system, with the origin at the nominal collision point, the x axis pointing to the center of the LHC ring, the y axis pointing up (perpendicular to the LHC plane), and the z axis along the anticlockwise beam direction.

C. Analysis outline

As discussed above, the RPs measure the direction of the scattered proton. The transverse momentum is inferred under the assumption that the total momentum of the proton has not changed in the collision. The longitudinal momentum is computed from the conservation of energy and momentum, taking into account all produced particles. The acceptance of the stations is not azimuthally uniform [39] and the coverage in the y component of the scattered proton momentum is $0.175 < |p_{1/2,y}| < 0.670$ GeV. The acceptance maps of the two arms are correlated since signals from both arms are used for triggering. In addition, their efficiency depends on the individual silicon strip detector efficiencies, which in some cases change significantly over time.

The coverage of the silicon tracker translates into acceptance for centrally produced hadrons for rapidities $|y| < y_{\max}$, where $y_{\max} \approx 2.0$ in the case of $\pi^+\pi^-$ and ≈ 1.6 for K^+K^- and pp. Tracking is efficient for $p_T > 0.1$ GeV, but the particle identification capabilities are substantially reduced at momenta above 1.2 GeV.

The data are analyzed as functions of the four-momentum transfers squared (t_1, t_2), or equivalently $(p_{1,T}, p_{2,T})$, and the azimuthal angle ϕ between the momentum vectors of the two scattered protons in the transverse plane.

The measurement is corrected bin-by-bin and no unfolding is needed. The corrections are computed without using Monte Carlo simulations, except for those describing the low-energy phenomena (GEANT4 [41] v10.4.3) needed for the determination of the tracking efficiency. The results are corrected for the p_y acceptance and the effect of the RP trigger based on the collected events. This is done by exploiting the expected azimuthal symmetry of the scattered protons around the beam axis. The combined correction is given in bins of $(p_{1,T}, p_{2,T}, \phi)$. Corrections are also applied for the proton tracklet reconstruction efficiency in the RPs, based on the hit structure of each tracklet at the strip level.

The measurement is also corrected for trigger, reconstruction, and particle identification efficiencies of the charged-hadron pair in the silicon tracker. The first two are constructed using a realistic detector simulation of single-track events combined with information on the pixel layer occupancy in the barrel. This combined tracker correction is applied in bins of $(p_{1,T}, p_{2,T})$, where in each of them a four-dimensional correction table $[\phi, m_{h^+h^-}, (\cos\theta, \varphi)_{GJ}]$ is employed based on a kinematic simulation. Here GJ refers to the Gottfried-Jackson frame [42] in the center of mass of the centrally produced hadron pair, where the z axis is in the direction of the hadron pair in the laboratory frame, the y axis is perpendicular to both $\hat{z}$ and the incoming proton direction, $\hat{x} = \hat{y} \times \hat{z}$, and θ and φ are the polar and azimuthal angles of the positively charged hadron in that frame.

The corrections are applied for each event separately in the form of products of independent weight factors. This is possible since there are no efficiency gaps (zero efficiency) in the $[\phi, m_{h^+h^-}, (\cos\theta, \varphi)_{GJ}]$ space of the two-hadron system in the rapidity range.

II. DATA-TAKING CONDITIONS

The data were taken in a special $\beta^* = 90$ m run of the LHC, in the period 2–7 July, 2018 (β^* is the value of the amplitude function at the collision point [43]). With such a high-β^* setting, the beam divergence is reduced, and the forward detectors are thus able to measure elastically scattered protons at low angles and small transverse momenta.

For this dataset, the level 1 (hardware) trigger requires detected protons in each RP arm, in various configurations. Only the data from double-pomeron exchange triggers are used in the analysis, not those from the elastic trigger (Secs. III A and III B). In the following, the term "parallel" refers to cases where only RPs above or below the beam-line have signals over predefined thresholds in the two arms (top-top or TT, bottom-bottom or BB), whereas the "diagonal" configuration refers to the other two cases (top-bottom or TB, bottom-top or BT). The high-level trigger (HLT) has multiple components [44]. The pixel activity filters require at least five pixel clusters and at least three layers with pixel clusters in the barrel pixel detector. The pixel track filters require at least one track (having at least three pixel clusters) in the entire pixel detector.

Part of the dataset was recorded with a proton bunch spacing of 100 ns and part with 50 ns. To reduce the readout rate, not all bunch crossings were read out in the case of the diagonal trigger configuration. The reduction of the selected bunches does not simply translate into the reduction of the recorded luminosity, since the bunch-by-bunch luminosity can greatly vary. A detailed recalculation of the integrated luminosity was performed at the level of bunch crossings and data segments. A data segment is a fraction of a run that contains 2^{18} orbits, i.e., lasting about 23.3 sec. This yields an integrated luminosity of 4.7 pb^{-1} for the present data.

In practice, sometimes more than one pp collision happens in a bunch crossing (pileup) with the average in the range 0.1–0.3. The detector-level signatures required for the present study are two slightly scattered but intact protons, two oppositely charged centrally produced hadrons, and the sum of the proton and hadron momenta close to zero (within the combined momentum resolution of 50 MeV in x and 20 MeV in y). A $p(h^+h^-)p$ event can be correctly recorded if there is exactly one detectable

$p(h^+h^-)p$ final state, no other double-pomeron exchange, single-, double-diffractive, or nondiffractive collision in the same bunch crossing (they would be visible in the tracker), and no visible elastic collisions (no detectable scattered protons in RPs). In the analysis, events with more than one pp collision are rejected.

The average pileup of visible interactions is $\langle\mu_{\rm vis}\rangle = L_{\rm int}\sigma_{\rm vis}/(n_{\rm bunch}n_{\rm orbit})$, where $\sigma_{\rm vis}$ is the cross section for visible collisions, $L_{\rm int}$ is the average integrated luminosity in a given time period with $n_{\rm orbit}$ orbits, and $n_{\rm bunch}$ is the number of selected colliding bunches. The integrated luminosity loss due to the selection of events with a single collision per bunch crossing is quantified by the factor $\exp(-\mu_{\rm vis})$. Most of the elastic pp collisions are rejected by the elastic RP proton pair veto (Sec. III A), whereas a large fraction of events with the $p(h^+h^-)p$ final state is selected. In this way the inelastic pp cross section is a good approximation for the visible cross section, $\sigma_{\rm vis} \sim \sigma_{\rm inel}$. There are several measurements of the inelastic pp cross section at $\sqrt{s} = 13$ TeV at the LHC [45–48], with an average value of 79 ± 1 mb. For comparison, the recommended cross section for inelastic events selected with a loose "minimum bias" trigger by CMS is 69.2 mb. We use $\sigma_{\rm vis} = 79 \pm 5$ mb.

The values of beam-related quantities (instantaneous luminosity, bunch crossing selection) and of the detector-related ones (acceptance, trigger efficiency) are checked by comparing the numbers of observed and expected events, in all RP trigger configurations (TB, BT, TT, and BB), separately in each data segment. Overall a good agreement is found.

III. SCATTERED PROTONS IN THE ROMAN POTS

Details of proton reconstruction, including specific aspects relevant for the high-β^* run (strip-level efficiencies, local and global alignment, optics determination), are reported in Ref. [49].

A. Proton-pair trigger acceptance (elastic veto)

The elastic pp cross section is much larger than that for central exclusive production events and, in the absence of an appropriate trigger algorithm, would saturate the available bandwidth of the data acquisition system. Therefore, elastic events need to be rejected. Triggering is based on "trigger roads," each consisting of 32 adjacent silicon strips with the aim of reducing the number of channels to handle. Since there are 512 strips in a plane, there are 16 trigger roads for each orientation (u and v). The trigger bit is set if trigger roads at the same location have signals above a predefined threshold in at least three planes. Suitable combinations of these trigger bits from RPs in diagonal configuration are used to reject elastic events. This algorithm is referred to as "elastic veto."

To determine the efficiency loss due to the elastic veto algorithm, proton tracks from events with parallel trigger configurations are used. A track from a TT event is combined with one from a BB event, and the resulting diagonal event is used as input to the veto algorithm. These events are used to build an efficiency table as a function of $(p_{1,y}, p_{2,y})$, which is used later for the calculation of the RP-related corrections (Sec. III B). The fraction of elastic-like events left after veto trigger is shown in Fig. 3 (left) as a function of p_y for arms 1 and 2. It compares well with the measured $(p_{1,y}, p_{2,y})$ distribution of the events obtained with the diagonal trigger configurations, as shown in Fig. 3 (middle).

B. Coverage and trigger acceptance

The combined trigger and detection acceptance, as well as the efficiency of the RP system are calculated in bins of $(p_{1,\rm T}, p_{2,\rm T}, \phi)$ using 400×10^6 simulated two-proton events. These events are generated with uniform and independent $p_{1,\rm T}$ and $p_{2,\rm T}$ distributions in the range (0,1) GeV and uniform ϕ distribution in the range $(0, \pi)$, using the single-proton and proton-pair trigger acceptances discussed above. The detection efficiencies for a pair of scattered protons in selected bins of the pp azimuthal angle ϕ are shown in Fig. 4, where the rightmost column displays the joint efficiency using all configurations, i.e., the coverage of the measurement. In general, large regions are populated by all four configurations. Some corners of phase space are not covered: they are at high $p_{1,\rm T}$ and low $p_{2,\rm T}$ (and vice versa), if $\phi < 20°$ or $\phi > 160°$; at low $p_{1,\rm T}$ and $p_{2,\rm T}$, if $70 < \phi < 110°$; and at high $p_{1,\rm T}$ and $p_{2,\rm T}$, if $80 < \phi < 100°$. Regions where the proton detection efficiency is below 2% are not used in the analysis.

IV. PARTICLES PRODUCED IN THE CENTRAL REGION

The finding and fitting of the charged-particle trajectories in the silicon tracker are performed with well-tested methods [50], which include the results of an optimization for low-momentum particles. In the following, we discuss some single- and two-track parameters using events with exactly two oppositely charged reconstructed particles. The distribution of the z coordinate of the reconstructed charged particles at their closest approach to the beamline is Gaussian with a fitted mean value of $\langle z\rangle = -0.37$ cm and standard deviation $\sigma_z = 4.63$ cm. The distribution of the transverse impact parameter of the reconstructed charged particles has a Cauchy distribution with $\Gamma = 0.046$ cm. The distribution of the difference $z_4 - z_3$ of the reconstructed charged-particle pair has again a Cauchy distribution with $\Gamma = 0.139$ cm. Events are selected if the z values of both tracks satisfy $|z - \langle z\rangle| < 4\sigma_z$ and their vertex is closer to the beamline than 1 cm. The latter requirement eliminates photon conversions in the beam pipe and pixel tracker layers, while significantly reducing the contribution of long-lived decays. Low $p_{\rm T}$ particles looping in the

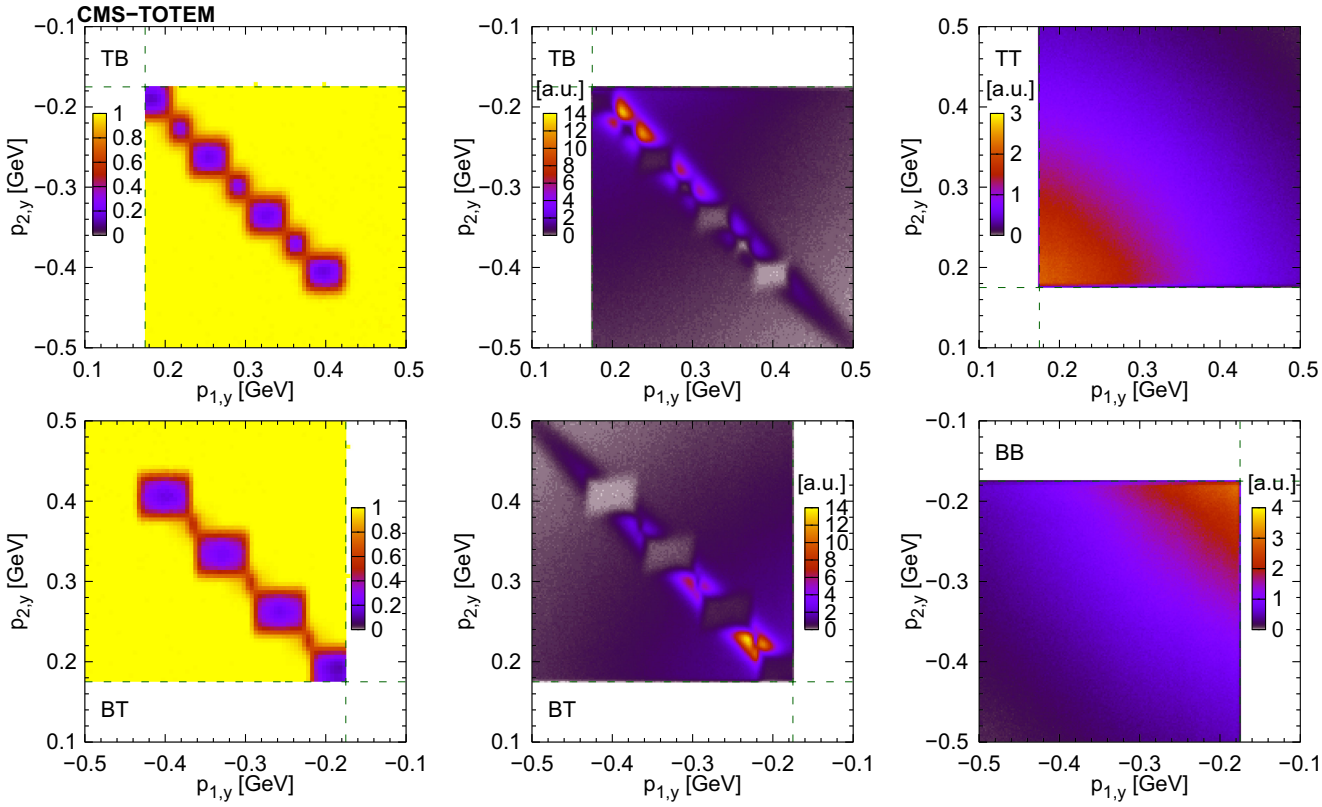

FIG. 3. Left: fraction of elasticlike events left after the veto trigger as functions of momentum components in the y direction in arms 1 and 2, shown here for the two diagonal trigger configurations: bottom pots in arm 2 with top pots in arm 1 (upper left) and top pots in arm 2 with bottom pots in arm 1 (lower left). Center and right: joint distribution of detected proton momenta $(p_{1,y}, p_{2,y})$ in arms 1 and 2 for all four trigger configurations (center, TB and BT; right, TT and BB). Limits of single-proton acceptance are indicated with long dashed lines.

solenoidal magnetic field might rarely (rate below 0.5%) be reconstructed as two oppositely charged particles with opposite momentum vectors. Their contribution is visible in the distribution of $|\vec{p}_3 + \vec{p}_4|/m$ as peaks near zero. In the analysis, events containing a looper are removed by requiring $|\vec{p}_3 + \vec{p}_4|/m > 0.2$, where m is the mass of the identified hadron. The corresponding event loss is negligible.

A. High-level trigger and tracking efficiency

The distributions of charged particles in the (η, p_{T}) plane reveal "valleys" corresponding to inefficiencies at low p_{T}. These are present because the HLT contains pixel activity filters and various pixel track filters (Sec. II). Having a simple single-track tracking efficiency table is not sufficient, and a combined "track-pair HLT and tracking" efficiency is necessary. We have generated, simulated, and reconstructed single pions, kaons, and protons of both electric charges uniformly in the kinematic range $-3 < \eta < 3$, $0 < p_{\mathrm{T}} < 2$ GeV (30×10^6 events for each species). These events are used to determine the reconstruction efficiency and to study the distribution of the hit patterns in the pixel layers. The combination of these is then used to determine the HLT and reconstruction efficiency of two-track events (Sec. II). The extracted single-particle reconstruction efficiencies show the acceptance edge near $|\eta| \approx 2.5$ and the efficiency losses at low total momenta because of multiple Coulomb scattering and energy loss. Fragments of a charged-particle trajectory are rarely reconstructed as separate tracks. These are concentrated at $\eta \approx 0$ for pions (loopers) and around $|\eta| \sim 2$ for kaons (scatters or decays), but their frequency is at or below the 1% level. The combined reconstruction and HLT efficiencies for single particles are shown in Fig. 5, projected onto the (η, p_{T}) plane. These plots show a significant decrease of efficiency in the region of the barrel–end cap transition because of the small number of clusters of pixel detector layers with hits.

B. Particle identification

Details on the determination of the silicon strip properties, detector gain calibration, model validation, and on the estimation of the most probable energy loss rate ε (or its logarithm) and its variance $\sigma^2_{\ln\varepsilon}$ based on control samples in data are identical to those already discussed in Ref. [51]. The distributions of $\ln\varepsilon$ as a function of momentum, for reconstructed charged particles in selected two-track

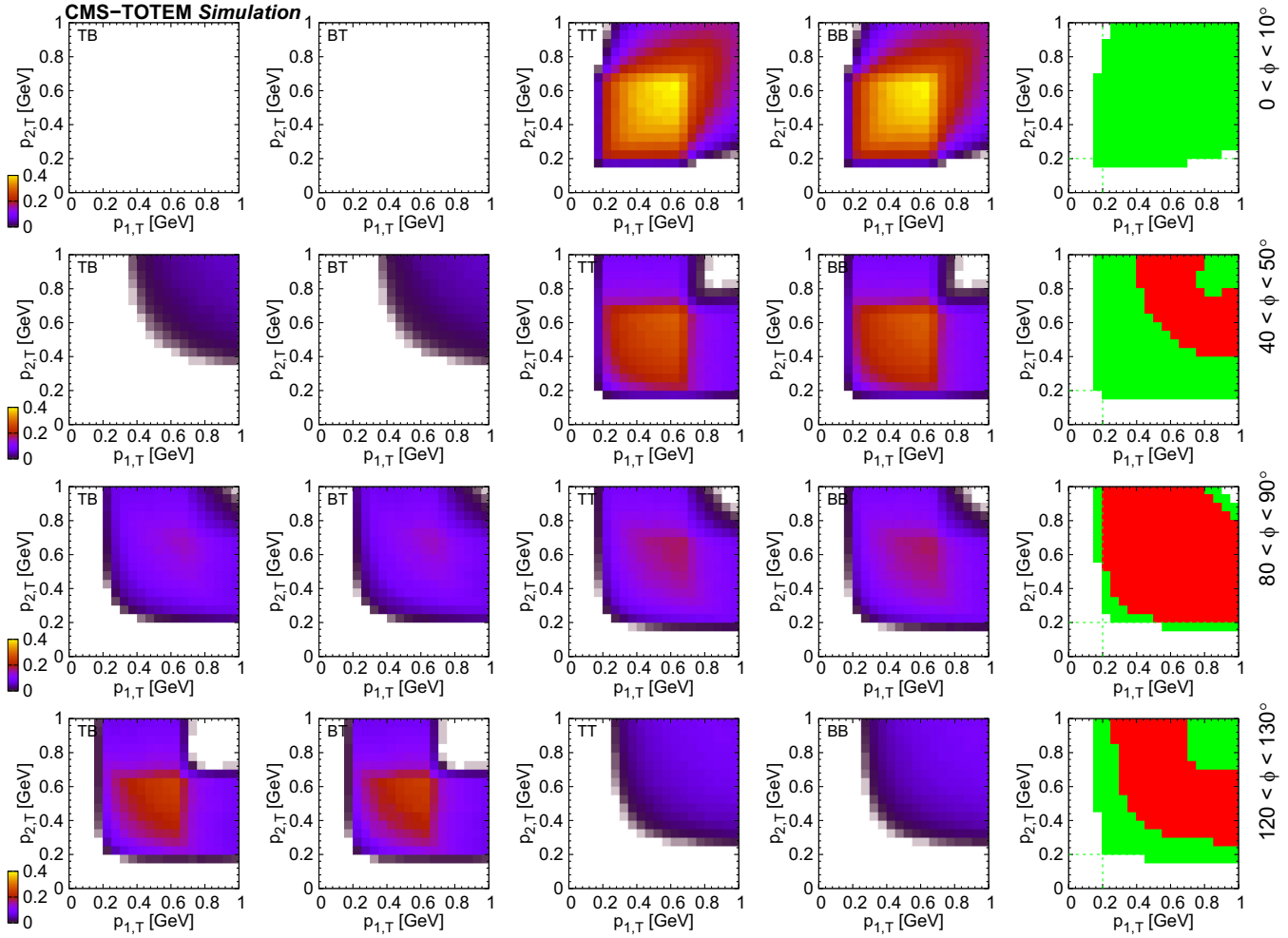

FIG. 4. Calculated detection efficiencies for the pair of scattered protons as functions of their transverse momenta $(p_{1,\mathrm{T}}, p_{2,\mathrm{T}})$ in some selected bins of the pp azimuthal angle ϕ (indicated on the right side of each row). The first four columns show the efficiencies for each trigger configuration, the four rows show four different angular ranges, and the rightmost column displays the coverage of the measurement with color codes (white, not covered; green, covered by at least one configuration; red, covered by all configurations). Lines corresponding to 0.2 GeV are drawn in the rightmost plots.

events, are shown in Fig. 6, including identified $\pi^+\pi^-$, K^+K^-, and pp pairs (without track-RP momentum matching), as well as signal and sideband distributions, which correspond to events where momentum is not conserved in the transverse plane (Sec. V). The curves show the expected values according to Eq. (34.12) in Ref. [1]. While the sideband region displays a reasonable amount of pions, kaons, and protons, the signal region reveals only few protons in the sample (Fig. 6, lower left). The exclusive production of pp pairs is suppressed because of the limited energy and phase space available for pair creation. For two-track identification, the knowledge of $\sigma_{\ln\varepsilon}$ is essential and is extracted from data using identified pions, kaons, and protons in narrow bins for the ranges $-3 < \eta < 3$ and $p_{\mathrm{T}} < 2$ GeV.

The probability density function P_k for identifying a charged particle with momentum p and estimated values $\ln\varepsilon$ and $\sigma^2_{\ln\varepsilon}$ as being of type k (e.g., a pion, kaon, or proton) is a Gaussian function with mean $\langle\ln\varepsilon\rangle_k(p)$. A particle pair is identified of type $\mathrm{h}^+\mathrm{h}^-$ if that choice is at least 10 times more likely than the others, $P_{1,\mathrm{h}}P_{2,\mathrm{h}} > 10P_{1,k}P_{2,k}$, where $k \neq h$. If no type choice fulfils any of the above conditions, the particle pair is left unidentified. To verify the particle identification capabilities, a detailed simulation was set up. Samples with oppositely charged particles ($\pi^+\pi^-$, K^+K^-, and pp) were generated uniformly in the range $-3 < \eta < 3$ and in total momentum (p_3, p_4) up to 2 GeV; each sample has 100 000 events. The most probable value of ε was taken from a model [1] using the density correction according to Ref. [52]; its relative standard deviation was sampled from the measured distribution of $\sigma_{\ln\varepsilon}$. The identification efficiencies are close to 100% at low momenta and slowly decrease above approximately 1 GeV (pions and kaons) or 2 GeV (protons).

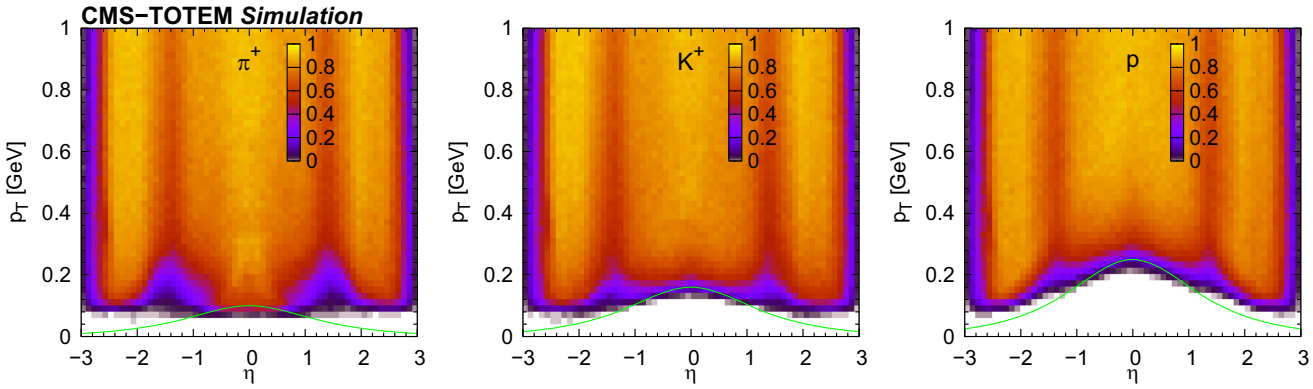

FIG. 5. The combined reconstruction and HLT efficiency (reconstructed and passing the HLT selection) for positively charged pions, kaons, and protons as functions of (η, p_T). Curves indicate constant total momentum ($p = 0.1$ GeV for pions, 0.16 GeV for kaons, 0.25 GeV for protons). Plots for negatively charged particles are similar.

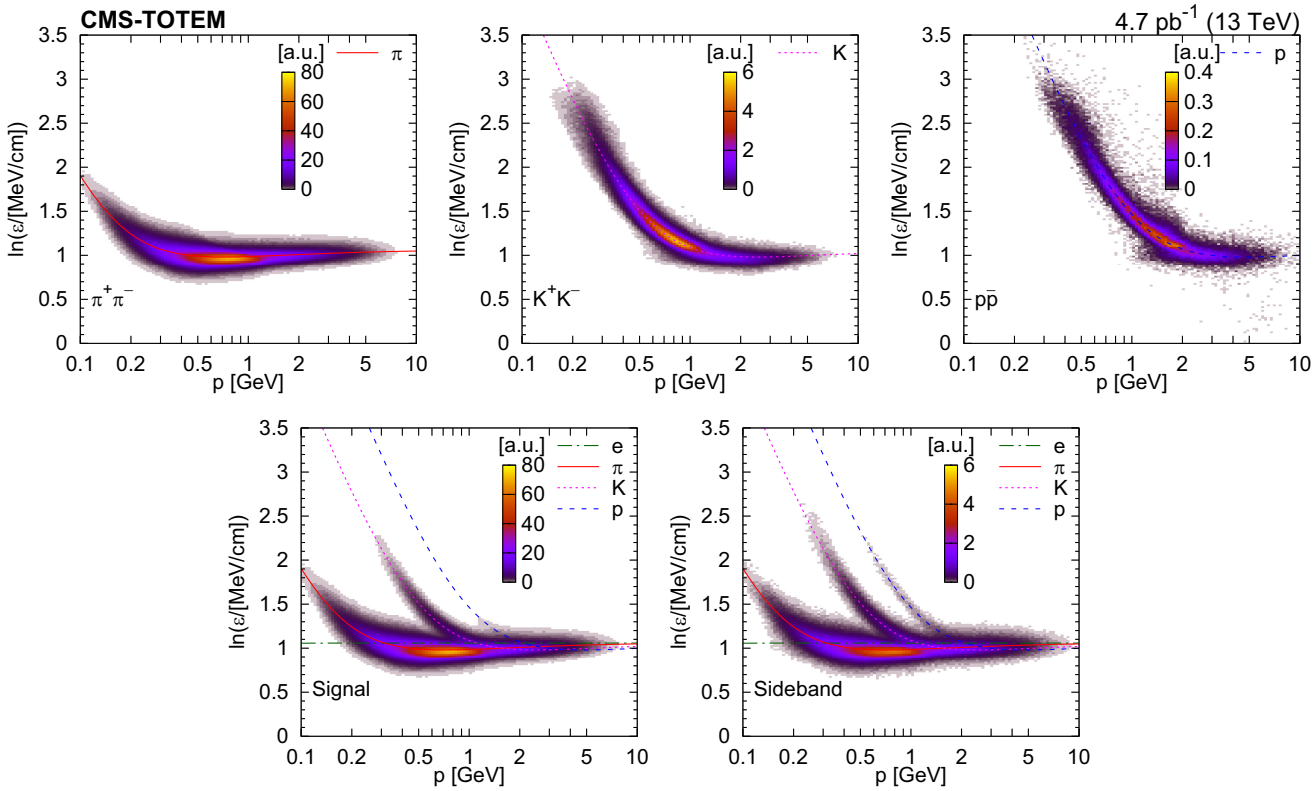

FIG. 6. Distribution of $\ln \varepsilon$ as a function of total momentum, for reconstructed charged particles in selected two-track events (identified $\pi^+\pi^-$, K^+K^-, $p\bar{p}$, signal, and sideband; Sec. V). The variable ε is the most probable energy loss rate at a reference path length $l_0 = 450$ μm. The color scale is shown in arbitrary units and is linear. The curves show the expected $\ln \varepsilon$ for electrons, pions, kaons, and protons [Eq. (34.12) in Ref. [1]].

C. Combined corrections for the silicon tracker

The combined HLT, reconstruction, and identification efficiencies are calculated in the four-dimensional space of $[\phi, m_{h^+h^-}, (\cos\theta, \varphi)_{GJ}]$ (Sec. I C), separately for each $(p_{1,T}, p_{2,T})$ bin, using exclusive two-track events generated with uniform distributions. The combined efficiency is usually above 10% and can reach 90%. It is lower than 1% only in small regions, specifically in the first 20 MeV wide mass bin, at the threshold $2m_{\pi/K/p}$ near $\phi \approx \pi$, and in the case of kaons for $m > 2.6$ GeV because of the reduced particle identification capabilities at higher momenta. In summary, we have coverage in $[\phi, m, (\cos\theta, \varphi)_{GJ}]$ through most of the RP trigger configurations. The corrections described so far are included in the analysis by weighting

TABLE I. Ranges (in parentheses) for bias and resolution of the reconstructed transverse momentum and the two-hadron invariant mass, shown for pions, kaons, and protons, in MeV units.

		π	K	p
Single hadrons	p_T bias	$(0,+5)$	$(-10,+5)$	$(-15,+5)$
	p_T resolution	(5, 15)	(10, 20)	(15, 25)
h^+h^- pairs	m bias	$(0,+4)$	$(-2,0)$	$(-2,0)$
	m resolution	15 at $m_{\pi^+\pi^-} \approx 0.6$ GeV		

events with the product of three factors,

$$\left(\frac{1}{L_{\text{int}}}\right)_{\text{trigger conf}} \left(\frac{\prod \text{tracklet weights}}{\text{azimuthal accep}}\right)_{\text{RPs}} \times \left(\frac{1}{\text{combined effic}}\right)_{\text{tracker}}, \quad (6)$$

which refer to the actual RP trigger configuration of the event, the Roman pot, and the tracker-related corrections, respectively.

D. Momentum and mass resolutions

The bias and resolution of the reconstructed transverse momentum and the two-hadron invariant mass are shown in Table I for pions, kaons, and protons. The p_T bias for kaons and protons occurs because all particles are reconstructed with the pion mass assumption, but the physical effects of particle passage through matter are mass and momentum dependent. The p_T resolutions also show some phase space dependence. The uncertainties seen in momentum sum distributions below (Sec. V) mostly come from the proton momentum reconstruction of the RP system. The bias of the two-hadron invariant mass is proportional to the decay momentum of the daughter in the center-of-mass frame. In summary, the observed shifts are much smaller than the bin width of 20 MeV, but become comparable with it at higher masses. For uneven mass distributions (narrow resonances), these effects should be properly unfolded, but for smooth distributions (nonresonant continuum) an unfolding is not needed.

V. EVENT CLASSIFICATION

The classification of events is largely based on momentum conservation in the transverse plane. Once corrected for the effects of the beam crossing angle (120 μrad), the system of the colliding protons has zero momentum. Therefore, the sum of the momenta of the scattered protons and the other particles created in the collision should also be zero. Momentum conservation in the z direction is already utilized for the calculation of longitudinal momenta of the scattered protons, since the resolution from a direct measurement would be poor.

The sum of scattered proton transverse momenta ($\sum_2 \vec{p}_T$ for these two particles) and the sum of scattered proton and central hadron transverse momenta ($\sum_4 \vec{p}_T$ for these four particles) play an important role. The joint distributions of their components ($\sum_4 p_x$ vs $\sum_2 p_x$, $\sum_4 p_y$ vs $\sum_2 p_y$) are shown for each trigger configuration for two-track events in Fig. 7. The contributions of elastic pileup (two scattered protons and two unrelated central charged hadrons, vertical band) and central exclusive events (two scattered protons and two central charged hadrons, horizontal band) are visible. In addition, a slanted area of nonexclusive or inelastic background is present. In the case of TT and BB trigger configurations, the vertical band is absent, since such configurations ($\sum_2 p_y > 2 \times 0.2$ GeV) prevent the recording of elastic events.

The classification variable is the Mahalanobis distance χ, which is a multidimensional generalization of the standard deviation taking into account internal correlations [53]. It is based on the value and covariance of momentum sums, defined in the multivariate normal case as $\chi(\vec{s}) = (\vec{s}^T V^{-1} \vec{s})^{1/2}$, where $V(\vec{s})$ is the covariance matrix. For two-dimensional vectors (s_x, s_y) it can be written as

$$\chi(\vec{s}) = \left(\frac{V_{yy} s_x^2 - 2V_{xy} s_x s_y + V_{xx} s_y^2}{V_{xx} V_{yy} - V_{xy}^2}\right)^{1/2}. \quad (7)$$

For each event, the classification variable χ_2 is based on $\vec{s} = \sum_2 \vec{p}_T$, whereas the value of χ_4 is computed from $\vec{s} = \sum_4 \vec{p}_T$. They both follow the χ distribution of 2 degrees of freedom (d.o.f.) with a parameterless probability density function $\chi \exp(-\chi^2/2)$. Distributions and joint distributions of χ_2 and χ_4 are shown in Fig. 8 without any preselection (integrated over the azimuthal angle between the scattered protons ϕ). The distributions are fitted with a two-component model: a sum of a χ distribution (signal) and a phase space motivated term (background) as $A\chi \exp(-\chi^2/2) + B\chi \exp(-k\chi)$. The functional form fits the measured distribution well, with two relevant parameters only (B/A and k).

An event is used in the analysis if it is more likely a central exclusive signal than an elastic + pileup background, $\chi_4 < \chi_2$. Signal events are defined by $\chi_4 \leq \chi_{\text{sign}} = 3.4$, where the numerical choice for χ_{sign} translates into a signal loss below 0.5%. Sideband events in the region $\chi_{\text{sign}} \leq \chi_4 < \chi_{\text{side}}$ are subtracted with weight of -1 to compensate for nonexclusive events in the signal region. For this subtraction scheme to work, we must have equal numbers of nonexclusive events in the signal and sideband regions. We need a χ_{side} value that satisfies $\int_0^{\chi_{\text{sign}}} \chi \exp(-k\chi) d\chi = \int_{\chi_{\text{sign}}}^{\chi_{\text{side}}} \chi \exp(-k\chi) d\chi$. Although the choice of signal cutoff is fixed, the value of the sideband cutoff depends on the actual distribution of χ_4. The fitted coefficient k and the value of χ_{side} for χ_4 as a function ϕ are shown in Fig. 8 (lower right).

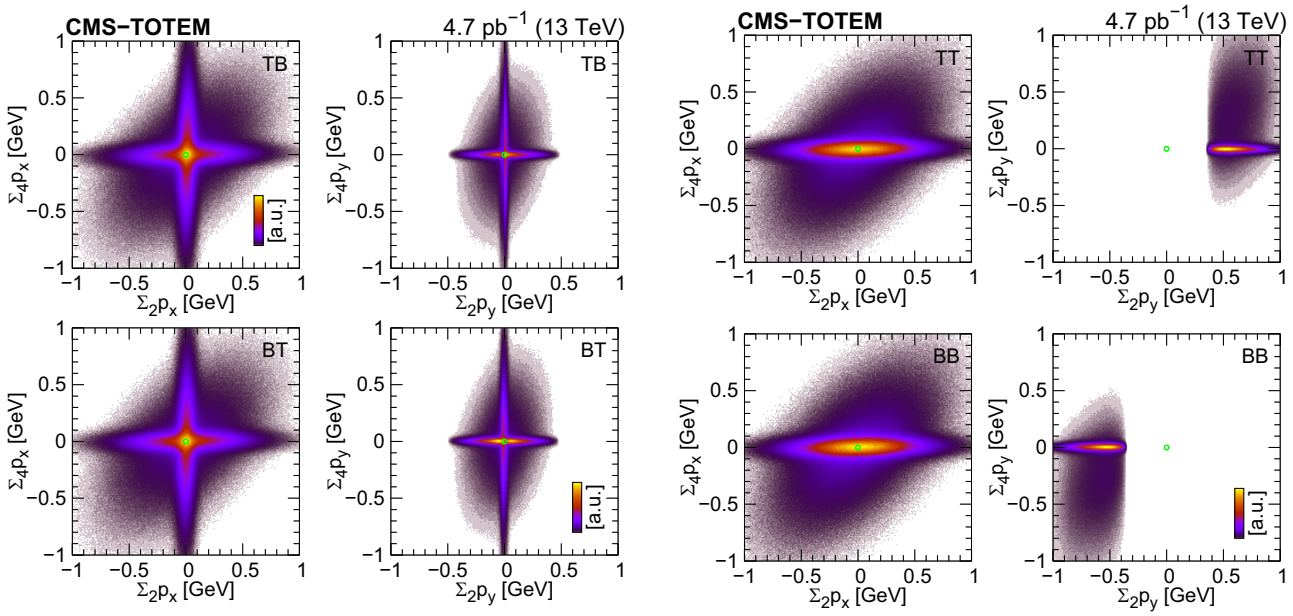

FIG. 7. Distribution of the sum of the scattered proton and central hadron momenta and the sum of the scattered proton momenta ($\sum_4 p_x$ vs $\sum_2 p_x$, $\sum_4 p_y$ vs $\sum_2 p_y$) shown for the diagonal trigger configurations (TB and BT, left) and the parallel ones (TT and BB, right) in the case of two-track events.

VI. RESULTS

The measured distributions are the following: distribution of the azimuthal angle ϕ between the scattered proton momenta, $d^3\sigma/dp_{1,\mathrm{T}}dp_{2,\mathrm{T}}d\phi$; invariant mass of two hadrons m, $d^3\sigma/dp_{1,\mathrm{T}}dp_{2,\mathrm{T}}dm$; squared four-momentum $\max(\hat{t},\hat{u})$ of the virtual meson, $d^3\sigma/dp_{1,\mathrm{T}}dp_{2,\mathrm{T}}d\max(\hat{t},\hat{u})$, in the range $0.2 < (p_{1,\mathrm{T}}, p_{2,\mathrm{T}}) < 0.8$ GeV. In the plots the scattered protons are indexed such that $p_{1,\mathrm{T}} \geq p_{2,\mathrm{T}}$. Tabulated results are provided in HEPData [54].

A. Systematic uncertainties

The relevant systematic uncertainties are listed in Table II, where values propagated to the final differential cross sections are given. The sources are the pileup correction (because of the uncertainty in the visible cross section), the reduced RPs availability, the integrated luminosity, the efficiency of the RPs, the removal of the nonexclusive background, the fraction of signal events mistaken as background or lost because of the selection against looping particles, and the efficiency of single-particle tracking.

The systematic uncertainty of the visible cross section σ_{vis} is estimated as half the difference between the value used and the minimum bias value. This uncertainty is propagated to the final differential cross sections through the pileup correction factor, and its contribution to the systematic uncertainty is 1.0%. A few short periods with reduced data-taking efficiency are due to the loss of one out of the four data streams. About 2%–3% of the data segments are affected, leading to about 0.5% systematic uncertainty. The systematic uncertainty in the integrated luminosity (per data segment) is 2.5% [55]. The efficiency of tracklet reconstruction in the RPs depends on the knowledge of the individual strip efficiencies. These were determined by a tag-and-probe method [56] using zero- and two-track datasets. The effect on proton reconstruction efficiency is about 3%. To estimate the systematics related to the removal of nonexclusive background (χ_4 distribution), the functional form of the background model was varied (uncertainty below 0.5%). Signal events are lost because of the sideband removal procedure. Their fraction is estimated with the help of the signal and the background components of the χ_4 distributions, resulting in an uncertainty of 0.16%, which is neglected. The fraction of events lost because of the looper removal procedure is estimated by fitting the $|\vec{p_3} + \vec{p_4}|/m$ distribution with a signal and a background component. The estimated value is below 0.5%, which is again neglected. The systematic uncertainty in the single-particle tracking efficiency of centrally produced hadrons in the relevant low-momentum regions is 1.4%, according to a study based on control samples in data [57]. To demonstrate the particle identification capabilities for particle-antiparticle hadron pairs, a detailed simulation was set up. The probability of misidentification is low, and in the most populated low-momentum regions it is below 1%.

The uncertainty of the RP and single-particle tracking efficiencies are included for both arms and for both centrally reconstructed charged hadrons. The estimated total systematic uncertainty of the differential cross section measurements is 5.4%, with the various contributions treated as independent and added in quadrature.

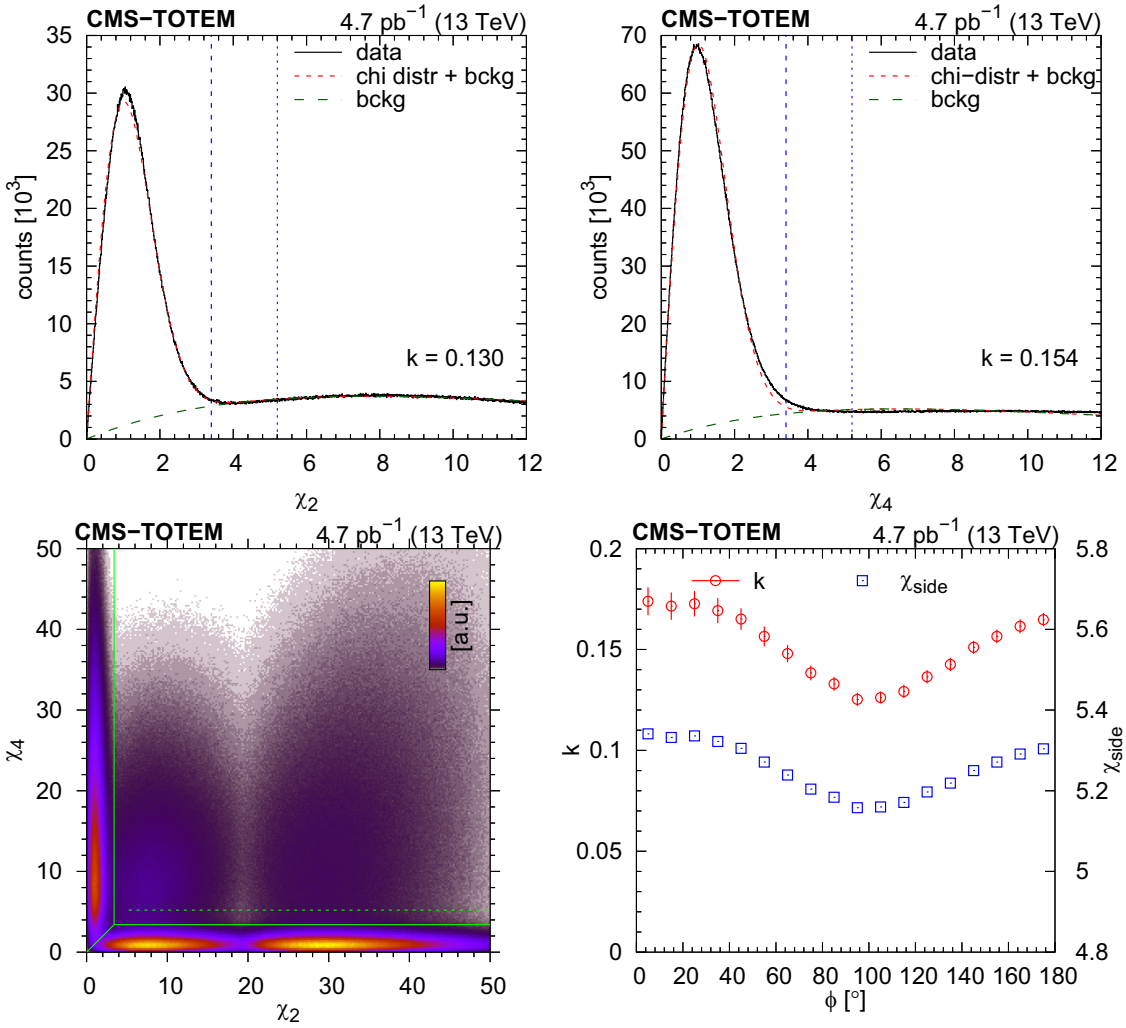

FIG. 8. Distributions of the classification variables χ_2 (upper left) and χ_4 (upper right). Fits using a two-component model are indicated. The distributions are integrated over the angle between the scattered protons ϕ. Selection lines at $\chi_{\text{sign}} = 3.4$ (green solid) and $\chi_{\text{side}} \approx 5.2$ (green dotted) are also plotted. Lower left: joint distributions of classification variables χ_2 and χ_4. Central exclusive signal events are at the bottom, whereas elastic events are at the left margin. Lower right: coefficient k and the position of the upper cutoff χ_{side} for χ_4 to describe the background component as a function of the angle between the scattered protons ϕ, in the plane transverse to the beam direction.

B. The ϕ distributions

We focus on $\pi^+\pi^-$ production because this system has a wide invariant mass window ($0.35 < m_{\pi^+\pi^-} < 0.65$ GeV) without resonance contributions, contrary to the K^+K^- case. The distributions of $d^3\sigma/dp_{1,\mathrm{T}}dp_{2,\mathrm{T}}d\phi$ as functions of ϕ in several $(p_{1,\mathrm{T}}, p_{2,\mathrm{T}})$ bins are shown in Figs. 9–11. The differential cross sections are given in units of $\mu\mathrm{b/GeV}^2$. Values based on data from each RP trigger configuration (TB, BT, TT, and BB) are shown separately with colored symbols, whereas the weighted average is indicated with black symbols. The error bars show the statistical uncertainties. Gaps (missing data points) in some $(p_{1,\mathrm{T}})$ bins of Fig. 9 are due to the vanishing acceptance in those bins.

The distributions from the different trigger configurations are consistent. Except for the lowest p_{T} bins, they feature a minimum where the differential cross section gets close to zero, while local maxima at $\phi = 0$ and π are also present. The distributions are asymmetric at low and high transverse momenta, but there exists a symmetric region around $p_{1,\mathrm{T}} + p_{2,\mathrm{T}} \approx 0.8$–$0.9$ GeV.

The data can be fitted with a simple functional form

$$\frac{d^3\sigma}{dp_{1,\mathrm{T}}dp_{2,\mathrm{T}}d\phi} = [A(R - \cos\phi)]^2 + c^2, \tag{8}$$

where A, R, and c are functions of $(p_{1,\mathrm{T}}, p_{2,\mathrm{T}})$. The χ^2/d.o.f. values corresponding to individual fits are mostly

TABLE II. Systematic uncertainties of the differential cross sections.

Source	Value (%)	Remark
Pileup correction	1.0	Through σ_{vis}
Periods with reduced RP availability	0.5	
Integrated luminosity (L_{int})	2.5	
HLT efficiency	<0.1	Neglected
Total normalization type	2.7	
Roman pot efficiency	3.0	Twice
Background removal	<0.5	Neglected
Lost events during background removal	0.16	Neglected
Lost events due to looper removal	<0.5	Neglected
Single-particle tracking efficiency	1.4	Twice
Particle identification efficiency	<1.0	Neglected
Total efficiency type	4.7	
Total systematics	5.4	

in the range 1–10. The formula features a sum of squared amplitudes (Sec. I A) and is inspired by previous theoretical and experimental studies [13,15], where $A(R-\cos\phi)$ is connected to the quantum mechanical amplitude of the process. If the total amplitude crosses zero at a given ϕ, its squared value will have a parabolic minimum. Such a dip at $\phi = \arccos R$ can be understood as an effect of additional pomeron exchanges between the incoming protons, resulting from the interference between the bare and the rescattered amplitudes [30]. The term containing c is added incoherently; it is small and is present to improve the quality of the fit.

The dependences of the parameters A, R, and c on (t_1, t_2) are shown in Fig. 12. Although A and c can be approximated with a simple $t_1 + t_2$ dependence, the results for R do not all have the same dependence. The measured points are fitted with model-motivated [13,15] functional forms

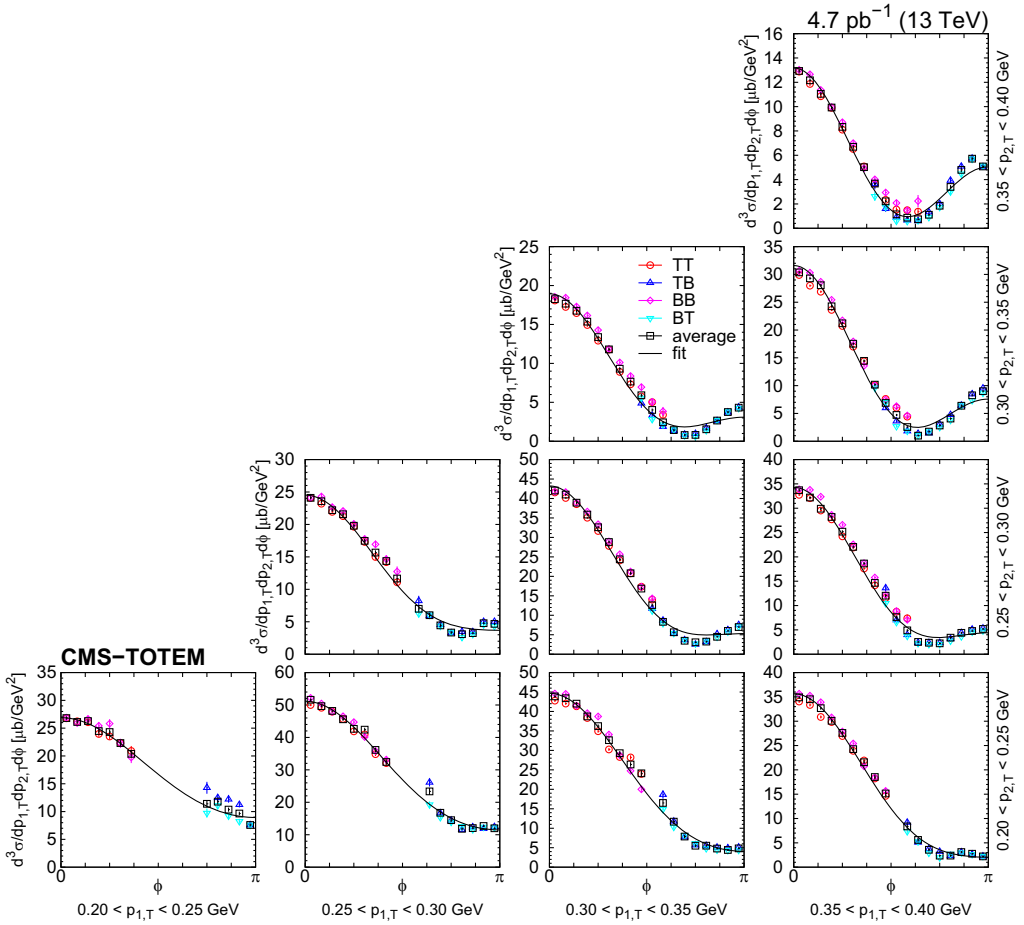

FIG. 9. Distributions of $d^3\sigma/dp_{1,\text{T}}dp_{2,\text{T}}d\phi$ as functions of ϕ in the $\pi^+\pi^-$ nonresonant region ($0.35 < m_{\pi^+\pi^-} < 0.65$ GeV) in several $(p_{1,\text{T}}, p_{2,\text{T}})$ bins in the range $0.20 < p_{1,\text{T}} < 0.40$ and $0.20 < p_{2,\text{T}} < 0.40$ GeV, in units of μb/GeV^2. Values based on data from each RP trigger configuration (TB, BT, TT, and TT) are shown separately with colored symbols, whereas the weighted average is indicated with black symbols. Results of individual fits with the form $[A(R-\cos\phi)]^2 + c^2$ [Eq. (8)] are plotted with the curves. The error bars indicate the statistical uncertainties.

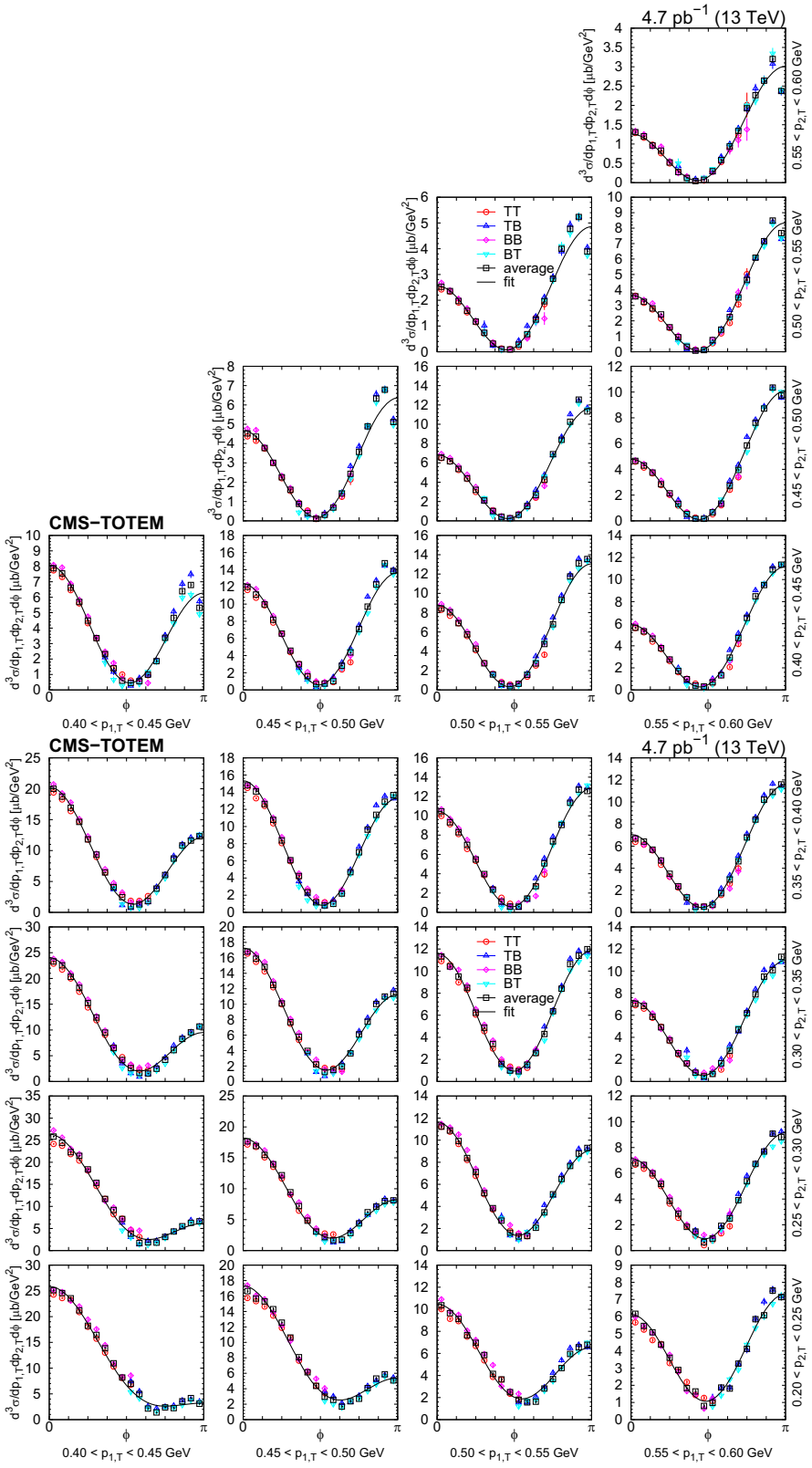

FIG. 10. Distributions of $d^3\sigma/dp_{1,\mathrm{T}}dp_{2,\mathrm{T}}d\phi$ as functions of ϕ in the $\pi^+\pi^-$ nonresonant region ($0.35 < m_{\pi^+\pi^-} < 0.65$ GeV) in several $(p_{1,\mathrm{T}}, p_{2,\mathrm{T}})$ bins in the range $0.40 < p_{1,\mathrm{T}} < 0.60$ and $0.20 < p_{2,\mathrm{T}} < 0.60$ GeV, in units of $\mu\mathrm{b}/\mathrm{GeV}^2$. Values based on data from each RP trigger configuration (TB, BT, TT, and TT) are shown separately with colored symbols, whereas the weighted average is indicated with black symbols. Results of individual fits with the form $[A(R - \cos\phi)]^2 + c^2$ [Eq. (8)] are plotted with the curves. The error bars indicate the statistical uncertainties.

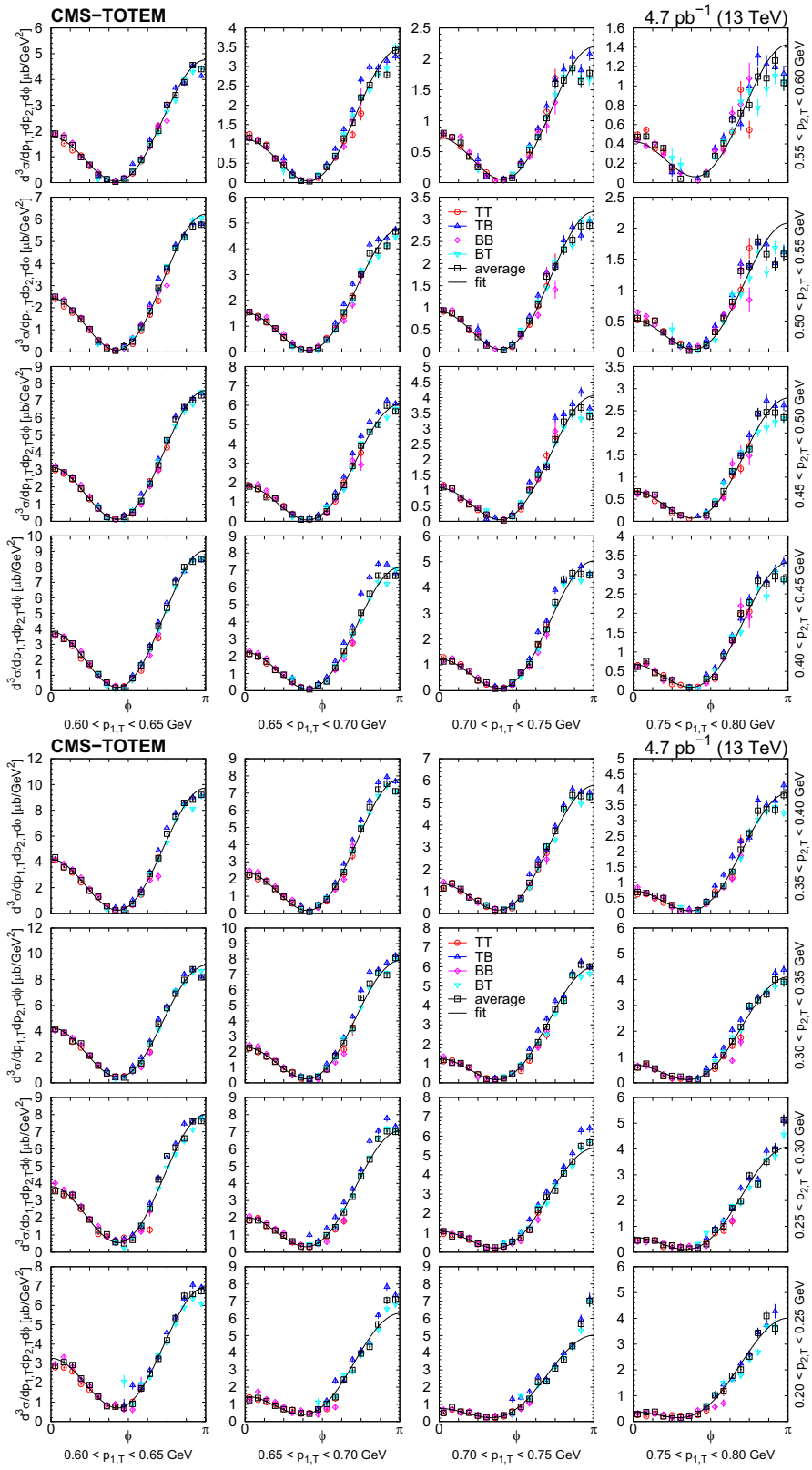

FIG. 11. Distributions of $d^3\sigma/dp_{1,\mathrm{T}}dp_{2,\mathrm{T}}d\phi$ as functions of ϕ in the $\pi^+\pi^-$ nonresonant region ($0.35 < m_{\pi^+\pi^-} < 0.65$ GeV) in several $(p_{1,\mathrm{T}}, p_{2,\mathrm{T}})$ bins in the range $0.60 < p_{1,\mathrm{T}} < 0.80$ and $0.20 < p_{2,\mathrm{T}} < 0.60$ GeV, in units of μb/GeV^2. Values based on data from each RP trigger configuration (TB, BT, TT, and TT) are shown separately with colored symbols, whereas the weighted average is indicated with black symbols. Results of individual fits with the form $[A(R - \cos\phi)]^2 + c^2$ [Eq. (8)] are plotted with the curves. The error bars indicate the statistical uncertainties.

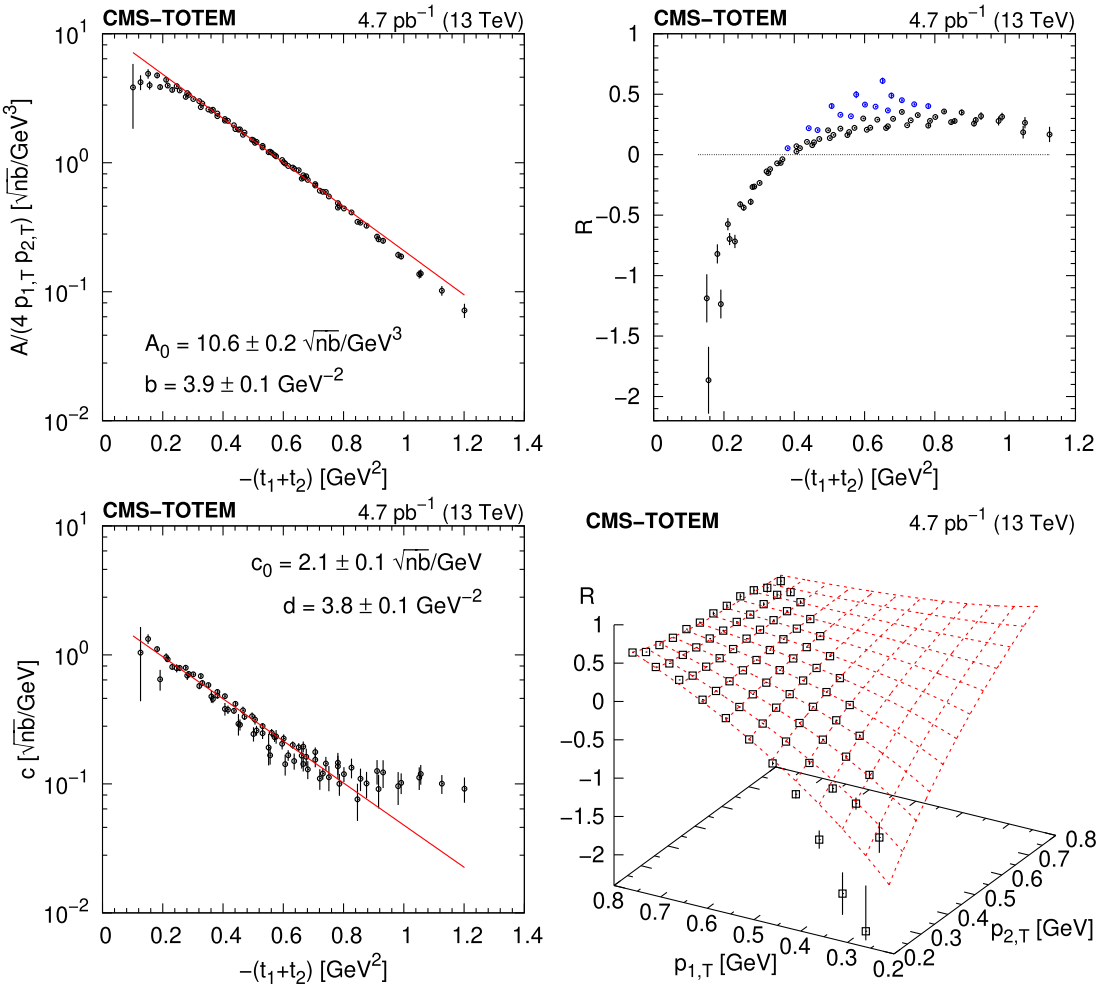

FIG. 12. Dependence of the parameters A, R, and c [Eq. (8)] on (t_1, t_2). The fits correspond to the functional forms displayed in Eqs. (9). In the upper right plot, points with significantly different proton transverse momenta ($|p_{1,\mathrm{T}} - p_{2,\mathrm{T}}| > 0.35$ GeV) are colored blue. The lower right plot shows the dependence of R on the two scattered proton transverse momenta.

$$
\begin{aligned}
A(t_1, t_2) &= 4\sqrt{t_1 t_2} A_0 \mathrm{e}^{b(t_1+t_2)}, \\
R(t_1, t_2) &\approx \frac{1.2(\sqrt{-t_1} + \sqrt{-t_2}) - 1.6\sqrt{t_1 t_2} - 0.8}{\sqrt{t_1 t_2} + 0.1}, \\
c(t_1, t_2) &= c_0 \mathrm{e}^{d(t_1+t_2)}.
\end{aligned} \tag{9}
$$

Although the parametrization overall gives a good description of the data, there are some deviations at low and high $-(t_1 + t_2)$ values for A and c, respectively. Both A and c have very similar dependence on $(t_1 + t_2)$ since $b \approx d$.

The parametrization of the invariant triple-differential cross section is

$$
\begin{aligned}
\frac{d^3\sigma}{dt_1 dt_2 d\phi} &= 4\sqrt{t_1 t_2} A_0^2 \mathrm{e}^{2b(t_1+t_2)} [R(t_1, t_2) - \cos\phi]^2 \\
&\quad + \frac{1}{4\sqrt{t_1 t_2}} c_0^2 \mathrm{e}^{2d(t_1+t_2)},
\end{aligned} \tag{10}
$$

where $A_0 = 10.6 \pm 0.2\sqrt{\text{nb}}/\text{GeV}^3$, $b = 3.9 \pm 0.1$ GeV^{-2}, $c_0 = 2.1 \pm 0.1\sqrt{\text{nb}}/\text{GeV}$, and $d = 3.8 \pm 0.1$ GeV^{-2}.

C. Available MC event generators

The DIME [30] (v1.07) MC event generator for exclusive meson pair production via double-pomeron exchange was used in previous STAR [18] and CMS [20] analyses. It generates central exclusive nonresonant $\pi^+\pi^-$ and K^+K^- production events via the double-pomeron exchange mechanism. This generator is based on previous work on proton opacity [27] and the two-channel model [29] (Good-Walker approach). It includes a fully differential treatment of the eikonal survival factor. The SuperChic2 generator [58] can be regarded as an evolution of DIME, but only provides events with hadron pair invariant masses above 2 GeV. The GenEx code [59] follows an approach quite similar to that of DIME, but does not include the absorption corrections [18]. The model developers estimated the corresponding suppression factor to be large,

of the order of 2–5, and cross sections have to be scaled down by such suppression factor at masses $m < 1.2$ GeV. The GRANIITTI (v1.051) MC event generator [60] for high-energy diffraction includes differential screening, an extendable set of scattering amplitudes with adaptive MC sampling and spin effects.

In the following we consider three models (empirical, one channel, and two channel) and three parametrizations [exponential, Orear-type, and power law, Eq. (3)] of the proton-pomeron form factor. In the case of the empirical model, the rescattering amplitude comes from a simple parametrization of the elastic differential pp amplitude [31,32], fitted to the measured cross sections [61,62]. The one-channel model assumes ground state protons (one eigenstate), whereas the two-channel model works with two diffractive proton eigenstates (Sec. I A). The one-channel model is disfavored in describing the elastic differential cross section data [63].

D. Model tuning

There exist loose estimates of the numerous parameters of the theoretical model illustrated in Sec. I A, including cross sections, slopes, proton-pomeron, and meson-pomeron form factors. Our aim here is to determine the best values and corresponding uncertainties in these quantities with the present data. For the tuning of physics parameters, the tool PROFESSOR [64] (v2.3.3) is employed. It quantifies the per-bin generator response to parameter variations and numerically optimizes the behavior of the generator.

The measured distributions included in model tuning are from events with $\pi^+\pi^-$ central final state in the resonance-free region:

(i) that of azimuthal angle between the scattered proton momenta, $d^3\sigma/dp_{1,\mathrm{T}}dp_{2,\mathrm{T}}d\phi$, if $0.35 < m < 0.65$ GeV;
(ii) that of two-hadron invariant mass at low masses, $d^3\sigma/dp_{1,\mathrm{T}}dp_{2,\mathrm{T}}dm$, if $m < 0.7$ GeV;
(iii) the distribution of the two-hadron invariant mass at high masses, $d^3\sigma/dp_{1,\mathrm{T}}dp_{2,\mathrm{T}}dm$, if $1.8 < m < 2.2$ GeV;
(iv) that of squared four-momentum of the virtual meson, $d^3\sigma/dp_{1,\mathrm{T}}dp_{2,\mathrm{T}}d\max(\hat{t},\hat{u})$, if $1.8 < m < 2.2$ GeV;

all of them in the range $0.2 < (p_{1,\mathrm{T}}, p_{2,\mathrm{T}}) < 0.8$ GeV. The ϕ distributions are sensitive to any resonant contribution; for this reason their mass window is a bit more restricted ($0.35 < m < 0.65$ GeV) than that of the invariant mass distribution. Information about the exchanged virtual meson is present in the distribution of $\max(\hat{t},\hat{u})$ and can be exploited if one of $\hat{t}$ or $\hat{u}$ is close to zero, when the hadron is nearly on shell. Such cases occur if the difference of q_1 and q_2 is large. In other words, the invariant mass of the two-hadron system should be large, hence the choice of a resonance-free window at higher mass values.

The parameter space has many dimensions, and there are up to 13 parameters to tune. The ranges of the parameters are chosen such that the variation of the model output, i.e., its envelope, covers the measured distributions. The sampling is random and uniform, and 512 pseudoexperiments are performed for each form factor parametrization. Each pseudoexperiment contains 1×10^6 generated events, whose average cross section per event is recorded. The distributions from these MC pseudoexperiments are interpolated with a first-order polynomial in the parameter space. The tuning, i.e., the minimization of the global goodness of fit, converges to unique minima for each model and all three form factor options. The χ^2/d.o.f. values are in the range 1.6–2.0 (empirical), 1.2–1.5 (one channel), and 1.0–1.3 (two channel). Good fits are achieved with the one- or two-channel models using exponential or Orear-type form factors, whereas the numerically best one is the two-channel model with the exponential parametrization of the proton-pomeron form factor. It is clear that the power-law parametrization of the proton-pomeron form factor is least favored by our results. The empirical model also has a poor goodness-of-fit value, although with fairly few parameters.

The values of the fitted parameters are listed in Table III and shown in Fig. 13, with notations $\Delta|a|^2 = (|a_1|^2 - |a_2|^2)/2$ and $\Delta\gamma = (\gamma_1 - \gamma_2)/2$. In the case of the two-channel model, parameter values of two models describing the elastic differential pp cross section from Ref. [29] are also indicated (DIME 1 and 2). Settings of DIME 1 agree well with the best tuned values of the parameters, with the exception of the $\Delta|a^2|$, $\Delta\gamma$, and b factors. The extracted values of σ_0 are stable, except for the one-channel exponential case, and disagree with earlier estimates (Sec. I A). The matrix of correlation coefficients for the two-channel model is displayed in Fig. 14 for several choices of the proton-pomeron form factor.

E. Data-MC comparisons

The distributions of $d^3\sigma/dp_{1,\mathrm{T}}dp_{2,\mathrm{T}}d\phi$ in the nonresonant region ($0.35 < m_{\pi^+\pi^-} < 0.65$ GeV) as a function of ϕ in several $(p_{1,\mathrm{T}}, p_{2,\mathrm{T}})$ bins are shown in Figs. 15–17. The measured values are shown together with the predictions of the empirical and the two-channel models using the tuned parameters for the exponential proton-pomeron form factors. Curves corresponding to DIME (model 1) are also plotted: this generator gives a poor description of the data for $\phi > \pi/2$. Although the various tuned models give a better description, there are some regions with sizable disagreements pointing to the need for further theoretical developments, specially for low $p_{1,\mathrm{T}}$ and low $p_{2,\mathrm{T}}$, as well as high $p_{1,\mathrm{T}}$ and high $p_{2,\mathrm{T}}$ combinations.

The plain exponential proton-pomeron form factor (from the fit with the empirical model) and those of the two diffractive proton eigenstates are shown in Fig. 18 (left). One of the eigenstates is quite close to the exponential form. Various options of the meson-pomeron form factor

TABLE III. Values and statistical uncertainties of the parameters tuned using the PROFESSOR tool, given for the empirical, one-channel, and two-channel models along with the DIME soft models 1 and 2 with the exponential, power-law, and Orear-type parametrizations of the proton-pomeron form factor. Goodness-of-fit (χ^2/d.o.f.) values are also listed.

Parameter	Exponential	Orear-type	Power law	DIME 1/2
Empirical model				
a_{ore}(GeV)	⋯	0.735 ± 0.015	⋯	
$b_{\text{exp/ore/pow}}$(GeV$^{-2\text{ or }-1}$)	1.084 ± 0.004	1.782 ± 0.014	1.356 ± 0.001	
$B_{\mathbb{P}}$(GeV^{-2})	3.757 ± 0.033	3.934 ± 0.027	4.159 ± 0.019	
χ^2/d.o.f.	9470/5796	10059/5795	11409/5796	
One-channel model				
σ_0(mb)	34.99 ± 0.79	27.98 ± 0.40	26.87 ± 0.30	
$\alpha_P - 1$	0.129 ± 0.002	0.127 ± 0.001	0.134 ± 0.001	
α'_P(GeV^{-2})	0.084 ± 0.005	0.034 ± 0.002	0.037 ± 0.002	
a_{ore}(GeV)	⋯	0.578 ± 0.022	⋯	
$b_{\text{exp/ore/pow}}$(GeV$^{-2\text{ or }-1}$)	0.820 ± 0.011	1.385 ± 0.015	1.222 ± 0.004	
$B_{\mathbb{P}}$(GeV^{-2})	2.745 ± 0.046	4.271 ± 0.021	4.072 ± 0.017	
χ^2/d.o.f.	7356/5793	7448/5792	8339/5793	
Two-channel model				
σ_0 (mb)	20.97 ± 0.48	22.89 ± 0.17	23.02 ± 0.23	23/33
$\alpha_P - 1$	0.136 ± 0.001	0.129 ± 0.001	0.131 ± 0.001	0.13/0.115
α'_P(GeV^{-2})	0.078 ± 0.001	0.075 ± 0.001	0.071 ± 0.001	0.08/0.11
a_{ore}(GeV)	⋯	0.718 ± 0.012	⋯	
$b_{\text{exp/ore/pow}}$(GeV$^{-2\text{ or }-1}$)	0.917 ± 0.007	1.517 ± 0.008	0.931 ± 0.002	0.45
$\Delta\lvert a\rvert^2$	0.070 ± 0.026	-0.058 ± 0.009	0.042 ± 0.011	$-0.04/-0.25$
$\Delta\gamma$	0.052 ± 0.042	0.131 ± 0.018	0.273 ± 0.023	0.55/0.4
b_1(GeV^2)	8.438 ± 0.108	8.951 ± 0.041	8.877 ± 0.040	8.5/8.0
c_1(GeV^2)	0.298 ± 0.012	0.278 ± 0.004	0.266 ± 0.006	0.18/0.18
d_1	0.472 ± 0.007	0.465 ± 0.002	0.465 ± 0.003	0.45/0.63
b_2(GeV^2)	4.982 ± 0.133	4.222 ± 0.052	4.780 ± 0.060	4.5/6.0
c_2(GeV^2)	0.542 ± 0.015	0.522 ± 0.006	0.615 ± 0.006	0.58/0.58
d_2	0.453 ± 0.009	0.452 ± 0.003	0.431 ± 0.004	0.45/0.47
χ^2/d.o.f.	5741/5786	6415/5785	7879/5786	

in the two-channel model, for the exponential, power-law, and the Orear-type parametrizations are shown in Fig. 18 (right).

The distributions of $d^3\sigma/dp_{1,\text{T}}dp_{2,\text{T}}dm$ as a function of m in several $(p_{1,\text{T}}, p_{2,\text{T}})$ bins are shown for $\pi^+\pi^-$ in Figs. 19–21. Measured values are shown together with the predictions of models using the tuned parameters for the exponential proton-pomeron form factors. The tuned models do not satisfactorily describe the regions with high $p_{1,\text{T}}$ and high $p_{2,\text{T}}$ combinations, whereas the empirical model is not able to describe data well at low transverse momenta.

The distributions of the squared momentum transfer of the virtual pion at invariant masses $1.8 < m_{\pi^+\pi^-} < 2.2$ GeV in several $(p_{1,\text{T}}, p_{2,\text{T}})$ bins are shown for $\pi^+\pi^-$ in Figs. 22–23. Measured values are shown together with the predictions of the empirical and the two-channel models using the tuned parameters for the exponential proton-pomeron form factors. Curves corresponding to DIME (model 1, "Dime 1") and its modification [labeled "Dime 1 (mod)"] with $b_{\text{exp}} = 0.9$ GeV^{-2} are also plotted.

VII. SUMMARY

We examined the central exclusive production of charged-hadron pairs in proton-proton collisions at a center-of-mass energy of 13 TeV. Events are selected by requiring both scattered protons to be detected in the TOTEM Roman pots and exactly two oppositely charged identified pions in the CMS silicon tracker. The process is studied in the resonance-free region, for invariant masses of the centrally produced two-pion system $m_{\pi^+\pi^-} < 0.7$ or $m_{\pi^+\pi^-} > 1.8$ GeV. Differential cross sections are measured as a function of the azimuthal angle between the surviving protons in a wide region of scattered proton transverse momenta, between 0.2 and 0.8 GeV, and for pion rapidities $|y| < 2$. A rich structure of nonperturbative interactions

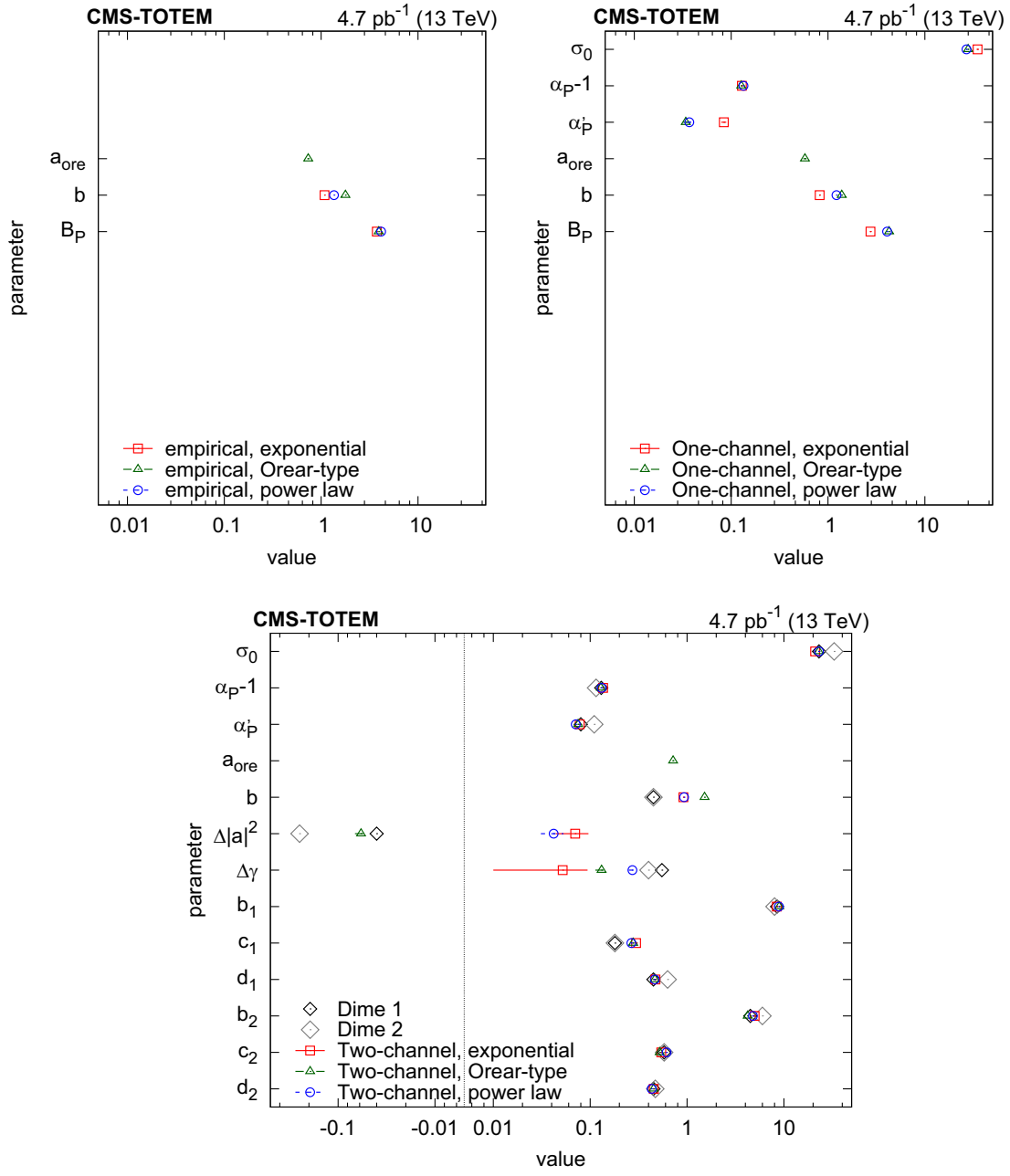

FIG. 13. Values of best parameters for the empirical (upper left), one-channel (upper right), and two-channel (lower) models with several choices of the proton-pomeron form factor (exponential, Orear-type, power law). In the case of the two-channel model, parameter values of models describing the elastic differential pp cross section from Ref. [29] are also indicated (DIME 1 and 2).

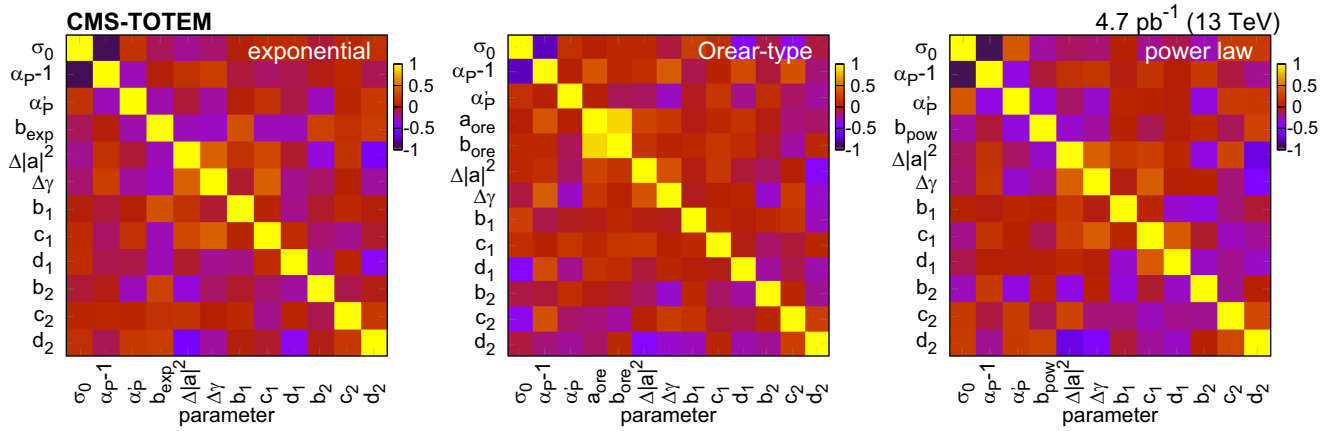

FIG. 14. Correlation coefficients among values of best parameters for the two-channel model, in the case of the exponential (left), Orear-type (center), and power-law (right) parametrizations of the proton-pomeron form factor.

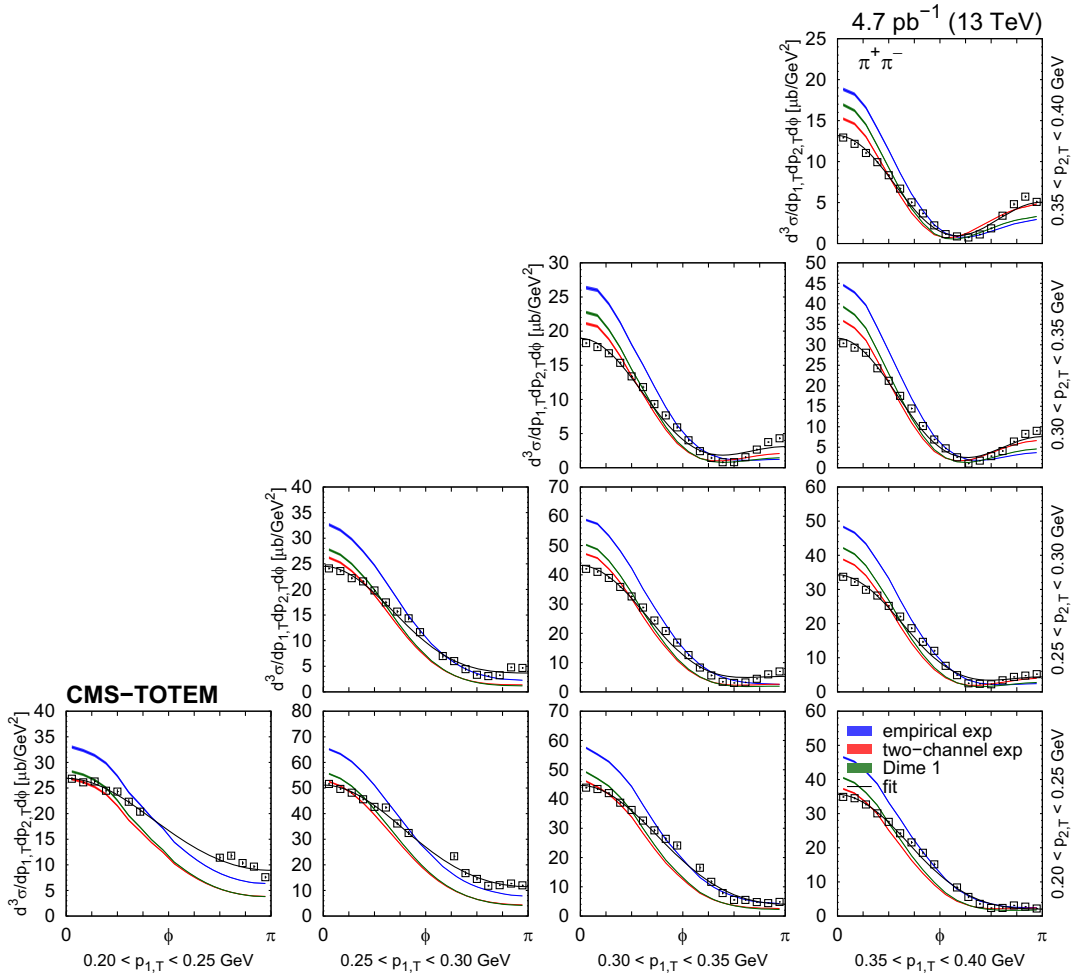

FIG. 15. Distribution of $d^3\sigma/dp_{1,\mathrm{T}}dp_{2,\mathrm{T}}d\phi$ as a function of ϕ in several $(p_{1,\mathrm{T}}, p_{2,\mathrm{T}})$ bins in the range $0.20 < p_{1,\mathrm{T}} < 0.40$ and $0.20 < p_{2,\mathrm{T}} < 0.60$ GeV, in units of $\mu\mathrm{b/GeV}^2$, for the mass range $0.35 < m_{\pi^+\pi^-} < 0.65$ GeV. Measured values (black symbols) are shown together with the predictions of the empirical and the two-channel models (colored curves) using the tuned parameters for the exponential proton-pomeron form factors (see text for details). Curves corresponding to DIME (model 1) are also plotted. Results of individual fits with the form $[A(R - \cos\phi)]^2 + c^2$ [Eq. (8)] are plotted with the curves. The error bars indicate the statistical uncertainties.

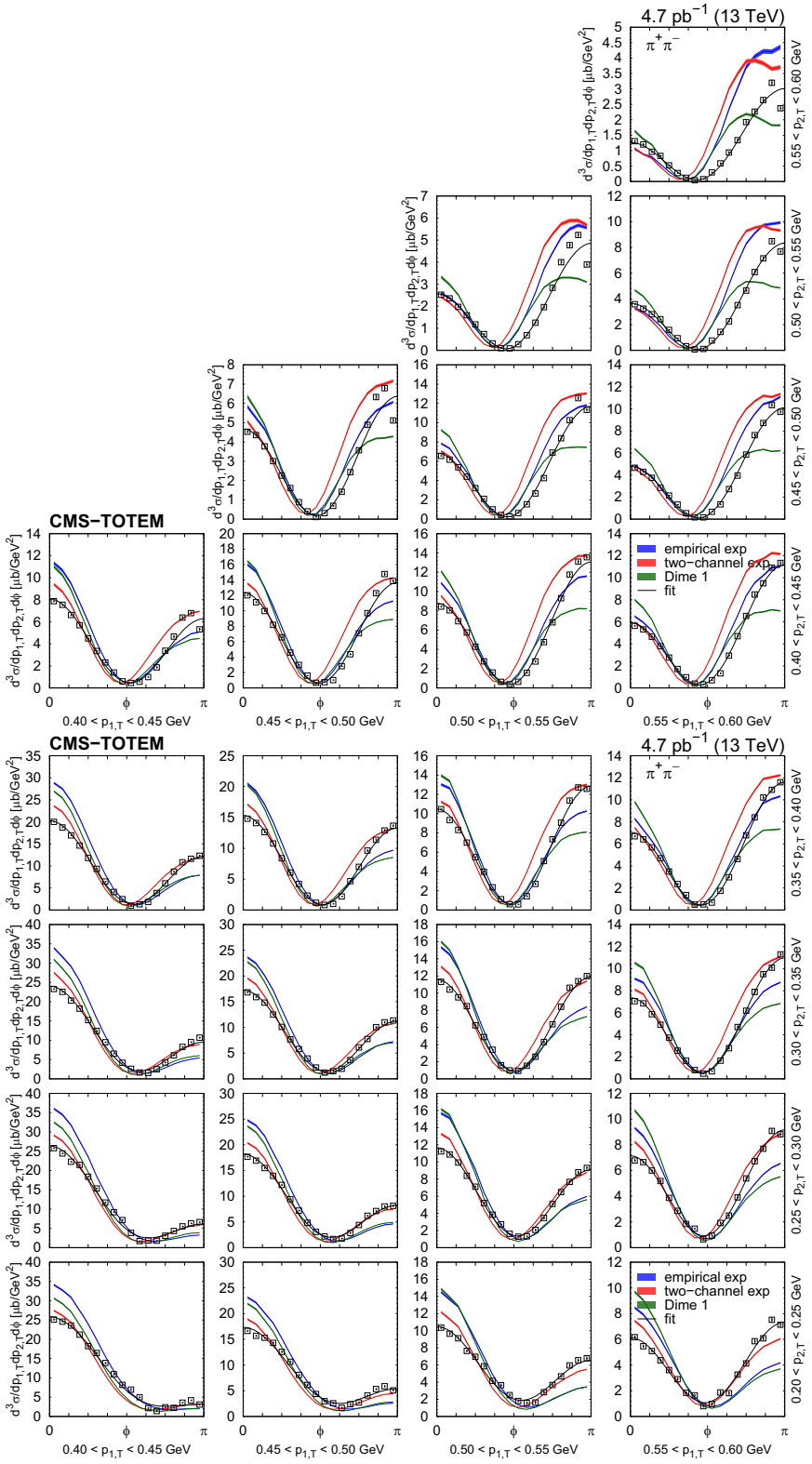

FIG. 16. Distribution of $d^3\sigma/dp_{1,\mathrm{T}}dp_{2,\mathrm{T}}d\phi$ as a function of ϕ in several $(p_{1,\mathrm{T}}, p_{2,\mathrm{T}})$ bins in the range $0.40 < p_{1,\mathrm{T}} < 0.60$ and $0.20 < p_{2,\mathrm{T}} < 0.60$ GeV, in units of μb/GeV^2, for the mass range $0.35 < m_{\pi^+\pi^-} < 0.65$ GeV. Measured values (black symbols) are shown together with the predictions of the empirical and the two-channel models (colored curves) using the tuned parameters for the exponential proton-pomeron form factors (see text for details). Curves corresponding to DIME (model 1) are also plotted. Results of individual fits with the form $[A(R - \cos\phi)]^2 + c^2$ [Eq. (8)] are plotted with the curves. The error bars indicate the statistical uncertainties.

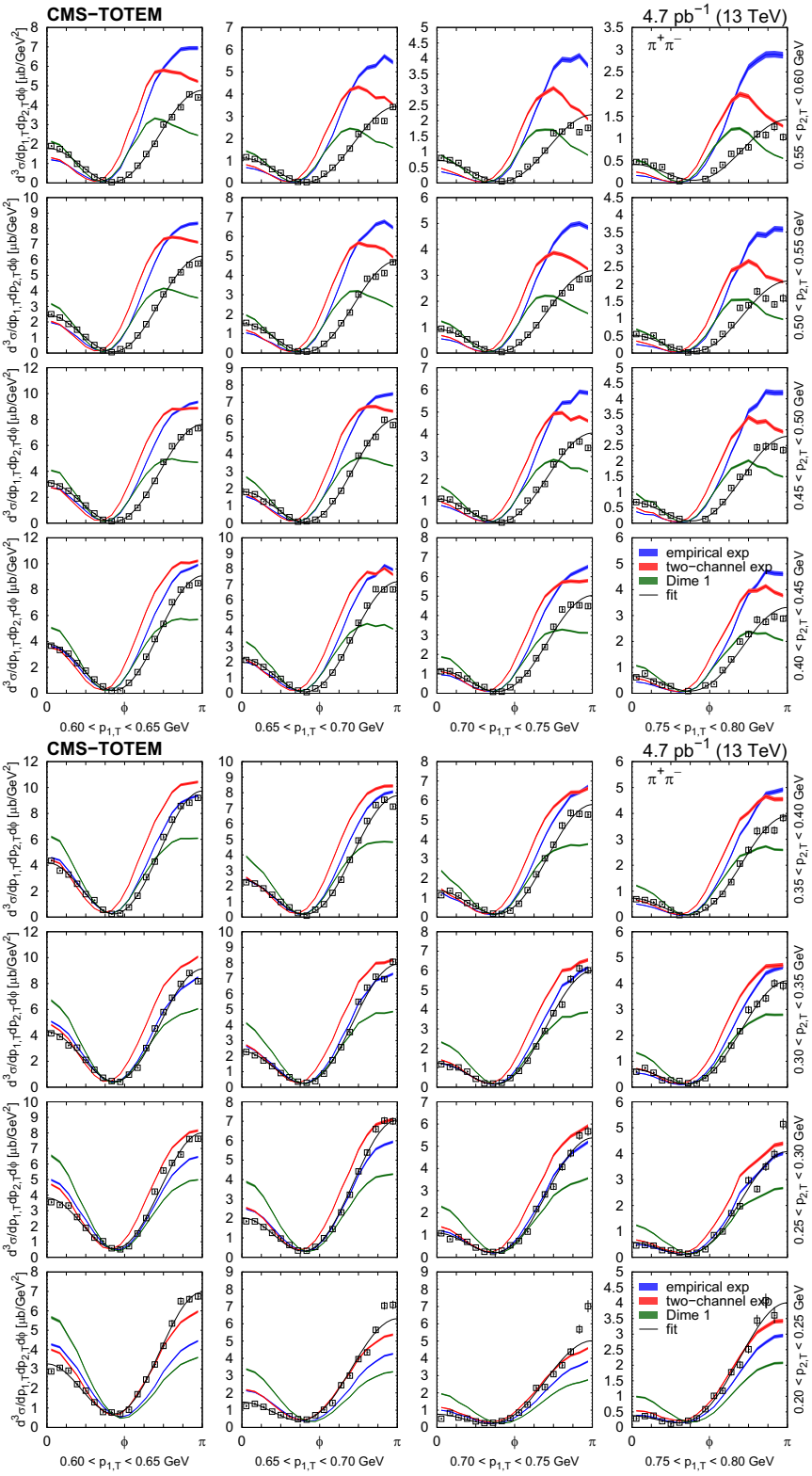

FIG. 17. Distribution of $d^3\sigma/dp_{1,\mathrm{T}}dp_{2,\mathrm{T}}d\phi$ as a function of ϕ in several $(p_{1,\mathrm{T}}, p_{2,\mathrm{T}})$ bins in the range $0.60 < p_{1,\mathrm{T}} < 0.80$ and $0.20 < p_{2,\mathrm{T}} < 0.60$ GeV, in units of μb/GeV^2, for the mass range $0.35 < m_{\pi^+\pi^-} < 0.65$ GeV. Measured values (black symbols) are shown together with the predictions of the empirical and the two-channel models (colored curves) using the tuned parameters for the exponential proton-pomeron form factors (see text for details). Curves corresponding to DIME (model 1) are also plotted. Results of individual fits with the form $[A(R - \cos\phi)]^2 + c^2$ [Eq. (8)] are plotted with the curves. The error bars indicate the statistical uncertainties.

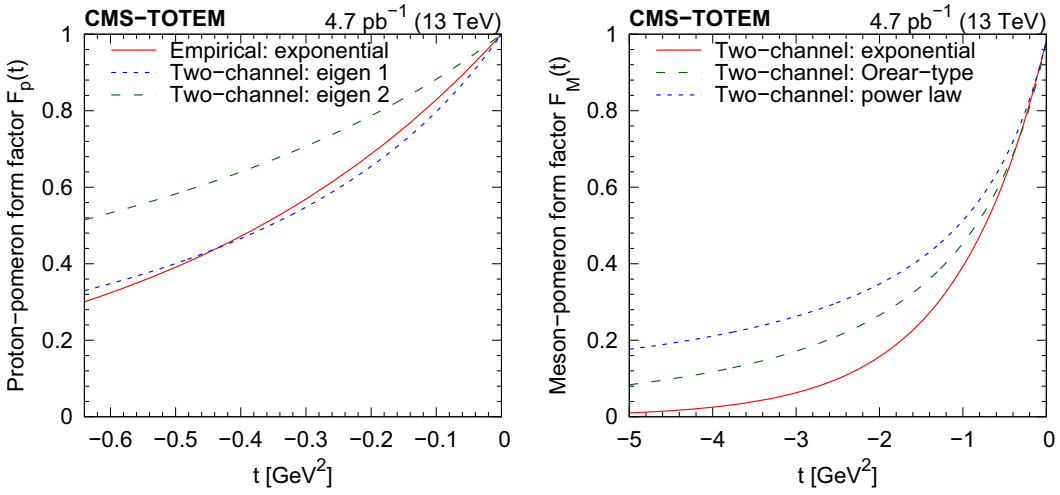

FIG. 18. Results of model tuning. Left: the plain exponential proton-pomeron form factor compared with those of the two diffractive proton eigenstates. Right: various options of the meson-pomeron form factor, shown for the exponential, Orear-type, and power-law parametrizations.

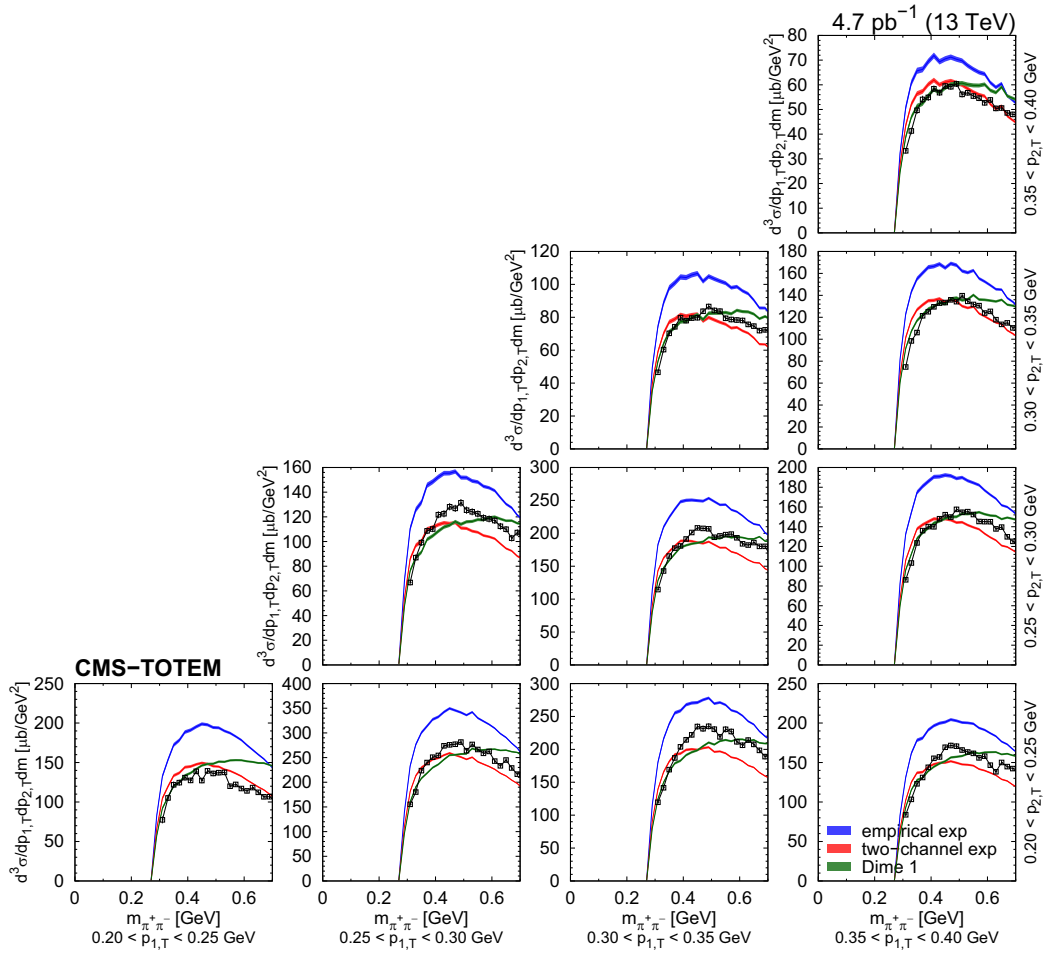

FIG. 19. Distribution of $d^3\sigma/dp_{1,\mathrm{T}}dp_{2,\mathrm{T}}dm$ as a function of m for $\pi^+\pi^-$ pairs in several $(p_{1,\mathrm{T}}, p_{2,\mathrm{T}})$ bins, in units of μb/GeV^3, for the mass range $0.35 < m_{\pi^+\pi^-} < 0.65$ GeV. Measured values (black symbols) are shown together with the predictions of the empirical and the two-channel models (colored curves) using the tuned parameters for the exponential proton-pomeron form factors (see text for details). Curves corresponding to DIME (model 1) are also plotted. The error bars indicate the statistical uncertainties. Lines connecting the data points are drawn to guide the eye.

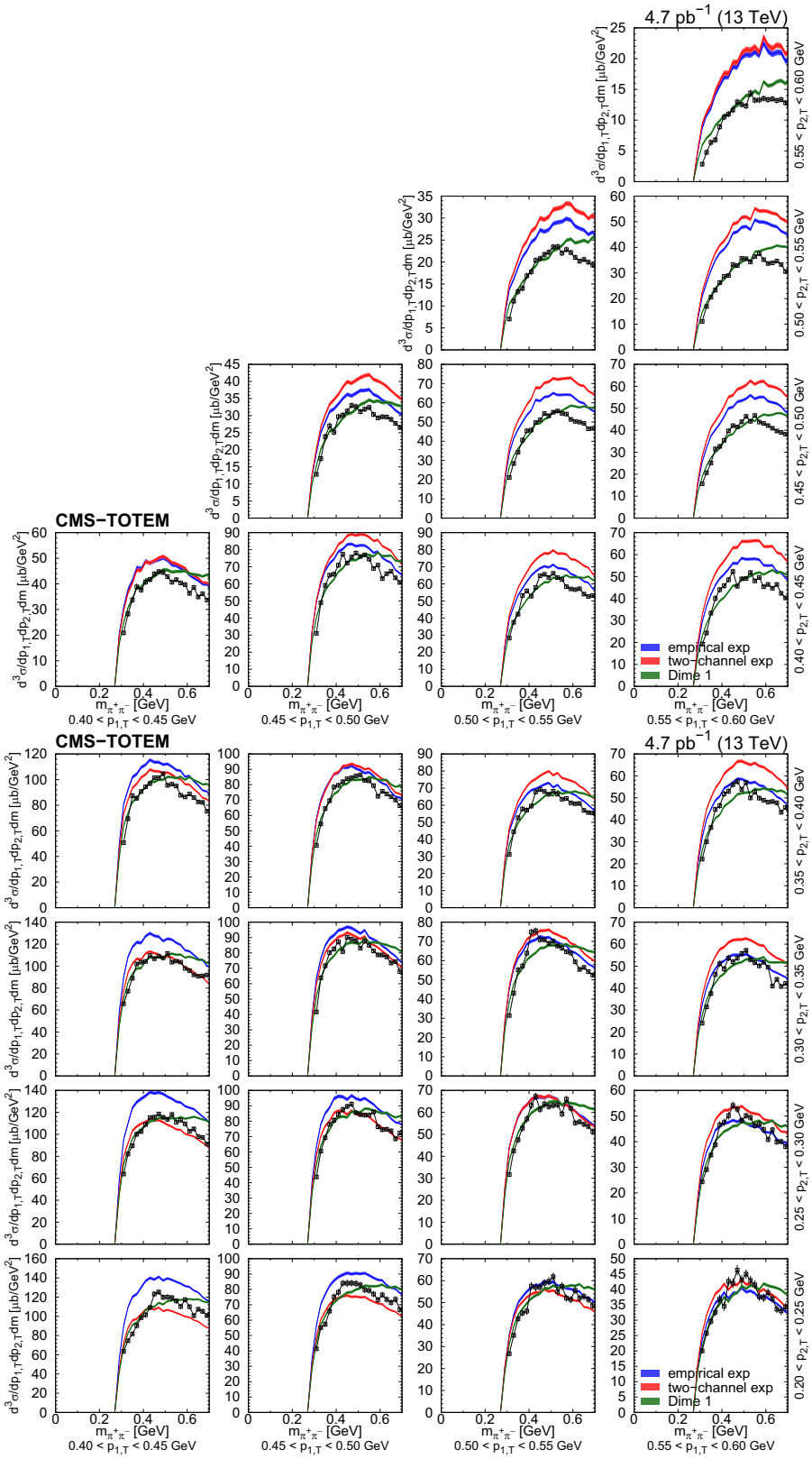

FIG. 20. Distribution of $d^3\sigma/dp_{1,T}dp_{2,T}dm$ as a function of m for $\pi^+\pi^-$ pairs in several $(p_{1,T}, p_{2,T})$ bins, in units of μb/GeV^3, for the mass range $0.35 < m_{\pi^+\pi^-} < 0.65$ GeV. Measured values (black symbols) are shown together with the predictions of the empirical and the two-channel models (colored curves) using the tuned parameters for the exponential proton-pomeron form factors (see text for details). Curves corresponding to DIME (model 1) are also plotted. The error bars indicate the statistical uncertainties. Lines connecting the data points are drawn to guide the eye.

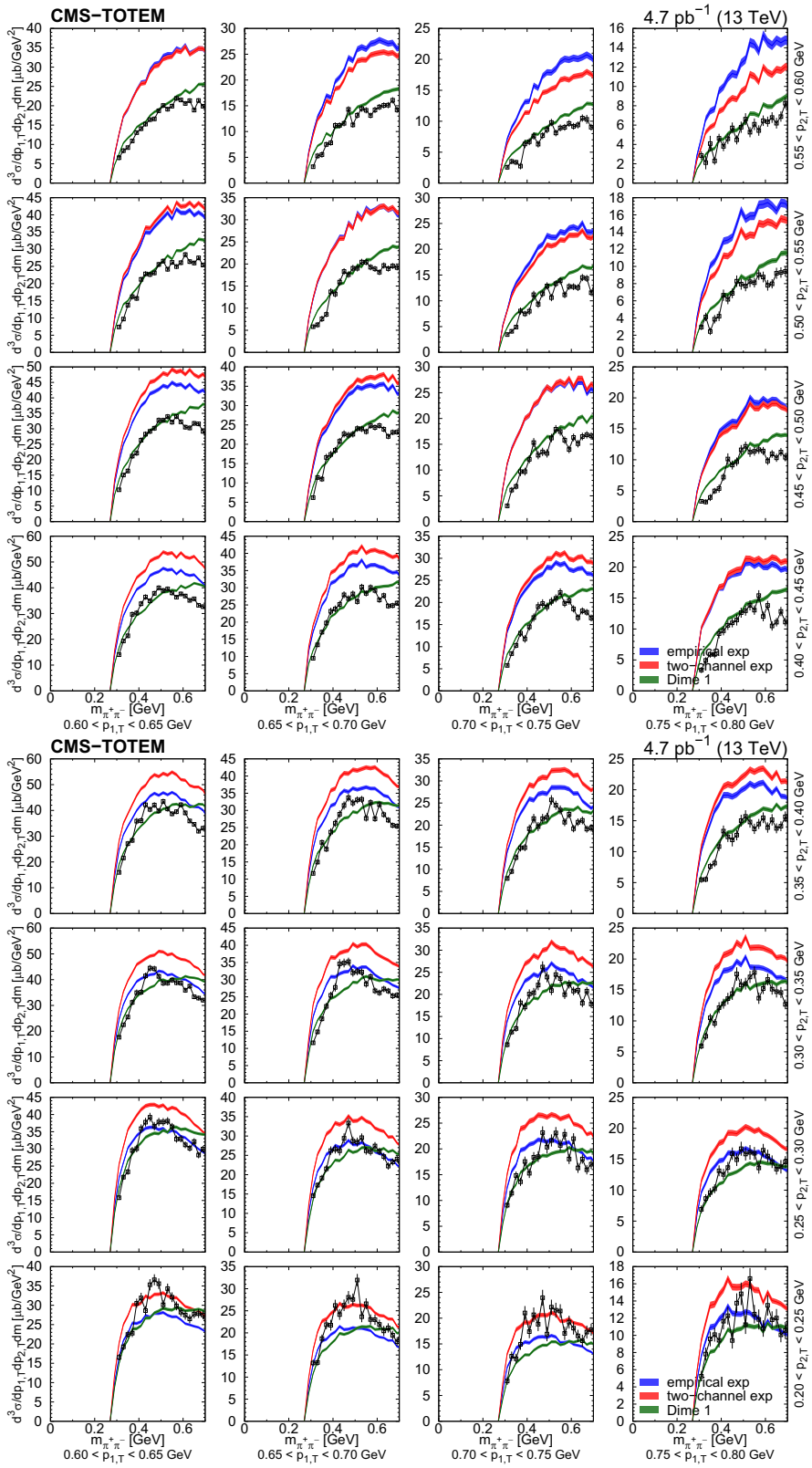

FIG. 21. Distribution of $d^3\sigma/dp_{1,\mathrm{T}}dp_{2,\mathrm{T}}dm$ as a function of m for $\pi^+\pi^-$ pairs in several $(p_{1,\mathrm{T}}, p_{2,\mathrm{T}})$ bins, in units of μb/GeV^3, for the mass range $0.35 < m_{\pi^+\pi^-} < 0.65$ GeV. Measured values (black symbols) are shown together with the predictions of the empirical and the two-channel models (colored curves) using the tuned parameters for the exponential proton-pomeron form factors (see text for details). Curves corresponding to DIME (model 1) are also plotted. The error bars indicate the statistical uncertainties. Lines connecting the data points are drawn to guide the eye.

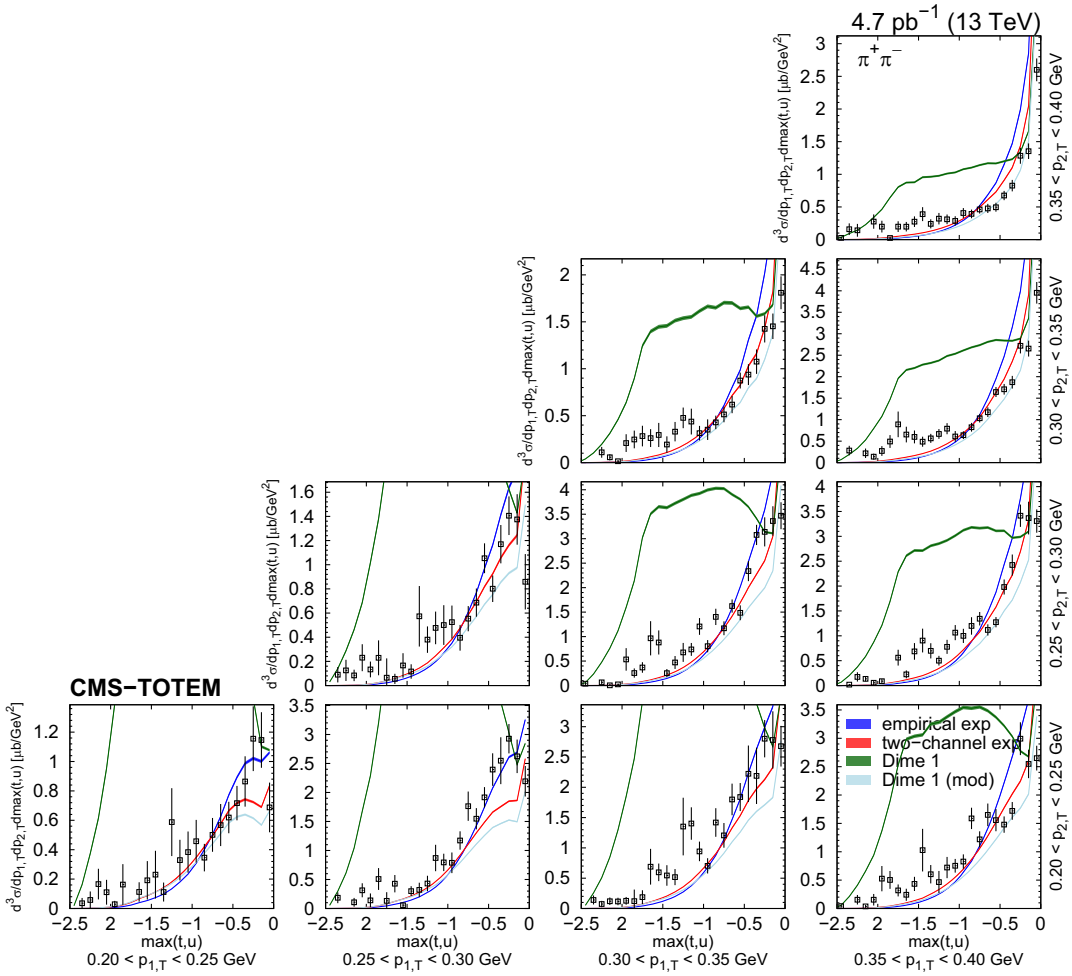

FIG. 22. Distribution of the squared momentum transfer of the virtual pion in several $(p_{1,T}, p_{2,T})$ bins, in units of μb/GeV^3, for the mass range $1.8 < m_{\pi^+\pi^-} < 2.2$ GeV. Measured values (black symbols) are shown together with the predictions of the empirical and the two-channel models (colored curves) using the tuned parameters for the exponential proton-pomeron form factors (see text for details). Curves corresponding to DIME (model 1, Dime 1) and its modification [labeled Dime 1 (mod)] with $b_{\text{exp}} = 0.9$ GeV^{-2} are also plotted. The error bars indicate the statistical uncertainties.

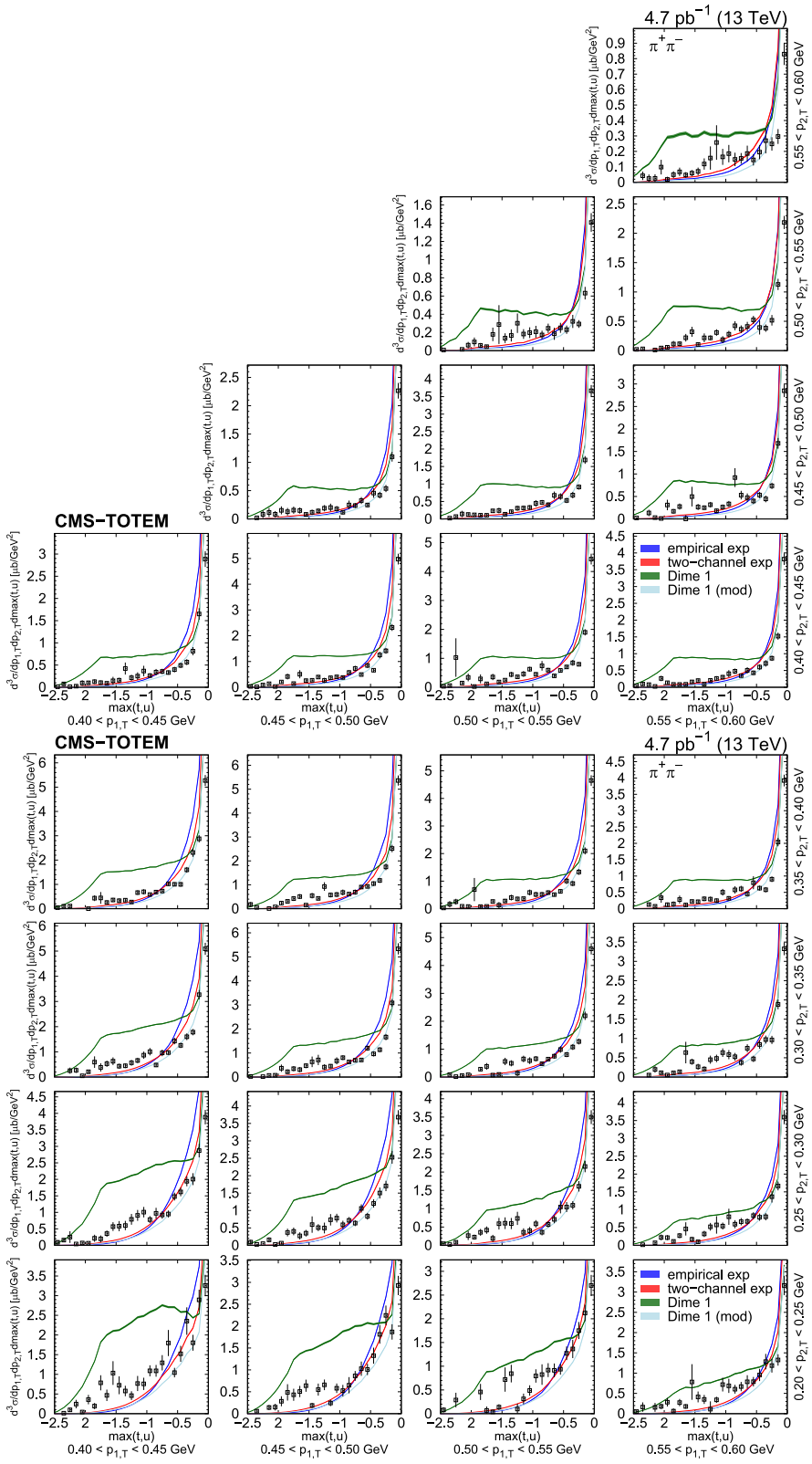

FIG. 23. Distribution of the squared momentum transfer of the virtual pion in several $(p_{1,T}, p_{2,T})$ bins, in units of μb/GeV^3, for the mass range $1.8 < m_{\pi^+\pi^-} < 2.2$ GeV. Measured values (black symbols) are shown together with the predictions of the empirical and the two-channel models (colored curves) using the tuned parameters for the exponential proton-pomeron form factors (see text for details). Curves corresponding to DIME (model 1, Dime 1) and its modification [labeled Dime 1 (mod)] with $b_{\rm exp} = 0.9$ GeV^{-2} are also plotted. The error bars indicate the statistical uncertainties.

related to double-pomeron exchange emerges and is measured with good precision. The parabolic minimum in the distribution of the two-proton azimuthal angle is observed for the first time. It can be understood as an effect of additional pomeron exchanges between the incoming protons, resulting from the interference of the bare and the rescattered amplitudes. With model tuning, various physical quantities related to the pomeron cross section, proton-pomeron, and meson-pomeron form factors, pomeron trajectory and intercept, as well as coefficients of diffractive eigenstates of the proton are determined.

ACKNOWLEDGMENTS

We congratulate our colleagues in the CERN accelerator departments for the excellent performance of the LHC and thank the technical and administrative staffs at CERN and at other CMS sand TOTEM institutes for their contributions to the success of the common CMS-TOTEM effort. In addition, we gratefully acknowledge the computing centers and personnel of the Worldwide LHC Computing Grid and other centers for delivering so effectively the computing infrastructure essential to our analyses. Finally, we acknowledge the enduring support for the construction and operation of the LHC, the CMS and TOTEM detectors, and the supporting computing infrastructure provided by the following funding agencies: SC (Armenia), BMBWF and FWF (Austria); FNRS and FWO (Belgium); CNPq, CAPES, FAPERJ, FAPERGS, and FAPESP (Brazil); MES and BNSF (Bulgaria); CERN; CAS, MoST, and NSFC (China); MINCIENCIAS (Colombia); MSES and CSF (Croatia); RIF (Cyprus); SENESCYT (Ecuador); MoER, ERC PUT, and ERDF (Estonia); Academy of Finland, Magnus Ehrnrooth Foundation, MEC, HIP, and Waldemar von Frenckell Foundation (Finland); CEA and CNRS/IN2P3 (France); SRNSF (Georgia); BMBF, DFG, and HGF (Germany); GSRI (Greece); NKFIH (Hungary); DAE and DST (India); IPM (Iran); SFI (Ireland); INFN (Italy); MSIP and NRF (Republic of Korea); MES (Latvia); LAS (Lithuania); MOE and UM (Malaysia); BUAP, CINVESTAV, CONACYT, LNS, SEP, and UASLP-FAI (Mexico); MOS (Montenegro); MBIE (New Zealand); PAEC (Pakistan); MES and NSC (Poland); FCT (Portugal); MESTD (Serbia); MCIN/AEI and PCTI (Spain); MOSTR (Sri Lanka); Swiss Funding Agencies (Switzerland); MST (Taipei); MHESI and NSTDA (Thailand); TUBITAK and TENMAK (Turkey); NASU (Ukraine); STFC (United Kingdom); DOE and NSF (U.S.). Individuals have received support from the Marie-Curie program and the European Research Council and Horizon 2020 Grant, Contracts No. 675440, No. 724704, No. 752730, No. 758316, No. 765710, No. 824093, and COST Action CA16108 (European Union); the Leventis Foundation; the Alfred P. Sloan Foundation; the Alexander von Humboldt Foundation; the Science Committee, Project No. 22rl-037 (Armenia); the Belgian Federal Science Policy Office; the Fonds pour la Formation *à la* Recherche dans l'Industrie et dans l'Agriculture (FRIA-Belgium); the Agentschap voor Innovatie door Wetenschap en Technologie (IWT-Belgium); the F. R. S.-FNRS and FWO (Belgium) under the "Excellence of Science—EOS"—be.h Project No. 30820817; the Beijing Municipal Science and Technology Commission, No. Z191100007219010 and Fundamental Research Funds for the Central Universities (China); the Ministry of Education, Youth and Sports (MEYS) of the Czech Republic; the Shota Rustaveli National Science Foundation, Grant No. FR-22-985 (Georgia); the Deutsche Forschungsgemeinschaft (DFG), under Germany's Excellence Strategy—EXC 2121 "Quantum Universe"—390833306, and under Project No. 400140256—GRK2497; the Hellenic Foundation for Research and Innovation (HFRI), Project No. 2288 (Greece); the Hungarian Academy of Sciences, the New National Excellence Program—ÚNKP, the NKFIH research Grants No. K 124845, No. K 124850, No. K 128713, No. K 128786, No. K 129058, No. K 131991, No. K 133046, No. K 138136, No. K 143460, No. K 143477, No. K 146913, No. K 146914, No. K 147048, No. 2020-2.2.1-ED-2021-00181, and No. TKP2021-NKTA-64 (Hungary); the Council of Science and Industrial Research, India; ICSC—National Research Centre for High Performance Computing, Big Data and Quantum Computing, funded by the NextGenerationEU program (Italy); the Latvian Council of Science; the Ministry of Education and Science, Project No. 2022/WK/14, and the National Science Center, Contracts Opus No. 2021/41/B/ST2/01369 and No. 2021/43/B/ST2/01552 (Poland); the Fundação para a Ciência e a Tecnologia, Grant No. CEECIND/01334/2018 (Portugal); the National Priorities Research Program by Qatar National Research Fund; MCIN/AEI/10.13039/501100011033, ERDF "a way of making Europe," and the Programa Estatal de Fomento de la Investigación Científica y Técnica de Excelencia María de Maeztu, Grant No. MDM-2017-0765 and Programa Severo Ochoa del Principado de Asturias (Spain); the Chulalongkorn Academic into Its 2nd Century Project Advancement Project and the National Science, Research, and Innovation Fund via the Program Management Unit for Human Resources and Institutional Development, Research, and Innovation, Grant No. B37G660013 (Thailand); the Kavli Foundation; the Nvidia Corporation; the SuperMicro Corporation; the Welch Foundation, Contract No. C-1845; and the Weston Havens Foundation (U.S.).

[1] R. L. Workman *et al.* (Particle Data Group), Review of particle physics, Prog. Theor. Exp. Phys. **2022**, 083C01 (2022).

[2] V. B. Berestetsky and I. Y. Pomeranchuk, On the asymptotic behaviour of cross sections at high energies, Nucl. Phys. **22**, 629 (1961).

[3] S. Donnachie, H. G. Dosch, O. Nachtmann, and P. Landshoff, *Pomeron Physics and QCD* (Cambridge University Press, Cambridge, England, 2004), Vol. 19.

[4] D. Amati, A. Stanghellini, and S. Fubini, Theory of high-energy scattering and multiple production, Nuovo Cimemto **26**, 896 (1962).

[5] H. B. Meyer and M. J. Teper, Glueball Regge trajectories and the pomeron: A lattice study, Phys. Lett. B **605**, 344 (2005).

[6] D0 and TOTEM Collaborations, Odderon exchange from elastic scattering differences between pp and $p\bar{p}$ data at 1.96 TeV and from pp forward scattering measurements, Phys. Rev. Lett. **127**, 062003 (2021).

[7] V. A. Khoze, A. D. Martin, and M. G. Ryskin, Prospects for new physics observations in diffractive processes at the LHC and Tevatron, Eur. Phys. J. C **23**, 311 (2002).

[8] M. G. Albrow, T. D. Coughlin, and J. R. Forshaw, Central exclusive particle production at high energy hadron colliders, Prog. Part. Nucl. Phys. **65**, 149 (2010).

[9] P. Lebiedowicz and A. Szczurek, Exclusive $pp \to pp\pi^+\pi^-$ reaction: From the threshold to LHC, Phys. Rev. D **81**, 036003 (2010).

[10] W. Ochs, The status of glueballs, J. Phys. G **40**, 043001 (2013).

[11] T. A. Armstrong *et al.* (WA76 Collaboration), Study of the centrally produced $\pi\pi$ and $K\bar{K}$ systems at 85 and 300 GeV/c, Z. Phys. C **51**, 351 (1991).

[12] F. Antinori *et al.* (WA91 Collaboration), A further study of the centrally produced $\pi^+\pi^-$ and $\pi^+\pi^-\pi^+\pi^-$ channels in pp interactions at 300 and 450 GeV/c, Phys. Lett. B **353**, 5894 (1995).

[13] F. E. Close and G. A. Schuler, Evidence that the pomeron transforms as a non-conserved vector current, Phys. Lett. B **464**, 279 (1999).

[14] D. Barberis *et al.* (WA102 Collaboration), Experimental evidence for a vector-like behavior of pomeron exchange, Phys. Lett. B **467**, 165 (1999).

[15] F. E. Close, A. Kirk, and G. Schuler, Dynamics of glueball and $q\bar{q}$ production in the central region of pp collisions, Phys. Lett. B **477**, 13 (2000).

[16] A. Kirk, Resonance production in central pp collisions at the CERN Omega spectrometer, Phys. Lett. B **489**, 29 (2000).

[17] T. A. Aaltonen *et al.* (CDF Collaboration), Measurement of central exclusive $\pi^+\pi^-$ production in $p\bar{p}$ collisions at $\sqrt{s} =$ 0.9 and 1.96 TeV at CDF, Phys. Rev. D **91**, 091101 (2015).

[18] J. Adam *et al.* (STAR Collaboration), Measurement of the central exclusive production of charged particle pairs in proton-proton collisions at $\sqrt{s} = 200$ GeV with the STAR detector at RHIC, J. High Energy Phys. 07 (2020) 178.

[19] ATLAS Collaboration, Measurement of exclusive pion pair production in proton–proton collisions at $\sqrt{s} = 7$ TeV with the ATLAS detector, Eur. Phys. J. C **83**, 627 (2023).

[20] CMS Collaboration, Study of central exclusive $\pi^+\pi^-$ production in proton-proton collisions at $\sqrt{s} = 5.02$ and 13 TeV, Eur. Phys. J. C **80**, 718 (2020).

[21] P. Lebiedowicz and A. Szczurek, Revised model of absorption corrections for the $pp \to pp\pi^+\pi^-$ process, Phys. Rev. D **92**, 054001 (2015).

[22] P. Lebiedowicz, O. Nachtmann, and A. Szczurek, Central exclusive diffractive production of $\pi^+\pi^-$ continuum, scalar and tensor resonances in pp and $p\bar{p}$ scattering within tensor Pomeron approach, Phys. Rev. D **93**, 054015 (2016).

[23] R. A. Ryutin, Central exclusive diffractive production of two pions from continuum and resonance decay in the Regge-eikonal model, Eur. Phys. J. C **83**, 172 (2023).

[24] P. Lebiedowicz, O. Nachtmann, and A. Szczurek, Towards a complete study of central exclusive production of K^+K^- pairs in proton-proton collisions within the tensor Pomeron approach, Phys. Rev. D **98**, 014001 (2018).

[25] P. Lebiedowicz, O. Nachtmann, and A. Szczurek, Central exclusive diffractive production of $p\bar{p}$ pairs in proton-proton collisions at high energies, Phys. Rev. D **97**, 094027 (2018).

[26] R. A. Ryutin, Central exclusive diffractive $p\bar{p}$ production in the Regge-eikonal model in the "scalar" proton approximation, Eur. Phys. J. C **83**, 647 (2023).

[27] M. G. Ryskin, A. D. Martin, and V. A. Khoze, Proton opacity in the light of LHC diffractive data, Eur. Phys. J. C **72**, 1937 (2012).

[28] L. A. Harland-Lang, V. A. Khoze, M. G. Ryskin, and W. J. Stirling, The phenomenology of central exclusive production at hadron colliders, Eur. Phys. J. C **72**, 2110 (2012).

[29] V. A. Khoze, A. D. Martin, and M. G. Ryskin, Diffraction at the LHC, Eur. Phys. J. C **73**, 2503 (2013).

[30] L. A. Harland-Lang, V. A. Khoze, and M. G. Ryskin, Modelling exclusive meson pair production at hadron colliders, Eur. Phys. J. C **74**, 2848 (2014).

[31] A. Grau, S. Pacetti, G. Pancheri, and Y. N. Srivastava, Checks of asymptotia in pp elastic scattering at LHC, Phys. Lett. B **714**, 70 (2012).

[32] D. A. Fagundes, G. Pancheri, A. Grau, S. Pacetti, and Y. N. Srivastava, Elastic pp scattering from the optical point to past the dip: An empirical parametrization from ISR to the LHC, Phys. Rev. D **88**, 094019 (2013).

[33] L. Lukaszuk and B. Nicolescu, A possible interpretation of pp rising total cross sections, Lett. Nuovo Cimento **8**, 405 (1973).

[34] A. Donnachie and P. V. Landshoff, Total cross sections, Phys. Lett. B **296**, 227 (1992).

[35] J. R. Cudell, V. V. Ezhela, P. Gauron, K. Kang, Y. V. Kuyanov, S. B. Lugovsky, B. Nicolescu, and N. P. Tkachenko, Hadronic scattering amplitudes: Medium-energy constraints on asymptotic behavior, Phys. Rev. D **65**, 074024 (2002).

[36] J. Orear, Transverse momentum distribution of protons in $p - p$ elastic scattering, Phys. Rev. Lett. **12**, 112 (1964).

[37] CMS Collaboration, Track impact parameter resolution for the full pseudorapidity coverage in the 2017 dataset with the CMS phase-1 pixel detector, CMS Detector Performance Note CMS-DP-2020-049, 2020, https://cds.cern.ch/record/2743740.

[38] CMS Collaboration, The CMS experiment at the CERN LHC, J. Instrum. **3**, S08004 (2008).
[39] G. Anelli *et al.* (TOTEM Collaboration), The TOTEM experiment at the CERN Large Hadron Collider, J. Instrum. **3**, S08007 (2008).
[40] G. Antchev *et al.* (TOTEM Collaboration), Performance of the TOTEM detectors at the LHC, Int. J. Mod. Phys. A **28**, 1330046 (2013).
[41] S. Agostinelli *et al.* (GEANT4 Collaboration), GEANT4—a simulation toolkit, Nucl. Instrum. Methods Phys. Res., Sect. A **506**, 250 (2003).
[42] K. Gottfried and J. D. Jackson, On the connection between production mechanism and decay of resonances at high-energies, Nuovo Cimento **33**, 309 (1964).
[43] H. Wiedemann, *Particle Accelerator Physics: Basic Principles and Linear Beam Dynamics* (Springer, Berlin, Heidelberg, 2013).
[44] CMS Collaboration, The CMS trigger system, J. Instrum. **12**, P01020 (2017).
[45] ATLAS Collaboration, Measurement of the inelastic proton-proton cross section at $\sqrt{s} = 13$ TeV with the ATLAS detector at the LHC, Phys. Rev. Lett. **117**, 182002 (2016).
[46] CMS Collaboration, Measurement of the inelastic proton-proton cross section at $\sqrt{s} = 13$ TeV, J. High Energy Phys. 07 (2018) 161.
[47] LHCb Collaboration, Measurement of the inelastic pp cross-section at a centre-of-mass energy of 13 TeV, J. High Energy Phys. 06 (2018) 100.
[48] G. Antchev *et al.* (TOTEM Collaboration), First measurement of elastic, inelastic and total cross-section at $\sqrt{s} =$ 13 TeV by TOTEM and overview of cross-section data at LHC energies, Eur. Phys. J. C **79**, 103 (2019).
[49] CMS and TOTEM Collaborations, Proton reconstruction using the TOTEM Roman pot detectors during the high-β^* data taking period (to be published).
[50] CMS Collaboration, Description and performance of track and primary-vertex reconstruction with the CMS tracker, J. Instrum. **9**, P10009 (2014).
[51] CMS Collaboration, Measurement of charged pion, kaon, and proton production in proton-proton collisions at $\sqrt{s} = 13$ TeV, Phys. Rev. D **96**, 112003 (2017).
[52] R. M. Sternheimer, M. J. Berger, and S. M. Seltzer, Density effect for the ionization loss of charged particles in various substances, At. Data Nucl. Data Tables **30**, 261 (1984).
[53] P. C. Mahalanobis, On the generalized distance in statistics, in *Proceedings of the National Institute of Sciences of India* (Institute of Science of India, 1936), Vol. 2, p. 49.
[54] HEPData record for this analysis (2023), 10.17182/hepdata.145998.
[55] CMS Collaboration, CMS luminosity measurement for the 2018 data-taking period at $\sqrt{s} = 13$ TeV, CMS Physics Analysis Summary, Report No. CMS-PAS-LUM-18-002, 2018, https://cds.cern.ch/record/2676164.
[56] CMS Collaboration, Measurements of inclusive W and Z cross sections in pp collisions at $\sqrt{s} = 7$ TeV, J. High Energy Phys. 01 (2011) 080.
[57] CMS Collaboration, Measurement of tracking efficiency, CMS Physics Analysis Summary, Report No. CMS-PAS-TRK-10-002, 2010, https://cds.cern.ch/record/1279139.
[58] L. A. Harland-Lang, V. A. Khoze, and M. G. Ryskin, Exclusive physics at the LHC with SuperChic2, Eur. Phys. J. C **76**, 9 (2016).
[59] R. A. Kycia, J. Chwastowski, R. Staszewski, and J. Turnau, GenEx: A simple generator structure for exclusive processes in high energy collisions, Commun. Comput. Phys. **24**, 860 (2018).
[60] M. Mieskolainen, GRANIITTI: A Monte Carlo event generator for high energy diffraction, arXiv:1910.06300.
[61] G. Antchev *et al.* (TOTEM Collaboration), First determination of the ρ parameter at $\sqrt{s} = 13$ TeV: Probing the existence of a colourless C-odd three-gluon compound state, Eur. Phys. J. C **79**, 785 (2019).
[62] G. Antchev *et al.* (TOTEM Collaboration), Elastic differential cross section measurement at $\sqrt{s} = 13$ TeV by TOTEM, Eur. Phys. J. C **79**, 861 (2019).
[63] V. A. Khoze, A. D. Martin, and M. G. Ryskin, t dependence of the slope of the high energy elastic pp cross section, J. Phys. G **42**, 025003 (2015).
[64] A. Buckley, H. Hoeth, H. Lacker, H. Schulz, and J. E. von Seggern, Systematic event generator tuning for the LHC, Eur. Phys. J. C **65**, 331 (2010).

A. Hayrapetyan,[1,†] A. Tumasyan,[1,b,†] W. Adam,[2,†] J. W. Andrejkovic,[2,†] T. Bergauer,[2,†] S. Chatterjee,[2,†] K. Damanakis,[2,†] M. Dragicevic,[2,†] P. S. Hussain,[2,†] M. Jeitler,[2,c,†] N. Krammer,[2,†] A. Li,[2,†] D. Liko,[2,†] I. Mikulec,[2,†] J. Schieck,[2,c,†] R. Schöfbeck,[2,†] D. Schwarz,[2,†] M. Sonawane,[2,†] S. Templ,[2,†] W. Waltenberger,[2,†] C.-E. Wulz,[2,c,†] M. R. Darwish,[3,d,†] T. Janssen,[3,†] P. Van Mechelen,[3,†] E. S. Bols,[4,†] J. D'Hondt,[4,†] S. Dansana,[4,†] A. De Moor,[4,†] M. Delcourt,[4,†] H. El Faham,[4,†] S. Lowette,[4,†] I. Makarenko,[4,†] D. Müller,[4,†] A. R. Sahasransu,[4,†] S. Tavernier,[4,†] M. Tytgat,[4,e,†] G. P. Van Onsem,[4,†] S. Van Putte,[4,†] D. Vannerom,[4,†] B. Clerbaux,[5,†] A. K. Das,[5,†] G. De Lentdecker,[5,†] L. Favart,[5,†] P. Gianneios,[5,†] D. Hohov,[5,†] J. Jaramillo,[5,†] A. Khalilzadeh,[5,†] K. Lee,[5,†] M. Mahdavikhorrami,[5,†] A. Malara,[5,†] S. Paredes,[5,†] L. Pétré,[5,†] N. Postiau,[5,†] L. Thomas,[5,†] M. Vanden Bemden,[5,†] C. Vander Velde,[5,†] P. Vanlaer,[5,†] M. De Coen,[6,†] D. Dobur,[6,†] Y. Hong,[6,†] J. Knolle,[6,†] L. Lambrecht,[6,†] G. Mestdach,[6,†] K. Mota Amarilo,[6,†] C. Rendón,[6,†] A. Samalan,[6,†] K. Skovpen,[6,†] N. Van Den Bossche,[6,†] J. van der Linden,[6,†] L. Wezenbeek,[6,†] A. Benecke,[7,†] A. Bethani,[7,†] G. Bruno,[7,†] C. Caputo,[7,†] C. Delaere,[7,†] I. S. Donertas,[7,†] A. Giammanco,[7,†] K. Jaffel,[7,†] Sa. Jain,[7,†] V. Lemaitre,[7,†]

J. Lidrych,[7,†] P. Mastrapasqua,[7,†] K. Mondal,[7,†] T. T. Tran,[7,†] S. Wertz,[7,†] G. A. Alves,[8,†] E. Coelho,[8,†] C. Hensel,[8,†] T. Menezes De Oliveira,[8,†] A. Moraes,[8,†] P. Rebello Teles,[8,†] M. Soeiro,[8,†] W. L. Aldá Júnior,[9,†] M. Alves Gallo Pereira,[9,†] M. Barroso Ferreira Filho,[9,†] H. Brandao Malbouisson,[9,†] W. Carvalho,[9,†] J. Chinellato,[9,f,†] E. M. Da Costa,[9,†] G. G. Da Silveira,[9,g,†] D. De Jesus Damiao,[9,†] S. Fonseca De Souza,[9,†] R. Gomes De Souza,[9,†] J. Martins,[9,h,†] C. Mora Herrera,[9,†] L. Mundim,[9,†] H. Nogima,[9,†] J. P. Pinheiro,[9,†] A. Santoro,[9,†] A. Sznajder,[9,†] M. Thiel,[9,†] A. Vilela Pereira,[9,†] C. A. Bernardes,[10,g,†] L. Calligaris,[10,†] T. R. Fernandez Perez Tomei,[10,†] E. M. Gregores,[10,†] P. G. Mercadante,[10,†] S. F. Novaes,[10,†] B. Orzari,[10,†] Sandra S. Padula,[10,†] A. Aleksandrov,[11,†] R. Hadjiiska,[11,†] P. Iaydjiev,[11,†] M. Misheva,[11,†] M. Shopova,[11,†] G. Sultanov,[11,†] A. Dimitrov,[12,†] L. Litov,[12,†] B. Pavlov,[12,†] P. Petkov,[12,†] A. Petrov,[12,†] E. Shumka,[12,†] S. Keshri,[13,†] S. Thakur,[13,†] T. Cheng,[14,†] Q. Guo,[14,†] T. Javaid,[14,†] L. Yuan,[14,†] Z. Hu,[15,†] J. Liu,[15,†] K. Yi,[15,i,j,†] G. M. Chen,[16,k,†] H. S. Chen,[16,k,†] M. Chen,[16,k,†] F. Iemmi,[16,†] C. H. Jiang,[16,†] A. Kapoor,[16,l,†] H. Liao,[16,†] Z.-A. Liu,[16,m,†] R. Sharma,[16,n,†] J. N. Song,[16,m,†] J. Tao,[16,†] C. Wang,[16,k,†] J. Wang,[16,†] Z. Wang,[16,k,†] H. Zhang,[16,†] A. Agapitos,[17,†] Y. Ban,[17,†] A. Levin,[17,†] C. Li,[17,†] Q. Li,[17,†] Y. Mao,[17,†] S. J. Qian,[17,†] X. Sun,[17,†] D. Wang,[17,†] H. Yang,[17,†] L. Zhang,[17,†] C. Zhou,[17,†] Z. You,[18,†] N. Lu,[19,†] G. Bauer,[20,o,†] X. Gao,[21,p,†] D. Leggat,[21,†] H. Okawa,[21,†] Z. Lin,[22,†] C. Lu,[22,†] M. Xiao,[22,†] C. Avila,[23,†] D. A. Barbosa Trujillo,[23,†] A. Cabrera,[23,†] C. Florez,[23,†] J. Fraga,[23,†] J. A. Reyes Vega,[23,†] J. Mejia Guisao,[24,†] F. Ramirez,[24,†] M. Rodriguez,[24,†] J. D. Ruiz Alvarez,[24,†] D. Giljanovic,[25,†] N. Godinovic,[25,†] D. Lelas,[25,†] A. Sculac,[25,†] M. Kovac,[26,†] T. Sculac,[26,q,†] P. Bargassa,[27,†] V. Brigljevic,[27,†] B. K. Chitroda,[27,†] D. Ferencek,[27,†] S. Mishra,[27,†] A. Starodumov,[27,r,†] T. Susa,[27,†] A. Attikis,[28,†] K. Christoforou,[28,†] S. Konstantinou,[28,†] J. Mousa,[28,†] C. Nicolaou,[28,†] F. Ptochos,[28,†] P. A. Razis,[28,†] H. Rykaczewski,[28,†] H. Saka,[28,†] A. Stepennov,[28,†] M. Finger,[29,†] M. Finger Jr.,[29,†] A. Kveton,[29,†] E. Ayala,[30,†] E. Carrera Jarrin,[31,†] H. Abdalla,[32,s,†] Y. Assran,[32,t,u,†] A. Lotfy,[33,†] M. A. Mahmoud,[33,†] K. Ehataht,[34,†] M. Kadastik,[34,†] T. Lange,[34,†] S. Nandan,[34,†] C. Nielsen,[34,†] J. Pata,[34,†] M. Raidal,[34,†] L. Tani,[34,†] C. Veelken,[34,†] H. Kirschenmann,[35,†] M. Voutilainen,[35,†] S. Bharthuar,[36,†] E. Brücken,[36,†] K. T. S. Kallonen,[36,†] R. Kinnunen,[36,†] T. Lampén,[36,†] K. Lassila-Perini,[36,†] S. Lehti,[36,†] T. Lindén,[36,†] L. Martikainen,[36,†] M. Myllymäki,[36,†] M. m. Rantanen,[36,†] H. Siikonen,[36,†] E. Tuominen,[36,†] J. Tuominiemi,[36,†] P. Luukka,[37,†] H. Petrow,[37,†] M. Besancon,[38,†] F. Couderc,[38,†] M. Dejardin,[38,†] D. Denegri,[38,†] J. L. Faure,[38,†] F. Ferri,[38,†] S. Ganjour,[38,†] P. Gras,[38,†] G. Hamel de Monchenault,[38,†] V. Lohezic,[38,†] J. Malcles,[38,†] J. Rander,[38,†] A. Rosowsky,[38,†] M. Ö. Sahin,[38,†] A. Savoy-Navarro,[38,v,†] P. Simkina,[38,†] M. Titov,[38,†] M. Tornago,[38,†] F. Beaudette,[39,†] A. Buchot Perraguin,[39,†] P. Busson,[39,†] A. Cappati,[39,†] C. Charlot,[39,†] F. Damas,[39,†] O. Davignon,[39,†] A. De Wit,[39,†] B. A. Fontana Santos Alves,[39,†] S. Ghosh,[39,†] A. Gilbert,[39,†] R. Granier de Cassagnac,[39,†] A. Hakimi,[39,†] B. Harikrishnan,[39,†] L. Kalipoliti,[39,†] G. Liu,[39,†] J. Motta,[39,†] M. Nguyen,[39,†] C. Ochando,[39,†] L. Portales,[39,†] R. Salerno,[39,†] J. B. Sauvan,[39,†] Y. Sirois,[39,†] A. Tarabini,[39,†] E. Vernazza,[39,†] A. Zabi,[39,†] A. Zghiche,[39,†] J.-L. Agram,[40,w,†] J. Andrea,[40,†] D. Apparu,[40,†] D. Bloch,[40,†] J.-M. Brom,[40,†] E. C. Chabert,[40,†] C. Collard,[40,†] S. Falke,[40,†] U. Goerlach,[40,†] C. Grimault,[40,†] R. Haeberle,[40,†] A.-C. Le Bihan,[40,†] M. Meena,[40,†] G. Saha,[40,†] M. A. Sessini,[40,†] P. Van Hove,[40,†] S. Beauceron,[41,†] B. Blancon,[41,†] G. Boudoul,[41,†] N. Chanon,[41,†] J. Choi,[41,†] D. Contardo,[41,†] P. Depasse,[41,†] C. Dozen,[41,x,†] H. El Mamouni,[41,†] J. Fay,[41,†] S. Gascon,[41,†] M. Gouzevitch,[41,†] C. Greenberg,[41,†] G. Grenier,[41,†] B. Ille,[41,†] I. B. Laktineh,[41,†] M. Lethuillier,[41,†] L. Mirabito,[41,†] S. Perries,[41,†] A. Purohit,[41,†] M. Vander Donckt,[41,†] P. Verdier,[41,†] J. Xiao,[41,†] G. Adamov,[42,†] I. Lomidze,[42,†] Z. Tsamalaidze,[42,r,†] V. Botta,[43,†] L. Feld,[43,†] K. Klein,[43,†] M. Lipinski,[43,†] D. Meuser,[43,†] A. Pauls,[43,†] N. Röwert,[43,†] M. Teroerde,[43,†] S. Diekmann,[44,†] A. Dodonova,[44,†] N. Eich,[44,†] D. Eliseev,[44,†] F. Engelke,[44,†] J. Erdmann,[44,†] M. Erdmann,[44,†] P. Fackeldey,[44,†] B. Fischer,[44,†] T. Hebbeker,[44,†] K. Hoepfner,[44,†] F. Ivone,[44,†] A. Jung,[44,†] M. y. Lee,[44,†] L. Mastrolorenzo,[44,†] F. Mausolf,[44,†] M. Merschmeyer,[44,†] A. Meyer,[44,†] S. Mukherjee,[44,†] D. Noll,[44,†] A. Novak,[44,†] F. Nowotny,[44,†] A. Pozdnyakov,[44,†] Y. Rath,[44,†] W. Redjeb,[44,†] F. Rehm,[44,†] H. Reithler,[44,†] U. Sarkar,[44,†] V. Sarkisovi,[44,†] A. Schmidt,[44,†] A. Sharma,[44,†] J. L. Spah,[44,†] A. Stein,[44,†] F. Torres Da Silva De Araujo,[44,y,†] L. Vigilante,[44,†] S. Wiedenbeck,[44,†] S. Zaleski,[44,†] C. Dziwok,[45,†] G. Flügge,[45,†] W. Haj Ahmad,[45,z,†] T. Kress,[45,†] A. Nowack,[45,†] O. Pooth,[45,†] A. Stahl,[45,†] T. Ziemons,[45,†] A. Zotz,[45,†] H. Aarup Petersen,[46,†] M. Aldaya Martin,[46,†] J. Alimena,[46,†] S. Amoroso,[46,†] Y. An,[46,†] S. Baxter,[46,†] M. Bayatmakou,[46,†] H. Becerril Gonzalez,[46,†] O. Behnke,[46,†] A. Belvedere,[46,†] S. Bhattacharya,[46,†] F. Blekman,[46,aa,†] K. Borras,[46,bb,†] A. Campbell,[46,†] A. Cardini,[46,†] C. Cheng,[46,†] F. Colombina,[46,†]

S. Consuegra Rodríguez,[46,†] G. Correia Silva,[46,†] M. De Silva,[46,†] G. Eckerlin,[46,†] D. Eckstein,[46,†] L. I. Estevez Banos,[46,†] O. Filatov,[46,†] E. Gallo,[46,aa,†] A. Geiser,[46,†] A. Giraldi,[46,†] G. Greau,[46,†] V. Guglielmi,[46,†] M. Guthoff,[46,†] A. Hinzmann,[46,†] A. Jafari,[46,cc,†] L. Jeppe,[46,†] N. Z. Jomhari,[46,†] B. Kaech,[46,†] M. Kasemann,[46,†] C. Kleinwort,[46,†] R. Kogler,[46,†] M. Komm,[46,†] D. Krücker,[46,†] W. Lange,[46,†] D. Leyva Pernia,[46,†] K. Lipka,[46,dd,†] W. Lohmann,[46,ee,†] R. Mankel,[46,†] I.-A. Melzer-Pellmann,[46,†] M. Mendizabal Morentin,[46,†] A. B. Meyer,[46,†] G. Milella,[46,†] A. Mussgiller,[46,†] L. P. NAIR,[46,†] A. Nürnberg,[46,†] Y. Otarid,[46,†] J. Park,[46,†] D. Pérez Adán,[46,†] E. Ranken,[46,†] A. Raspereza,[46,†] B. Ribeiro Lopes,[46,†] J. Rübenach,[46,†] A. Saggio,[46,†] M. Scham,[46,ff,bb,†] S. Schnake,[46,bb,†] P. Schütze,[46,†] C. Schwanenberger,[46,aa,†] D. Selivanova,[46,†] K. Sharko,[46,†] M. Shchedrolosiev,[46,†] R. E. Sosa Ricardo,[46,†] D. Stafford,[46,†] F. Vazzoler,[46,†] A. Ventura Barroso,[46,†] R. Walsh,[46,†] Q. Wang,[46,†] Y. Wen,[46,†] K. Wichmann,[46,†] L. Wiens,[46,bb,†] C. Wissing,[46,†] Y. Yang,[46,†] A. Zimermmane Castro Santos,[46,†] A. Albrecht,[47,†] S. Albrecht,[47,†] M. Antonello,[47,†] S. Bein,[47,†] L. Benato,[47,†] M. Bonanomi,[47,†] P. Connor,[47,†] M. Eich,[47,†] K. El Morabit,[47,†] Y. Fischer,[47,†] A. Fröhlich,[47,†] C. Garbers,[47,†] E. Garutti,[47,†] A. Grohsjean,[47,†] M. Hajheidari,[47,†] J. Haller,[47,†] H. R. Jabusch,[47,†] G. Kasieczka,[47,†] P. Keicher,[47,†] R. Klanner,[47,†] W. Korcari,[47,†] T. Kramer,[47,†] V. Kutzner,[47,†] F. Labe,[47,†] J. Lange,[47,†] A. Lobanov,[47,†] C. Matthies,[47,†] A. Mehta,[47,†] L. Moureaux,[47,†] M. Mrowietz,[47,†] A. Nigamova,[47,†] Y. Nissan,[47,†] A. Paasch,[47,†] K. J. Pena Rodriguez,[47,†] T. Quadfasel,[47,†] B. Raciti,[47,†] M. Rieger,[47,†] D. Savoiu,[47,†] J. Schindler,[47,†] P. Schleper,[47,†] M. Schröder,[47,†] J. Schwandt,[47,†] M. Sommerhalder,[47,†] H. Stadie,[47,†] G. Steinbrück,[47,†] A. Tews,[47,†] M. Wolf,[47,†] S. Brommer,[48,†] M. Burkart,[48,†] E. Butz,[48,†] T. Chwalek,[48,†] A. Dierlamm,[48,†] A. Droll,[48,†] N. Faltermann,[48,†] M. Giffels,[48,†] A. Gottmann,[48,†] F. Hartmann,[48,gg,†] R. Hofsaess,[48,†] M. Horzela,[48,†] U. Husemann,[48,†] J. Kieseler,[48,†] M. Klute,[48,†] R. Koppenhöfer,[48,†] J. M. Lawhorn,[48,†] M. Link,[48,†] A. Lintuluoto,[48,†] S. Maier,[48,†] S. Mitra,[48,†] M. Mormile,[48,†] Th. Müller,[48,†] M. Neukum,[48,†] M. Oh,[48,†] M. Presilla,[48,†] G. Quast,[48,†] K. Rabbertz,[48,†] B. Regnery,[48,†] N. Shadskiy,[48,†] I. Shvetsov,[48,†] H. J. Simonis,[48,†] M. Toms,[48,†] N. Trevisani,[48,†] R. Ulrich,[48,†] R. F. Von Cube,[48,†] M. Wassmer,[48,†] S. Wieland,[48,†] F. Wittig,[48,†] R. Wolf,[48,†] X. Zuo,[48,†] G. Anagnostou,[49,†] G. Daskalakis,[49,†] A. Kyriakis,[49,†] A. Papadopoulos,[49,gg,†] A. Stakia,[49,†] P. Kontaxakis,[50,†] G. Melachroinos,[50,†] A. Panagiotou,[50,†] I. Papavergou,[50,†] I. Paraskevas,[50,†] N. Saoulidou,[50,†] K. Theofilatos,[50,†] E. Tziaferi,[50,†] K. Vellidis,[50,†] I. Zisopoulos,[50,†] G. Bakas,[51,†] T. Chatzistavrou,[51,†] G. Karapostoli,[51,†] K. Kousouris,[51,†] I. Papakrivopoulos,[51,†] E. Siamarkou,[51,†] G. Tsipolitis,[51,†] A. Zacharopoulou,[51,†] K. Adamidis,[52,†] I. Bestintzanos,[52,†] I. Evangelou,[52,†] C. Foudas,[52,†] C. Kamtsikis,[52,†] P. Katsoulis,[52,†] P. Kokkas,[52,†] P. G. Kosmoglou Kioseoglou,[52,†] N. Manthos,[52,†] I. Papadopoulos,[52,†] J. Strologas,[52,†] M. Bartók,[53,hh,†] C. Hajdu,[53,†] D. Horvath,[53,ii,jj,†] F. Sikler,[53,†] V. Veszpremi,[53,†] M. Csanád,[54,†] K. Farkas,[54,†] M. M. A. Gadallah,[54,kk,†] Á. Kadlecsik,[54,†] P. Major,[54,†] K. Mandal,[54,†] G. Pásztor,[54,†] A. J. Rádl,[54,ll,†] G. I. Veres,[54,†] P. Raics,[55,†] B. Ujvari,[55,†] G. Zilizi,[55,†] G. Bencze,[56,†] S. Czellar,[56,†] J. Molnar,[56,†] Z. Szillasi,[56,†] T. Csorgo,[57,ll,†] T. Novak,[57,†] J. Babbar,[58,†] S. Bansal,[58,†] S. B. Beri,[58,†] V. Bhatnagar,[58,†] G. Chaudhary,[58,†] S. Chauhan,[58,†] N. Dhingra,[58,mm,†] A. Kaur,[58,†] A. Kaur,[58,†] H. Kaur,[58,†] M. Kaur,[58,†] S. Kumar,[58,†] K. Sandeep,[58,†] T. Sheokand,[58,†] J. B. Singh,[58,†] A. Singla,[58,†] A. Ahmed,[59,†] A. Bhardwaj,[59,†] A. Chhetri,[59,†] B. C. Choudhary,[59,†] A. Kumar,[59,†] A. Kumar,[59,†] M. Naimuddin,[59,†] K. Ranjan,[59,†] S. Saumya,[59,†] S. Baradia,[60,†] S. Barman,[60,nn,†] S. Bhattacharya,[60,†] S. Dutta,[60,†] S. Dutta,[60,†] S. Sarkar,[60,†] M. M. Ameen,[61,†] P. K. Behera,[61,†] S. C. Behera,[61,†] S. Chatterjee,[61,†] P. Jana,[61,†] P. Kalbhor,[61,†] J. R. Komaragiri,[61,oo,†] D. Kumar,[61,oo,†] L. Panwar,[61,oo,†] P. R. Pujahari,[61,†] N. R. Saha,[61,†] A. Sharma,[61,†] A. K. Sikdar,[61,†] S. Verma,[61,†] S. Dugad,[62,†] M. Kumar,[62,†] G. B. Mohanty,[62,†] P. Suryadevara,[62,†] A. Bala,[63,†] S. Banerjee,[63,†] R. M. Chatterjee,[63,†] R. K. Dewanjee,[63,pp,†] M. Guchait,[63,†] Sh. Jain,[63,†] S. Karmakar,[63,†] S. Kumar,[63,†] G. Majumder,[63,†] K. Mazumdar,[63,†] S. Parolia,[63,†] A. Thachayath,[63,†] S. Bahinipati,[64,qq,†] C. Kar,[64,†] D. Maity,[64,rr,†] P. Mal,[64,†] T. Mishra,[64,†] V. K. Muraleedharan Nair Bindhu,[64,rr,†] K. Naskar,[64,rr,†] A. Nayak,[64,rr,†] P. Sadangi,[64,†] P. Saha,[64,†] S. K. Swain,[64,†] S. Varghese,[64,rr,†] D. Vats,[64,rr,†] S. Acharya,[65,ss,†] A. Alpana,[65,†] S. Dube,[65,†] B. Gomber,[65,ss,†] B. Kansal,[65,†] A. Laha,[65,†] B. Sahu,[65,ss,†] S. Sharma,[65,†] H. Bakhshiansohi,[66,tt,†] E. Khazaie,[66,uu,†] M. Zeinali,[66,vv,†] S. Chenarani,[67,ww,†] S. M. Etesami,[67,†] M. Khakzad,[67,†] M. Mohammadi Najafabadi,[67,†] M. Grunewald,[68,†] M. Abbrescia,[69a,69b,†] R. Aly,[69a,69c,xx,†] A. Colaleo,[69a,69b,†] D. Creanza,[69a,69c,†] B. D'Anzi,[69a,69b,†] N. De Filippis,[69a,69c,†] M. De Palma,[69a,69b,†] A. Di Florio,[69a,69c,†] W. Elmetenawee,[69a,69b,xx,†] L. Fiore,[69a,†] G. Iaselli,[69a,69c,†] M. Louka,[69a,69b,†] G. Maggi,[69a,69c,†] M. Maggi,[69a,†] I. Margjeka,[69a,69b,†]

V. Mastrapasqua,[69a,69b,†] S. My,[69a,69b,†] S. Nuzzo,[69a,69b,†] A. Pellecchia,[69a,69b,†] A. Pompili,[69a,69b,†] G. Pugliese,[69a,69c,†] R. Radogna,[69a,†] G. Ramirez-Sanchez,[69a,69c,†] D. Ramos,[69a,†] A. Ranieri,[69a,†] L. Silvestris,[69a,†] F. M. Simone,[69a,69b,†] Ü. Sözbilir,[69a,†] A. Stamerra,[69a,†] R. Venditti,[69a,†] P. Verwilligen,[69a,†] A. Zaza,[69a,69b,†] G. Abbiendi,[70a,†] C. Battilana,[70a,70b,†] D. Bonacorsi,[70a,70b,†] L. Borgonovi,[70a,†] R. Campanini,[70a,70b,†] P. Capiluppi,[70a,70b,†] A. Castro,[70a,70b,†] F. R. Cavallo,[70a,†] M. Cuffiani,[70a,70b,†] G. M. Dallavalle,[70a,†] T. Diotalevi,[70a,70b,†] F. Fabbri,[70a,†] A. Fanfani,[70a,70b,†] D. Fasanella,[70a,70b,†] L. Giommi,[70a,70b,†] C. Grandi,[70a,†] L. Guiducci,[70a,70b,†] S. Lo Meo,[70a,yy,†] L. Lunerti,[70a,70b,†] S. Marcellini,[70a,†] G. Masetti,[70a,†] F. L. Navarria,[70a,70b,†] A. Perrotta,[70a,†] F. Primavera,[70a,70b,†] A. M. Rossi,[70a,70b,†] T. Rovelli,[70a,70b,†] G. P. Siroli,[70a,70b,†] S. Costa,[71a,71b,zz,†] A. Di Mattia,[71a,†] R. Potenza,[71a,71b,†] A. Tricomi,[71a,71b,zz,†] C. Tuve,[71a,71b,†] P. Assiouras,[72a,†] G. Barbagli,[72a,†] G. Bardelli,[72a,72b,†] B. Camaiani,[72a,72b,†] A. Cassese,[72a,†] R. Ceccarelli,[72a,†] V. Ciulli,[72a,72b,†] C. Civinini,[72a,†] R. D'Alessandro,[72a,72b,†] E. Focardi,[72a,72b,†] T. Kello,[72a,†] G. Latino,[72a,72b,†] P. Lenzi,[72a,72b,†] M. Lizzo,[72a,†] M. Meschini,[72a,†] S. Paoletti,[72a,†] A. Papanastassiou,[72a,72b,†] G. Sguazzoni,[72a,†] L. Viliani,[72a,†] L. Benussi,[73,†] S. Bianco,[73,†] S. Meola,[73,aaa,†] D. Piccolo,[73,†] P. Chatagnon,[74a,†] F. Ferro,[74a,†] E. Robutti,[74a,†] S. Tosi,[74a,74b,†] A. Benaglia,[75a,†] G. Boldrini,[75a,75b,†] F. Brivio,[75a,†] F. Cetorelli,[75a,†] F. De Guio,[75a,75b,†] M. E. Dinardo,[75a,75b,†] P. Dini,[75a,†] S. Gennai,[75a,†] R. Gerosa,[75a,75b,†] A. Ghezzi,[75a,75b,†] P. Govoni,[75a,75b,†] L. Guzzi,[75a,†] M. T. Lucchini,[75a,75b,†] M. Malberti,[75a,†] S. Malvezzi,[75a,†] A. Massironi,[75a,†] D. Menasce,[75a,†] L. Moroni,[75a,†] M. Paganoni,[75a,75b,†] D. Pedrini,[75a,†] B. S. Pinolini,[75a,†] S. Ragazzi,[75a,75b,†] T. Tabarelli de Fatis,[75a,75b,†] D. Zuolo,[75a,†] S. Buontempo,[76a,†] A. Cagnotta,[76a,76b,†] F. Carnevali,[76a,76b,†] N. Cavallo,[76a,76c,†] A. De Iorio,[76a,76b,†] F. Fabozzi,[76a,76c,†] A. O. M. Iorio,[76a,76b,†] L. Lista,[76a,76b,bbb,†] P. Paolucci,[76a,gg,†] B. Rossi,[76a,†] C. Sciacca,[76a,76b,†] R. Ardino,[77a,†] P. Azzi,[77a,†] N. Bacchetta,[77a,ccc,†] A. Bergnoli,[77a,†] D. Bisello,[77a,77b,†] P. Bortignon,[77a,†] A. Bragagnolo,[77a,77b,†] R. Carlin,[77a,77b,†] T. Dorigo,[77a,†] F. Gasparini,[77a,77b,†] U. Gasparini,[77a,77b,†] E. Lusiani,[77a,†] M. Margoni,[77a,77b,†] F. Marini,[77a,†] A. T. Meneguzzo,[77a,77b,†] M. Migliorini,[77a,77b,†] J. Pazzini,[77a,77b,†] P. Ronchese,[77a,77b,†] R. Rossin,[77a,77b,†] F. Simonetto,[77a,77b,†] G. Strong,[77a,†] M. Tosi,[77a,77b,†] A. Triossi,[77a,77b,†] S. Ventura,[77a,†] H. Yarar,[77a,77b,†] M. Zanetti,[77a,77b,†] P. Zotto,[77a,77b,†] A. Zucchetta,[77a,77b,†] G. Zumerle,[77a,77b,†] S. Abu Zeid,[78a,ddd,†] C. Aimè,[78a,78b,†] A. Braghieri,[78a,†] S. Calzaferri,[78a,†] D. Fiorina,[78a,†] P. Montagna,[78a,78b,†] V. Re,[78a,†] C. Riccardi,[78a,78b,†] P. Salvini,[78a,†] I. Vai,[78a,78b,†] P. Vitulo,[78a,78b,†] S. Ajmal,[79a,79b,†] G. M. Bilei,[79a,†] D. Ciangottini,[79a,79b,†] L. Fanò,[79a,79b,†] M. Magherini,[79a,79b,†] G. Mantovani,[79a,79b,†] V. Mariani,[79a,79b,†] M. Menichelli,[79a,†] F. Moscatelli,[79a,eee,†] A. Rossi,[79a,79b,†] A. Santocchia,[79a,79b,†] D. Spiga,[79a,†] T. Tedeschi,[79a,79b,†] P. Asenov,[80a,80b,†] P. Azzurri,[80a,†] G. Bagliesi,[80a,†] R. Bhattacharya,[80a,†] L. Bianchini,[80a,80b,†] T. Boccali,[80a,†] D. Bruschini,[80a,80c,†] R. Castaldi,[80a,†] M. A. Ciocci,[80a,80b,†] M. Cipriani,[80a,80b,†] V. D'Amante,[80a,80d,†] R. Dell'Orso,[80a,†] S. Donato,[80a,†] A. Giassi,[80a,†] F. Ligabue,[80a,80c,†] D. Matos Figueiredo,[80a,†] A. Messineo,[80a,80b,†] M. Musich,[80a,80b,†] F. Palla,[80a,†] A. Rizzi,[80a,80b,†] G. Rolandi,[80a,80c,†] S. Roy Chowdhury,[80a,†] T. Sarkar,[80a,†] A. Scribano,[80a,†] P. Spagnolo,[80a,†] R. Tenchini,[80a,†] G. Tonelli,[80a,80b,†] N. Turini,[80a,80d,†] A. Venturi,[80a,†] P. G. Verdini,[80a,†] P. Barria,[81a,†] M. Campana,[81a,81b,†] F. Cavallari,[81a,†] L. Cunqueiro Mendez,[81a,81b,†] D. Del Re,[81a,81b,†] E. Di Marco,[81a,†] M. Diemoz,[81a,†] F. Errico,[81a,81b,†] E. Longo,[81a,81b,†] P. Meridiani,[81a,†] J. Mijuskovic,[81a,81b,†] G. Organtini,[81a,81b,†] F. Pandolfi,[81a,†] R. Paramatti,[81a,81b,†] C. Quaranta,[81a,81b,†] S. Rahatlou,[81a,81b,†] C. Rovelli,[81a,†] F. Santanastasio,[81a,81b,†] L. Soffi,[81a,†] N. Amapane,[82a,82b,†] R. Arcidiacono,[82a,82c,†] S. Argiro,[82a,82b,†] M. Arneodo,[82a,82c,†] N. Bartosik,[82a,†] R. Bellan,[82a,82b,†] A. Bellora,[82a,82b,†] C. Biino,[82a,†] N. Cartiglia,[82a,†] M. Costa,[82a,82b,†] R. Covarelli,[82a,82b,†] N. Demaria,[82a,†] L. Finco,[82a,†] M. Grippo,[82a,82b,†] B. Kiani,[82a,82b,†] F. Legger,[82a,†] F. Luongo,[82a,82b,†] C. Mariotti,[82a,†] L. Markovic,[82a,82b,†] S. Maselli,[82a,†] A. Mecca,[82a,82b,†] E. Migliore,[82a,82b,†] M. Monteno,[82a,†] R. Mulargia,[82a,†] M. M. Obertino,[82a,82b,†] G. Ortona,[82a,†] L. Pacher,[82a,82b,†] N. Pastrone,[82a,†] M. Pelliccioni,[82a,†] M. Ruspa,[82a,82c,†] F. Siviero,[82a,82b,†] V. Sola,[82a,82b,†] A. Solano,[82a,82b,†] A. Staiano,[82a,†] C. Tarricone,[82a,82b,†] D. Trocino,[82a,†] G. Umoret,[82a,82b,†] E. Vlasov,[82a,82b,†] S. Belforte,[83a,†] V. Candelise,[83a,83b,†] M. Casarsa,[83a,†] F. Cossutti,[83a,†] K. De Leo,[83a,83b,†] G. Della Ricca,[83a,83b,†] S. Dogra,[84,†] J. Hong,[84,†] C. Huh,[84,†] B. Kim,[84,†] D. H. Kim,[84,†] J. Kim,[84,†] H. Lee,[84,†] S. W. Lee,[84,†] C. S. Moon,[84,†] Y. D. Oh,[84,†] M. S. Ryu,[84,†] S. Sekmen,[84,†] Y. C. Yang,[84,†] M. S. Kim,[85,†] G. Bak,[86,†] P. Gwak,[86,†] H. Kim,[86,†] D. H. Moon,[86,†] E. Asilar,[87,†] D. Kim,[87,†] T. J. Kim,[87,†] J. A. Merlin,[87,†] S. Choi,[88,†] S. Han,[88,†] B. Hong,[88,†] K. Lee,[88,†] K. S. Lee,[88,†] S. Lee,[88,†] J. Park,[88,†] S. K. Park,[88,†] J. Yoo,[88,†] J. Goh,[89,†] S. Yang,[89,†] H. S. Kim,[90,†] Y. Kim,[90,†] S. Lee,[90,†] J. Almond,[91,†] J. H. Bhyun,[91,†] J. Choi,[91,†] W. Jun,[91,†]

J. Kim,[91,†] S. Ko,[91,†] H. Kwon,[91,†] H. Lee,[91,†] J. Lee,[91,†] J. Lee,[91,†] B. H. Oh,[91,†] S. B. Oh,[91,†] H. Seo,[91,†] U. K. Yang,[91,†] I. Yoon,[91,†] W. Jang,[92,†] D. Y. Kang,[92,†] Y. Kang,[92,†] S. Kim,[92,†] B. Ko,[92,†] J. S. H. Lee,[92,†] Y. Lee,[92,†] I. C. Park,[92,†] Y. Roh,[92,†] I. J. Watson,[92,†] S. Ha,[93,†] H. D. Yoo,[93,†] M. Choi,[94,†] M. R. Kim,[94,†] H. Lee,[94,†] Y. Lee,[94,†] I. Yu,[94,†] T. Beyrouthy,[95,†] Y. Maghrbi,[95,†] K. Dreimanis,[96,†] A. Gaile,[96,†] G. Pikurs,[96,†] A. Potrebko,[96,†] M. Seidel,[96,†] V. Veckalns,[96,fff,†] N. R. Strautnieks,[97,†] M. Ambrozas,[98,†] A. Juodagalvis,[98,†] A. Rinkevicius,[98,†] G. Tamulaitis,[98,†] N. Bin Norjoharuddeen,[99,†] I. Yusuff,[99,ggg,†] Z. Zolkapli,[99,†] J. F. Benitez,[100,†] A. Castaneda Hernandez,[100,†] H. A. Encinas Acosta,[100,†] L. G. Gallegos Maríñez,[100,†] M. León Coello,[100,†] J. A. Murillo Quijada,[100,†] A. Sehrawat,[100,†] L. Valencia Palomo,[100,†] G. Ayala,[101,†] H. Castilla-Valdez,[101,†] E. De La Cruz-Burelo,[101,†] I. Heredia-De La Cruz,[101,hhh,†] R. Lopez-Fernandez,[101,†] C. A. Mondragon Herrera,[101,†] A. Sánchez Hernández,[101,†] C. Oropeza Barrera,[102,†] M. Ramírez García,[102,†] I. Bautista,[103,†] I. Pedraza,[103,†] H. A. Salazar Ibarguen,[103,†] C. Uribe Estrada,[103,†] I. Bubanja,[104,†] N. Raicevic,[104,†] P. H. Butler,[105,†] A. Ahmad,[106,†] M. I. Asghar,[106,†] A. Awais,[106,†] M. I. M. Awan,[106,†] H. R. Hoorani,[106,†] W. A. Khan,[106,†] H. Bialkowska,[108,†] M. Bluj,[108,†] B. Boimska,[108,†] M. Górski,[108,†] M. Kazana,[108,†] M. Szleper,[108,†] P. Zalewski,[108,†] K. Bunkowski,[109,†] K. Doroba,[109,†] A. Kalinowski,[109,†] M. Konecki,[109,†] J. Krolikowski,[109,†] A. Muhammad,[109,†] K. Pozniak,[110,†] W. Zabolotny,[110,†] M. Araujo,[111,†] D. Bastos,[111,†] C. Beirão Da Cruz E Silva,[111,†] A. Boletti,[111,†] T. Camporesi,[111,†] G. Da Molin,[111,†] P. Faccioli,[111,†] M. Gallinaro,[111,†] J. Hollar,[111,†] N. Leonardo,[111,†] T. Niknejad,[111,†] A. Petrilli,[111,†] M. Pisano,[111,†] J. Seixas,[111,†] J. Varela,[111,†] J. W. Wulff,[111,†] P. Adzic,[112,†] P. Milenovic,[112,†] M. Dordevic,[113,†] J. Milosevic,[113,†] V. Rekovic,[113,†] M. Aguilar-Benitez,[114,†] J. Alcaraz Maestre,[114,†] Cristina F. Bedoya,[114,†] M. Cepeda,[114,†] M. Cerrada,[114,†] N. Colino,[114,†] B. De La Cruz,[114,†] A. Delgado Peris,[114,†] A. Escalante Del Valle,[114,†] D. Fernández Del Val,[114,†] J. P. Fernández Ramos,[114,†] J. Flix,[114,†] M. C. Fouz,[114,†] O. Gonzalez Lopez,[114,†] S. Goy Lopez,[114,†] J. M. Hernandez,[114,†] M. I. Josa,[114,†] D. Moran,[114,†] C. M. Morcillo Perez,[114,†] Á. Navarro Tobar,[114,†] C. Perez Dengra,[114,†] A. Pérez-Calero Yzquierdo,[114,†] J. Puerta Pelayo,[114,†] I. Redondo,[114,†] D. D. Redondo Ferrero,[114,†] L. Romero,[114,†] S. Sánchez Navas,[114,†] L. Urda Gómez,[114,†] J. Vazquez Escobar,[114,†] C. Willmott,[114,†] J. F. de Trocóniz,[115,†] B. Alvarez Gonzalez,[116,†] J. Cuevas,[116,†] J. Fernandez Menendez,[116,†] S. Folgueras,[116,†] I. Gonzalez Caballero,[116,†] J. R. González Fernández,[116,†] E. Palencia Cortezon,[116,†] C. Ramón Álvarez,[116,†] V. Rodríguez Bouza,[116,†] A. Soto Rodríguez,[116,†] A. Trapote,[116,†] C. Vico Villalba,[116,†] P. Vischia,[116,†] S. Bhowmik,[117,†] S. Blanco Fernández,[117,†] J. A. Brochero Cifuentes,[117,†] I. J. Cabrillo,[117,†] A. Calderon,[117,†] J. Duarte Campderros,[117,†] M. Fernandez,[117,†] G. Gomez,[117,†] C. Lasaosa García,[117,†] C. Martinez Rivero,[117,†] P. Martinez Ruiz del Arbol,[117,†] F. Matorras,[117,†] P. Matorras Cuevas,[117,†] E. Navarrete Ramos,[117,†] J. Piedra Gomez,[117,†] L. Scodellaro,[117,†] I. Vila,[117,†] J. M. Vizan Garcia,[117,†] M. K. Jayananda,[118,†] B. Kailasapathy,[118,iii,†] D. U. J. Sonnadara,[118,†] D. D. C. Wickramarathna,[118,†] W. G. D. Dharmaratna,[119,jjj,†] K. Liyanage,[119,†] N. Perera,[119,†] N. Wickramage,[119,†] D. Abbaneo,[120,†] C. Amendola,[120,†] E. Auffray,[120,†] G. Auzinger,[120,†] D. Barney,[120,†] A. Bermúdez Martínez,[120,†] M. Bianco,[120,†] B. Bilin,[120,†] A. A. Bin Anuar,[120,†] A. Bocci,[120,†] C. Botta,[120,†] E. Brondolin,[120,†] C. Caillol,[120,†] G. Cerminara,[120,†] N. Chernyavskaya,[120,†] D. d'Enterria,[120,†] A. Dabrowski,[120,†] A. David,[120,†] A. De Roeck,[120,†] M. M. Defranchis,[120,†] M. Deile,[120,†] M. Dobson,[120,†] L. Forthomme,[120,†] G. Franzoni,[120,†] W. Funk,[120,†] S. Giani,[120,†] D. Gigi,[120,†] K. Gill,[120,†] F. Glege,[120,†] L. Gouskos,[120,†] M. Haranko,[120,†] J. Hegeman,[120,†] B. Huber,[120,†] V. Innocente,[120,†] T. James,[120,†] P. Janot,[120,†] S. Laurila,[120,†] P. Lecoq,[120,†] E. Leutgeb,[120,†] C. Lourenço,[120,†] B. Maier,[120,†] L. Malgeri,[120,†] M. Mannelli,[120,†] A. C. Marini,[120,†] M. Matthewman,[120,†] F. Meijers,[120,†] S. Mersi,[120,†] E. Meschi,[120,†] V. Milosevic,[120,†] F. Monti,[120,†] F. Moortgat,[120,†] M. Mulders,[120,†] I. Neutelings,[120,†] S. Orfanelli,[120,†] F. Pantaleo,[120,†] G. Petrucciani,[120,†] A. Pfeiffer,[120,†] M. Pierini,[120,†] D. Piparo,[120,†] H. Qu,[120,†] D. Rabady,[120,†] G. Reales Gutiérrez,[120,†] M. Rovere,[120,†] H. Sakulin,[120,†] S. Scarfi,[120,†] C. Schwick,[120,†] M. Selvaggi,[120,†] A. Sharma,[120,†] K. Shchelina,[120,†] P. Silva,[120,†] P. Sphicas,[120,kkk,†] A. G. Stahl Leiton,[120,†] A. Steen,[120,†] S. Summers,[120,†] D. Treille,[120,†] P. Tropea,[120,†] A. Tsirou,[120,†] D. Walter,[120,†] J. Wanczyk,[120,lll,†] J. Wang,[120,†] S. Wuchterl,[120,†] P. Zehetner,[120,†] P. Zejdl,[120,†] W. D. Zeuner,[120,†] T. Bevilacqua,[121,mmm,†] L. Caminada,[121,mmm,†] A. Ebrahimi,[121,†] W. Erdmann,[121,†] R. Horisberger,[121,†] Q. Ingram,[121,†] H. C. Kaestli,[121,†] D. Kotlinski,[121,†] C. Lange,[121,†] M. Missiroli,[121,mmm,†] L. Noehte,[121,mmm,†] T. Rohe,[121,†] T. K. Aarrestad,[122,†] K. Androsov,[122,lll,†] M. Backhaus,[122,†] A. Calandri,[122,†] C. Cazzaniga,[122,†]

K. Datta,[122,†] A. De Cosa,[122,†] G. Dissertori,[122,†] M. Dittmar,[122,†] M. Donegà,[122,†] F. Eble,[122,†] M. Galli,[122,†] K. Gedia,[122,†] F. Glessgen,[122,†] C. Grab,[122,†] D. Hits,[122,†] W. Lustermann,[122,†] A.-M. Lyon,[122,†] R. A. Manzoni,[122,†] M. Marchegiani,[122,†] L. Marchese,[122,†] C. Martin Perez,[122,†] A. Mascellani,[122,lll,†] F. Nessi-Tedaldi,[122,†] F. Pauss,[122,†] V. Perovic,[122,†] S. Pigazzini,[122,†] C. Reissel,[122,†] T. Reitenspiess,[122,†] B. Ristic,[122,†] F. Riti,[122,†] D. Ruini,[122,†] R. Seidita,[122,†] J. Steggemann,[122,lll,†] D. Valsecchi,[122,†] R. Wallny,[122,†] C. Amsler,[123,nnn,†] P. Bärtschi,[123,†] D. Brzhechko,[123,†] M. F. Canelli,[123,†] K. Cormier,[123,†] J. K. Heikkilä,[123,†] M. Huwiler,[123,†] W. Jin,[123,†] A. Jofrehei,[123,†] B. Kilminster,[123,†] S. Leontsinis,[123,†] S. P. Liechti,[123,†] A. Macchiolo,[123,†] P. Meiring,[123,†] U. Molinatti,[123,†] A. Reimers,[123,†] P. Robmann,[123,†] S. Sanchez Cruz,[123,†] M. Senger,[123,†] Y. Takahashi,[123,†] R. Tramontano,[123,†] C. Adloff,[124,ooo,†] D. Bhowmik,[124,†] C. M. Kuo,[124,†] W. Lin,[124,†] P. K. Rout,[124,†] P. C. Tiwari,[124,oo,†] S. S. Yu,[124,†] L. Ceard,[125,†] Y. Chao,[125,†] K. F. Chen,[125,†] P. s. Chen,[125,†] Z. g. Chen,[125,†] W.-S. Hou,[125,†] T. h. Hsu,[125,†] Y. w. Kao,[125,†] R. Khurana,[125,†] G. Kole,[125,†] Y. y. Li,[125,†] R.-S. Lu,[125,†] E. Paganis,[125,†] X. f. Su,[125,†] J. Thomas-Wilsker,[125,†] L. s. Tsai,[125,†] H. y. Wu,[125,†] E. Yazgan,[125,†] C. Asawatangtrakuldee,[126,†] N. Srimanobhas,[126,†] V. Wachirapusitanand,[126,†] D. Agyel,[127,†] F. Boran,[127,†] Z. S. Demiroglu,[127,†] F. Dolek,[127,†] I. Dumanoglu,[127,ppp,†] E. Eskut,[127,†] Y. Guler,[127,qqq,†] E. Gurpinar Guler,[127,qqq,†] C. Isik,[127,†] O. Kara,[127,†] A. Kayis Topaksu,[127,†] U. Kiminsu,[127,†] G. Onengut,[127,†] K. Ozdemir,[127,rrr,†] A. Polatoz,[127,†] B. Tali,[127,sss,†] U. G. Tok,[127,†] S. Turkcapar,[127,†] E. Uslan,[127,†] I. S. Zorbakir,[127,†] M. Yalvac,[128,ttt,†] B. Akgun,[129,†] I. O. Atakisi,[129,†] E. Gülmez,[129,†] M. Kaya,[129,uuu,†] O. Kaya,[129,vvv,†] S. Tekten,[129,www,†] A. Cakir,[130,†] K. Cankocak,[130,ppp,xxx,†] Y. Komurcu,[130,†] S. Sen,[130,yyy,†] O. Aydilek,[131,†] S. Cerci,[131,sss,†] V. Epshteyn,[131,†] B. Hacisahinoglu,[131,†] I. Hos,[131,zzz,†] O. Potok,[131,†] H. Sert,[131,†] C. Simsek,[131,†] C. Zorbilmez,[131,†] B. Isildak,[132,aaaa,†] D. Sunar Cerci,[132,sss,†] A. Boyaryntsev,[133,†] B. Grynyov,[133,†] L. Levchuk,[134,†] D. Anthony,[135,†] J. J. Brooke,[135,†] A. Bundock,[135,†] F. Bury,[135,†] E. Clement,[135,†] D. Cussans,[135,†] H. Flacher,[135,†] M. Glowacki,[135,†] J. Goldstein,[135,†] H. F. Heath,[135,†] L. Kreczko,[135,†] S. Paramesvaran,[135,†] S. Seif El Nasr-Storey,[135,†] V. J. Smith,[135,†] N. Stylianou,[135,bbbb,†] K. Walkingshaw Pass,[135,†] R. White,[135,†] A. H. Ball,[136,†] K. W. Bell,[136,†] A. Belyaev,[136,cccc,†] C. Brew,[136,†] R. M. Brown,[136,†] D. J. A. Cockerill,[136,†] C. Cooke,[136,†] K. V. Ellis,[136,†] K. Harder,[136,†] S. Harper,[136,†] M.-L. Holmberg,[136,dddd,†] J. Linacre,[136,†] K. Manolopoulos,[136,†] D. M. Newbold,[136,†] E. Olaiya,[136,†] D. Petyt,[136,†] T. Reis,[136,†] G. Salvi,[136,†] T. Schuh,[136,†] C. H. Shepherd-Themistocleous,[136,†] I. R. Tomalin,[136,†] T. Williams,[136,†] R. Bainbridge,[137,†] P. Bloch,[137,†] C. E. Brown,[137,†] O. Buchmuller,[137,†] V. Cacchio,[137,†] C. A. Carrillo Montoya,[137,†] G. S. Chahal,[137,eeee,†] D. Colling,[137,†] J. S. Dancu,[137,†] I. Das,[137,†] P. Dauncey,[137,†] G. Davies,[137,†] J. Davies,[137,†] M. Della Negra,[137,†] S. Fayer,[137,†] G. Fedi,[137,†] G. Hall,[137,†] M. H. Hassanshahi,[137,†] A. Howard,[137,†] G. Iles,[137,†] M. Knight,[137,†] J. Langford,[137,†] J. León Holgado,[137,†] L. Lyons,[137,†] A.-M. Magnan,[137,†] S. Malik,[137,†] M. Mieskolainen,[137,†] J. Nash,[137,ffff,†] M. Pesaresi,[137,†] B. C. Radburn-Smith,[137,†] A. Richards,[137,†] A. Rose,[137,†] K. Savva,[137,†] C. Seez,[137,†] R. Shukla,[137,†] A. Tapper,[137,†] K. Uchida,[137,†] G. P. Uttley,[137,†] L. H. Vage,[137,†] T. Virdee,[137,gg,†] M. Vojinovic,[137,†] N. Wardle,[137,†] D. Winterbottom,[137,†] K. Coldham,[138,†] J. E. Cole,[138,†] A. Khan,[138,†] P. Kyberd,[138,†] I. D. Reid,[138,†] S. Abdullin,[139,†] A. Brinkerhoff,[139,†] B. Caraway,[139,†] J. Dittmann,[139,†] K. Hatakeyama,[139,†] J. Hiltbrand,[139,†] B. McMaster,[139,†] M. Saunders,[139,†] S. Sawant,[139,†] C. Sutantawibul,[139,†] J. Wilson,[139,†] R. Bartek,[140,†] A. Dominguez,[140,†] C. Huerta Escamilla,[140,†] A. E. Simsek,[140,†] R. Uniyal,[140,†] A. M. Vargas Hernandez,[140,†] B. Bam,[141,†] R. Chudasama,[141,†] S. I. Cooper,[141,†] S. V. Gleyzer,[141,†] C. U. Perez,[141,†] P. Rumerio,[141,gggg,†] E. Usai,[141,†] R. Yi,[141,†] A. Akpinar,[142,†] D. Arcaro,[142,†] C. Cosby,[142,†] Z. Demiragli,[142,†] C. Erice,[142,†] C. Fangmeier,[142,†] C. Fernandez Madrazo,[142,†] E. Fontanesi,[142,†] D. Gastler,[142,†] F. Golf,[142,†] S. Jeon,[142,†] I. Reed,[142,†] J. Rohlf,[142,†] K. Salyer,[142,†] D. Sperka,[142,†] D. Spitzbart,[142,†] I. Suarez,[142,†] A. Tsatsos,[142,†] S. Yuan,[142,†] A. G. Zecchinelli,[142,†] G. Benelli,[143,†] X. Coubez,[143,bb,†] D. Cutts,[143,†] M. Hadley,[143,†] U. Heintz,[143,†] J. M. Hogan,[143,hhhh,†] T. Kwon,[143,†] G. Landsberg,[143,†] K. T. Lau,[143,†] D. Li,[143,†] J. Luo,[143,†] S. Mondal,[143,†] M. Narain,[143,a,†] N. Pervan,[143,†] S. Sagir,[143,iiii,†] F. Simpson,[143,†] M. Stamenkovic,[143,†] W. Y. Wong,[143,†] X. Yan,[143,†] W. Zhang,[143,†] S. Abbott,[144,†] J. Bonilla,[144,†] C. Brainerd,[144,†] R. Breedon,[144,†] M. Calderon De La Barca Sanchez,[144,†] M. Chertok,[144,†] M. Citron,[144,†] J. Conway,[144,†] P. T. Cox,[144,†] R. Erbacher,[144,†] F. Jensen,[144,†] O. Kukral,[144,†] G. Mocellin,[144,†] M. Mulhearn,[144,†] D. Pellett,[144,†] W. Wei,[144,†] Y. Yao,[144,†] F. Zhang,[144,†] M. Bachtis,[145,†] R. Cousins,[145,†] A. Datta,[145,†] G. Flores Avila,[145,†] J. Hauser,[145,†] M. Ignatenko,[145,†] M. A. Iqbal,[145,†] T. Lam,[145,†] E. Manca,[145,†] A. Nunez Del Prado,[145,†] D. Saltzberg,[145,†]

V. Valuev,[145,†] R. Clare,[146,†] J. W. Gary,[146,†] M. Gordon,[146,†] G. Hanson,[146,†] W. Si,[146,†] S. Wimpenny,[146,a,†] J. G. Branson,[147,†] S. Cittolin,[147,†] S. Cooperstein,[147,†] D. Diaz,[147,†] J. Duarte,[147,†] L. Giannini,[147,†] J. Guiang,[147,†] R. Kansal,[147,†] V. Krutelyov,[147,†] R. Lee,[147,†] J. Letts,[147,†] M. Masciovecchio,[147,†] F. Mokhtar,[147,†] S. Mukherjee,[147,†] M. Pieri,[147,†] M. Quinnan,[147,†] B. V. Sathia Narayanan,[147,†] V. Sharma,[147,†] M. Tadel,[147,†] E. Vourliotis,[147,†] F. Würthwein,[147,†] Y. Xiang,[147,†] A. Yagil,[147,†] A. Barzdukas,[148,†] L. Brennan,[148,†] C. Campagnari,[148,†] A. Dorsett,[148,†] J. Incandela,[148,†] J. Kim,[148,†] A. J. Li,[148,†] P. Masterson,[148,†] H. Mei,[148,†] J. Richman,[148,†] U. Sarica,[148,†] R. Schmitz,[148,†] F. Setti,[148,†] J. Sheplock,[148,†] D. Stuart,[148,†] T. Á. Vámi,[148,†] S. Wang,[148,†] A. Bornheim,[149,†] O. Cerri,[149,†] A. Latorre,[149,†] J. Mao,[149,†] H. B. Newman,[149,†] M. Spiropulu,[149,†] J. R. Vlimant,[149,†] C. Wang,[149,†] S. Xie,[149,†] R. Y. Zhu,[149,†] J. Alison,[150,†] S. An,[150,†] M. B. Andrews,[150,†] P. Bryant,[150,†] M. Cremonesi,[150,†] V. Dutta,[150,†] T. Ferguson,[150,†] A. Harilal,[150,†] C. Liu,[150,†] T. Mudholkar,[150,†] S. Murthy,[150,†] P. Palit,[150,†] M. Paulini,[150,†] A. Roberts,[150,†] A. Sanchez,[150,†] W. Terrill,[150,†] J. P. Cumalat,[151,†] W. T. Ford,[151,†] A. Hassani,[151,†] G. Karathanasis,[151,†] E. MacDonald,[151,†] N. Manganelli,[151,†] A. Perloff,[151,†] C. Savard,[151,†] N. Schonbeck,[151,†] K. Stenson,[151,†] K. A. Ulmer,[151,†] S. R. Wagner,[151,†] N. Zipper,[151,†] J. Alexander,[152,†] S. Bright-Thonney,[152,†] X. Chen,[152,†] D. J. Cranshaw,[152,†] J. Fan,[152,†] X. Fan,[152,†] D. Gadkari,[152,†] S. Hogan,[152,†] P. Kotamnives,[152,†] J. Monroy,[152,†] M. Oshiro,[152,†] J. R. Patterson,[152,†] J. Reichert,[152,†] M. Reid,[152,†] A. Ryd,[152,†] J. Thom,[152,†] P. Wittich,[152,†] R. Zou,[152,†] M. Albrow,[153,†] M. Alyari,[153,†] O. Amram,[153,†] G. Apollinari,[153,†] A. Apresyan,[153,†] L. A. T. Bauerdick,[153,†] D. Berry,[153,†] J. Berryhill,[153,†] P. C. Bhat,[153,†] K. Burkett,[153,†] J. N. Butler,[153,†] A. Canepa,[153,†] G. B. Cerati,[153,†] H. W. K. Cheung,[153,†] F. Chlebana,[153,†] G. Cummings,[153,†] J. Dickinson,[153,†] I. Dutta,[153,†] V. D. Elvira,[153,†] Y. Feng,[153,†] J. Freeman,[153,†] A. Gandrakota,[153,†] Z. Gecse,[153,†] L. Gray,[153,†] D. Green,[153,†] A. Grummer,[153,†] S. Grünendahl,[153,†] D. Guerrero,[153,†] O. Gutsche,[153,†] R. M. Harris,[153,†] R. Heller,[153,†] T. C. Herwig,[153,†] J. Hirschauer,[153,†] L. Horyn,[153,†] B. Jayatilaka,[153,†] S. Jindariani,[153,†] M. Johnson,[153,†] U. Joshi,[153,†] T. Klijnsma,[153,†] B. Klima,[153,†] K. H. M. Kwok,[153,†] S. Lammel,[153,†] D. Lincoln,[153,†] R. Lipton,[153,†] T. Liu,[153,†] C. Madrid,[153,†] K. Maeshima,[153,†] C. Mantilla,[153,†] D. Mason,[153,†] P. McBride,[153,†] P. Merkel,[153,†] S. Mrenna,[153,†] S. Nahn,[153,†] J. Ngadiuba,[153,†] D. Noonan,[153,†] V. Papadimitriou,[153,†] N. Pastika,[153,†] K. Pedro,[153,†] C. Pena,[153,jjjj,†] F. Ravera,[153,†] A. Reinsvold Hall,[153,kkkk,†] L. Ristori,[153,†] E. Sexton-Kennedy,[153,†] N. Smith,[153,†] A. Soha,[153,†] L. Spiegel,[153,†] S. Stoynev,[153,†] J. Strait,[153,†] L. Taylor,[153,†] S. Tkaczyk,[153,†] N. V. Tran,[153,†] L. Uplegger,[153,†] E. W. Vaandering,[153,†] I. Zoi,[153,†] C. Aruta,[154,†] P. Avery,[154,†] D. Bourilkov,[154,†] L. Cadamuro,[154,†] P. Chang,[154,†] V. Cherepanov,[154,†] R. D. Field,[154,†] E. Koenig,[154,†] M. Kolosova,[154,†] J. Konigsberg,[154,†] A. Korytov,[154,†] K. H. Lo,[154,†] K. Matchev,[154,†] N. Menendez,[154,†] G. Mitselmakher,[154,†] K. Mohrman,[154,†] A. Muthirakalayil Madhu,[154,†] N. Rawal,[154,†] D. Rosenzweig,[154,†] S. Rosenzweig,[154,†] K. Shi,[154,†] J. Wang,[154,†] T. Adams,[155,†] A. Al Kadhim,[155,†] A. Askew,[155,†] N. Bower,[155,†] R. Habibullah,[155,†] V. Hagopian,[155,†] R. Hashmi,[155,†] R. S. Kim,[155,†] S. Kim,[155,†] T. Kolberg,[155,†] G. Martinez,[155,†] H. Prosper,[155,†] P. R. Prova,[155,†] M. Wulansatiti,[155,†] R. Yohay,[155,†] J. Zhang,[155,†] B. Alsufyani,[156,†] M. M. Baarmand,[156,†] S. Butalla,[156,†] T. Elkafrawy,[156,ddd,†] M. Hohlmann,[156,†] R. Kumar Verma,[156,†] M. Rahmani,[156,†] E. Yanes,[156,†] M. R. Adams,[157,†] A. Baty,[157,†] C. Bennett,[157,†] R. Cavanaugh,[157,†] R. Escobar Franco,[157,†] O. Evdokimov,[157,†] C. E. Gerber,[157,†] D. J. Hofman,[157,†] J. h. Lee,[157,†] D. S. Lemos,[157,†] A. H. Merrit,[157,†] C. Mills,[157,†] S. Nanda,[157,†] G. Oh,[157,†] B. Ozek,[157,†] D. Pilipovic,[157,†] R. Pradhan,[157,†] T. Roy,[157,†] S. Rudrabhatla,[157,†] M. B. Tonjes,[157,†] N. Varelas,[157,†] Z. Ye,[157,†] J. Yoo,[157,†] M. Alhusseini,[158,†] D. Blend,[158,†] K. Dilsiz,[158,llll,†] L. Emediato,[158,†] G. Karaman,[158,†] O. K. Köseyan,[158,†] J.-P. Merlo,[158,†] A. Mestvirishvili,[158,mmmm,†] J. Nachtman,[158,†] O. Neogi,[158,†] H. Ogul,[158,nnnn,†] Y. Onel,[158,†] A. Penzo,[158,†] C. Snyder,[158,†] E. Tiras,[158,oooo,†] B. Blumenfeld,[159,†] L. Corcodilos,[159,†] J. Davis,[159,†] A. V. Gritsan,[159,†] L. Kang,[159,†] S. Kyriacou,[159,†] P. Maksimovic,[159,†] M. Roguljic,[159,†] J. Roskes,[159,†] S. Sekhar,[159,†] M. Swartz,[159,†] A. Abreu,[160,†] L. F. Alcerro Alcerro,[160,†] J. Anguiano,[160,†] P. Baringer,[160,†] A. Bean,[160,†] Z. Flowers,[160,†] D. Grove,[160,†] J. King,[160,†] G. Krintiras,[160,†] M. Lazarovits,[160,†] C. Le Mahieu,[160,†] J. Marquez,[160,†] M. Murray,[160,†] M. Nickel,[160,†] M. Pitt,[160,†] S. Popescu,[160,pppp,†] C. Rogan,[160,†] R. Salvatico,[160,†] S. Sanders,[160,†] C. Smith,[160,†] Q. Wang,[160,†] G. Wilson,[160,†] B. Allmond,[161,†] A. Ivanov,[161,†] K. Kaadze,[161,†] A. Kalogeropoulos,[161,†] D. Kim,[161,†] Y. Maravin,[161,†] K. Nam,[161,†] J. Natoli,[161,†] D. Roy,[161,†] G. Sorrentino,[161,†] F. Rebassoo,[162,†] D. Wright,[162,†] A. Baden,[163,†] A. Belloni,[163,†] Y. M. Chen,[163,†] S. C. Eno,[163,†] N. J. Hadley,[163,†] S. Jabeen,[163,†]

R. G. Kellogg,[163,†] T. Koeth,[163,†] Y. Lai,[163,†] S. Lascio,[163,†] A. C. Mignerey,[163,†] S. Nabili,[163,†] C. Palmer,[163,†] C. Papageorgakis,[163,†] M. M. Paranjpe,[163,†] L. Wang,[163,†] J. Bendavid,[164,†] W. Busza,[164,†] I. A. Cali,[164,†] M. D'Alfonso,[164,†] J. Eysermans,[164,†] C. Freer,[164,†] G. Gomez-Ceballos,[164,†] M. Goncharov,[164,†] G. Grosso,[164,†] P. Harris,[164,†] D. Hoang,[164,†] D. Kovalskyi,[164,†] J. Krupa,[164,†] L. Lavezzo,[164,†] Y.-J. Lee,[164,†] K. Long,[164,†] C. Mironov,[164,†] C. Paus,[164,†] D. Rankin,[164,†] C. Roland,[164,†] G. Roland,[164,†] S. Rothman,[164,†] G. S. F. Stephans,[164,†] Z. Wang,[164,†] B. Wyslouch,[164,†] T. J. Yang,[164,†] B. Crossman,[165,†] B. M. Joshi,[165,†] C. Kapsiak,[165,†] M. Krohn,[165,†] D. Mahon,[165,†] J. Mans,[165,†] B. Marzocchi,[165,†] S. Pandey,[165,†] M. Revering,[165,†] R. Rusack,[165,†] R. Saradhy,[165,†] N. Schroeder,[165,†] N. Strobbe,[165,†] M. A. Wadud,[165,†] L. M. Cremaldi,[166,†] K. Bloom,[167,†] D. R. Claes,[167,†] G. Haza,[167,†] J. Hossain,[167,†] C. Joo,[167,†] I. Kravchenko,[167,†] J. E. Siado,[167,†] W. Tabb,[167,†] A. Vagnerini,[167,†] A. Wightman,[167,†] F. Yan,[167,†] D. Yu,[167,†] H. Bandyopadhyay,[168,†] L. Hay,[168,†] I. Iashvili,[168,†] A. Kharchilava,[168,†] M. Morris,[168,†] D. Nguyen,[168,†] S. Rappoccio,[168,†] H. Rejeb Sfar,[168,†] A. Williams,[168,†] G. Alverson,[169,†] E. Barberis,[169,†] J. Dervan,[169,†] Y. Haddad,[169,†] Y. Han,[169,†] A. Krishna,[169,†] J. Li,[169,†] M. Lu,[169,†] G. Madigan,[169,†] R. Mccarthy,[169,†] D. M. Morse,[169,†] V. Nguyen,[169,†] T. Orimoto,[169,†] A. Parker,[169,†] L. Skinnari,[169,†] A. Tishelman-Charny,[169,†] B. Wang,[169,†] D. Wood,[169,†] S. Bhattacharya,[170,†] J. Bueghly,[170,†] Z. Chen,[170,†] S. Dittmer,[170,†] K. A. Hahn,[170,†] Y. Liu,[170,†] Y. Miao,[170,†] D. G. Monk,[170,†] M. H. Schmitt,[170,†] A. Taliercio,[170,†] M. Velasco,[170,†] G. Agarwal,[171,†] R. Band,[171,†] R. Bucci,[171,†] S. Castells,[171,†] A. Das,[171,†] R. Goldouzian,[171,†] M. Hildreth,[171,†] K. W. Ho,[171,†] K. Hurtado Anampa,[171,†] T. Ivanov,[171,†] C. Jessop,[171,†] K. Lannon,[171,†] J. Lawrence,[171,†] N. Loukas,[171,†] L. Lutton,[171,†] J. Mariano,[171,†] N. Marinelli,[171,†] I. Mcalister,[171,†] T. McCauley,[171,†] C. Mcgrady,[171,†] C. Moore,[171,†] Y. Musienko,[171,r,†] H. Nelson,[171,†] M. Osherson,[171,†] A. Piccinelli,[171,†] R. Ruchti,[171,†] A. Townsend,[171,†] Y. Wan,[171,†] M. Wayne,[171,†] H. Yockey,[171,†] M. Zarucki,[171,†] L. Zygala,[171,†] A. Basnet,[172,†] B. Bylsma,[172,†] M. Carrigan,[172,†] L. S. Durkin,[172,†] C. Hill,[172,†] M. Joyce,[172,†] M. Nunez Ornelas,[172,†] K. Wei,[172,†] B. L. Winer,[172,†] B. R. Yates,[172,†] F. M. Addesa,[173,†] H. Bouchamaoui,[173,†] P. Das,[173,†] G. Dezoort,[173,†] P. Elmer,[173,†] A. Frankenthal,[173,†] B. Greenberg,[173,†] N. Haubrich,[173,†] G. Kopp,[173,†] S. Kwan,[173,†] D. Lange,[173,†] A. Loeliger,[173,†] D. Marlow,[173,†] I. Ojalvo,[173,†] J. Olsen,[173,†] A. Shevelev,[173,†] D. Stickland,[173,†] C. Tully,[173,†] S. Malik,[174,†] A. S. Bakshi,[175,†] V. E. Barnes,[175,†] S. Chandra,[175,†] R. Chawla,[175,†] S. Das,[175,†] A. Gu,[175,†] L. Gutay,[175,†] M. Jones,[175,†] A. W. Jung,[175,†] D. Kondratyev,[175,†] A. M. Koshy,[175,†] M. Liu,[175,†] G. Negro,[175,†] N. Neumeister,[175,†] G. Paspalaki,[175,†] S. Piperov,[175,†] V. Scheurer,[175,†] J. F. Schulte,[175,†] M. Stojanovic,[175,†] J. Thieman,[175,†] A. K. Virdi,[175,†] F. Wang,[175,†] W. Xie,[175,†] J. Dolen,[176,†] N. Parashar,[176,†] A. Pathak,[176,†] D. Acosta,[177,†] T. Carnahan,[177,†] K. M. Ecklund,[177,†] P. J. Fernández Manteca,[177,†] S. Freed,[177,†] P. Gardner,[177,†] F. J. M. Geurts,[177,†] W. Li,[177,†] O. Miguel Colin,[177,†] B. P. Padley,[177,†] R. Redjimi,[177,†] J. Rotter,[177,†] E. Yigitbasi,[177,†] Y. Zhang,[177,†] A. Bodek,[178,†] P. de Barbaro,[178,†] R. Demina,[178,†] J. L. Dulemba,[178,†] A. Garcia-Bellido,[178,†] O. Hindrichs,[178,†] A. Khukhunaishvili,[178,†] N. Parmar,[178,†] P. Parygin,[178,r,†] E. Popova,[178,r,†] R. Taus,[178,†] K. Goulianos,[179,†] B. Chiarito,[180,†] J. P. Chou,[180,†] Y. Gershtein,[180,†] E. Halkiadakis,[180,†] A. Hart,[180,†] M. Heindl,[180,†] D. Jaroslawski,[180,†] O. Karacheban,[180,ee,†] I. Laflotte,[180,†] A. Lath,[180,†] R. Montalvo,[180,†] K. Nash,[180,†] H. Routray,[180,†] S. Salur,[180,†] S. Schnetzer,[180,†] S. Somalwar,[180,†] R. Stone,[180,†] S. A. Thayil,[180,†] S. Thomas,[180,†] J. Vora,[180,†] H. Wang,[180,†] H. Acharya,[181,†] D. Ally,[181,†] A. G. Delannoy,[181,†] S. Fiorendi,[181,†] S. Higginbotham,[181,†] T. Holmes,[181,†] A. R. Kanuganti,[181,†] N. Karunarathna,[181,†] L. Lee,[181,†] E. Nibigira,[181,†] S. Spanier,[181,†] D. Aebi,[182,†] M. Ahmad,[182,†] O. Bouhali,[182,qqqq,†] R. Eusebi,[182,†] J. Gilmore,[182,†] T. Huang,[182,†] T. Kamon,[182,rrrr,†] H. Kim,[182,†] S. Luo,[182,†] R. Mueller,[182,†] D. Overton,[182,†] D. Rathjens,[182,†] A. Safonov,[182,†] N. Akchurin,[183,†] J. Damgov,[183,†] V. Hegde,[183,†] A. Hussain,[183,†] Y. Kazhykarim,[183,†] K. Lamichhane,[183,†] S. W. Lee,[183,†] A. Mankel,[183,†] T. Peltola,[183,†] I. Volobouev,[183,†] A. Whitbeck,[183,†] E. Appelt,[184,†] Y. Chen,[184,†] S. Greene,[184,†] A. Gurrola,[184,†] W. Johns,[184,†] R. Kunnawalkam Elayavalli,[184,†] A. Melo,[184,†] F. Romeo,[184,†] P. Sheldon,[184,†] S. Tuo,[184,†] J. Velkovska,[184,†] J. Viinikainen,[184,†] B. Cardwell,[185,†] B. Cox,[185,†] J. Hakala,[185,†] R. Hirosky,[185,†] A. Ledovskoy,[185,†] C. Neu,[185,†] C. E. Perez Lara,[185,†] P. E. Karchin,[186,†] A. Aravind,[187,†] S. Banerjee,[187,†] K. Black,[187,†] T. Bose,[187,†] S. Dasu,[187,†] I. De Bruyn,[187,†] P. Everaerts,[187,†] C. Galloni,[187,†] H. He,[187,†] M. Herndon,[187,†] A. Herve,[187,†] C. K. Koraka,[187,†] A. Lanaro,[187,†] R. Loveless,[187,†] J. Madhusudanan Sreekala,[187,†] A. Mallampalli,[187,†] A. Mohammadi,[187,†] S. Mondal,[187,†] G. Parida,[187,†] D. Pinna,[187,†] A. Savin,[187,†] V. Shang,[187,†] V. Sharma,[187,†] W. H. Smith,[187,†] D. Teague,[187,†] H. F. Tsoi,[187,†] W. Vetens,[187,†]

A. Warden,[187,†] S. Afanasiev,[188,†] V. Andreev,[188,†] Yu. Andreev,[188,†] T. Aushev,[188,†] M. Azarkin,[188,†] A. Babaev,[188,†] A. Belyaev,[188,†] V. Blinov,[188,r,†] E. Boos,[188,†] D. Budkouski,[188,†] M. Chadeeva,[188,r,†] V. Chekhovsky,[188,†] R. Chistov,[188,r,†] A. Dermenev,[188,†] T. Dimova,[188,r,†] M. Dubinin,[188,jjjj,†] L. Dudko,[188,†] G. Gavrilov,[188,†] V. Gavrilov,[188,†] S. Gninenko,[188,†] V. Golovtcov,[188,†] N. Golubev,[188,†] I. Golutvin,[188,†] I. Gorbunov,[188,†] A. Gribushin,[188,†] Y. Ivanov,[188,†] V. Kachanov,[188,†] V. Karjavine,[188,†] A. Karneyeu,[188,†] L. Khein,[188,†] V. Kim,[188,r,†] M. Kirakosyan,[188,†] D. Kirpichnikov,[188,†] M. Kirsanov,[188,†] V. Klyukhin,[188,†] O. Kodolova,[188,ssss,†] V. Korenkov,[188,†] A. Kozyrev,[188,r,†] N. Krasnikov,[188,†] A. Lanev,[188,†] P. Levchenko,[188,tttt,†] O. Lukina,[188,†] N. Lychkovskaya,[188,†] V. Makarenko,[188,†] A. Malakhov,[188,†] V. Matveev,[188,r,†] V. Murzin,[188,†] A. Nikitenko,[188,uuuu,ssss,†] S. Obraztsov,[188,†] V. Oreshkin,[188,†] V. Palichik,[188,†] V. Perelygin,[188,†] S. Petrushanko,[188,†] S. Polikarpov,[188,r,†] V. Popov,[188,†] O. Radchenko,[188,r,†] M. Savina,[188,†] V. Savrin,[188,†] V. Shalaev,[188,†] S. Shmatov,[188,†] S. Shulha,[188,†] Y. Skovpen,[188,r,†] S. Slabospitskii,[188,†] V. Smirnov,[188,†] A. Snigirev,[188,†] D. Sosnov,[188,†] V. Sulimov,[188,†] A. Terkulov,[188,†] O. Teryaev,[188,†] I. Tlisova,[188,†] A. Toropin,[188,†] L. Uvarov,[188,†] A. Uzunian,[188,†] A. Vorobyev,[188,a,†] N. Voytishin,[188,†] B. S. Yuldashev,[188,vvvv,†] A. Zarubin,[188,†] I. Zhizhin,[188,†] A. Zhokin,[188,†] G. Antchev,[11,‡] P. Aspell,[120,‡] I. Atanassov,[11,‡] V. Avati,[107,120,‡] J. Baechler,[120,‡] C. Baldenegro Barrera,[160,‡] V. Berardi,[69a,191a,‡] M. Berretti,[36,‡] V. Borshch,[194,‡] E. Bossini,[80a,‡] U. Bottigli,[192,‡] M. Bozzo,[74a,74b,‡] H. Burkhardt,[120,‡] F. S. Cafagna,[69a,‡] M. G. Catanesi,[69a,‡] M. Deile,[120,‡] F. De Leonardis,[69a,191b,‡] M. Doubek,[189c,‡] D. Druzhkin,[53,120,‡] K. Eggert,[193,‡] V. Eremin,[194,‡] A. Fiergolski,[120,‡] F. Garcia,[36,‡] V. Georgiev,[189a,‡] S. Giani,[120,‡] L. Grzanka,[107,‡] J. Hammerbauer,[189a,‡] T. Isidori,[160,‡] V. Ivanchenko,[194,‡] M. Janda,[189c,‡] A. Karev,[120,‡] J. Kašpar,[189b,120,‡] B. Kaynak,[131,‡] J. Kopal,[120,‡] V. Kundrát,[189b,‡] S. Lami,[80a,‡] R. Linhart,[189a,‡] C. Lindsey,[160,‡] M. V. Lokajíček,[189b,a,‡] L. Losurdo,[192,‡] F. Lucas Rodríguez,[120,‡] M. Macrí,[74a,a,‡] M. Malawski,[107] N. Minafra,[160,‡] S. Minutoli,[74a,‡] K. Misan,[107,‡] T. Naaranoja,[35,36,‡] F. Nemes,[53,120,190,‡] H. Niewiadomski,[193,‡] E. Oliveri,[120,‡] F. Oljemark,[35,36,‡] M. Oriunno,[195,‡] K. Österberg,[35,36,‡] S. Ozkorucuklu,[131,‡] P. Palazzi,[120,‡] V. Passaro,[69a,191b,‡] Z. Peroutka,[189a,‡] O. Potok,[131,‡] J. Procházka,[189b,a,‡] M. Quinto,[69a,191a,‡] E. Radermacher,[120,‡] E. Radicioni,[69a,‡] F. Ravotti,[120,‡] C. Royon,[160,‡] G. Ruggiero,[120,‡] H. Saarikko,[35,36,‡] V. D. Samoylenko,[194,‡] A. Scribano,[80a,160,‡] J. Široký,[189a,‡] J. Smajek,[120,‡] W. Snoeys,[120,‡] R. Stefanovitch,[53,120,‡] C. Taylor,[193,‡] E. Tcherniaev,[194,‡] N. Turini,[192,‡] O. Urban,[189a,‡] V. Vacek,[189c,‡] O. Vavroch,[189a,‡] J. Welti,[35,36,‡] J. Williams,[160,‡] and J. Zich[189a,‡]

[†](CMS Collaboration)

[‡](TOTEM Collaboration)

[1]*Yerevan Physics Institute, Yerevan, Armenia*
[2]*Institut für Hochenergiephysik, Vienna, Austria*
[3]*Universiteit Antwerpen, Antwerpen, Belgium*
[4]*Vrije Universiteit Brussel, Brussel, Belgium*
[5]*Université Libre de Bruxelles, Bruxelles, Belgium*
[6]*Ghent University, Ghent, Belgium*
[7]*Université Catholique de Louvain, Louvain-la-Neuve, Belgium*
[8]*Centro Brasileiro de Pesquisas Fisicas, Rio de Janeiro, Brazil*
[9]*Universidade do Estado do Rio de Janeiro, Rio de Janeiro, Brazil*
[10]*Universidade Estadual Paulista, Universidade Federal do ABC, São Paulo, Brazil*
[11]*Institute for Nuclear Research and Nuclear Energy, Bulgarian Academy of Sciences, Sofia, Bulgaria*
[12]*University of Sofia, Sofia, Bulgaria*
[13]*Instituto De Alta Investigación, Universidad de Tarapacá, Casilla 7 D, Arica, Chile*
[14]*Beihang University, Beijing, China*
[15]*Department of Physics, Tsinghua University, Beijing, China*
[16]*Institute of High Energy Physics, Beijing, China*
[17]*State Key Laboratory of Nuclear Physics and Technology, Peking University, Beijing, China*
[18]*Sun Yat-Sen University, Guangzhou, China*
[19]*University of Science and Technology of China, Hefei, China*
[20]*Nanjing Normal University, Nanjing, China*
[21]*Institute of Modern Physics and Key Laboratory of Nuclear Physics and Ion-beam Application (MOE)—Fudan University, Shanghai, China*
[22]*Zhejiang University, Hangzhou, Zhejiang, China*
[23]*Universidad de Los Andes, Bogota, Colombia*
[24]*Universidad de Antioquia, Medellin, Colombia*

[25]*University of Split, Faculty of Electrical Engineering, Mechanical Engineering and Naval Architecture, Split, Croatia*
[26]*University of Split, Faculty of Science, Split, Croatia*
[27]*Institute Rudjer Boskovic, Zagreb, Croatia*
[28]*University of Cyprus, Nicosia, Cyprus*
[29]*Charles University, Prague, Czech Republic*
[30]*Escuela Politecnica Nacional, Quito, Ecuador*
[31]*Universidad San Francisco de Quito, Quito, Ecuador*
[32]*Academy of Scientific Research and Technology of the Arab Republic of Egypt, Egyptian Network of High Energy Physics, Cairo, Egypt*
[33]*Center for High Energy Physics (CHEP-FU), Fayoum University, El-Fayoum, Egypt*
[34]*National Institute of Chemical Physics and Biophysics, Tallinn, Estonia*
[35]*Department of Physics, University of Helsinki, Helsinki, Finland*
[36]*Helsinki Institute of Physics, Helsinki, Finland*
[37]*Lappeenranta-Lahti University of Technology, Lappeenranta, Finland*
[38]*IRFU, CEA, Université Paris-Saclay, Gif-sur-Yvette, France*
[39]*Laboratoire Leprince-Ringuet, CNRS/IN2P3, Ecole Polytechnique, Institut Polytechnique de Paris, Palaiseau, France*
[40]*Université de Strasbourg, CNRS, IPHC UMR 7178, Strasbourg, France*
[41]*Institut de Physique des 2 Infinis de Lyon (IP2I), Villeurbanne, France*
[42]*Georgian Technical University, Tbilisi, Georgia*
[43]*RWTH Aachen University, I. Physikalisches Institut, Aachen, Germany*
[44]*RWTH Aachen University, III. Physikalisches Institut A, Aachen, Germany*
[45]*RWTH Aachen University, III. Physikalisches Institut B, Aachen, Germany*
[46]*Deutsches Elektronen-Synchrotron, Hamburg, Germany*
[47]*University of Hamburg, Hamburg, Germany*
[48]*Karlsruher Institut fuer Technologie, Karlsruhe, Germany*
[49]*Institute of Nuclear and Particle Physics (INPP), NCSR Demokritos, Aghia Paraskevi, Greece*
[50]*National and Kapodistrian University of Athens, Athens, Greece*
[51]*National Technical University of Athens, Athens, Greece*
[52]*University of Ioánnina, Ioánnina, Greece*
[53]*HUN-REN Wigner Research Centre for Physics, Budapest, Hungary*
[54]*MTA-ELTE Lendület CMS Particle and Nuclear Physics Group, Eötvös Loránd University, Budapest, Hungary*
[55]*Faculty of Informatics, University of Debrecen, Debrecen, Hungary*
[56]*Institute of Nuclear Research ATOMKI, Debrecen, Hungary*
[57]*Karoly Robert Campus, MATE Institute of Technology, Gyongyos, Hungary*
[58]*Panjab University, Chandigarh, India*
[59]*University of Delhi, Delhi, India*
[60]*Saha Institute of Nuclear Physics, HBNI, Kolkata, India*
[61]*Indian Institute of Technology Madras, Madras, India*
[62]*Tata Institute of Fundamental Research-A, Mumbai, India*
[63]*Tata Institute of Fundamental Research-B, Mumbai, India*
[64]*National Institute of Science Education and Research, An OCC of Homi Bhabha National Institute, Bhubaneswar, Odisha, India*
[65]*Indian Institute of Science Education and Research (IISER), Pune, India*
[66]*Isfahan University of Technology, Isfahan, Iran*
[67]*Institute for Research in Fundamental Sciences (IPM), Tehran, Iran*
[68]*University College Dublin, Dublin, Ireland*
[69a]*INFN Sezione di Bari, Bari, Italy*
[69b]*Università di Bari, Bari, Italy*
[69c]*Politecnico di Bari, Bari, Italy*
[70a]*INFN Sezione di Bologna, Bologna, Italy*
[70b]*Università di Bologna, Bologna, Italy*
[71a]*INFN Sezione di Catania, Catania, Italy*
[71b]*Università di Catania, Catania, Italy*
[72a]*INFN Sezione di Firenze, Firenze, Italy*
[72b]*Università di Firenze, Firenze, Italy*
[73]*INFN Laboratori Nazionali di Frascati, Frascati, Italy*
[74a]*INFN Sezione di Genova, Genova, Italy*

[74b]Università di Genova, Genova, Italy
[75a]INFN Sezione di Milano-Bicocca, Milano, Italy
[75b]Università di Milano-Bicocca, Milano, Italy
[76a]INFN Sezione di Napoli, Napoli, Italy
[76b]Università di Napoli 'Federico II', Napoli, Italy
[76c]Università della Basilicata, Potenza, Italy
[76d]Scuola Superiore Meridionale (SSM), Napoli, Italy
[77a]INFN Sezione di Padova, Padova, Italy
[77b]Università di Padova, Padova, Italy
[77c]Università di Trento, Trento, Italy
[78a]INFN Sezione di Pavia, Pavia, Italy
[78b]Università di Pavia, Pavia, Italy
[79a]INFN Sezione di Perugia, Perugia, Italy
[79b]Università di Perugia, Perugia, Italy
[80a]INFN Sezione di Pisa, Pisa, Italy
[80b]Università di Pisa, Pisa, Italy
[80c]Scuola Normale Superiore di Pisa, Pisa, Italy
[80d]Università di Siena, Siena, Italy
[81a]INFN Sezione di Roma, Roma, Italy
[81b]Sapienza Università di Roma, Roma, Italy
[82a]INFN Sezione di Torino, Torino, Italy
[82b]Università di Torino, Torino, Italy
[82c]Università del Piemonte Orientale, Novara, Italy
[83a]INFN Sezione di Trieste, Trieste, Italy
[83b]Università di Trieste, Trieste, Italy
[84]Kyungpook National University, Daegu, Korea
[85]Department of Mathematics and Physics—GWNU, Gangneung, Korea
[86]Chonnam National University, Institute for Universe and Elementary Particles, Kwangju, Korea
[87]Hanyang University, Seoul, Korea
[88]Korea University, Seoul, Korea
[89]Kyung Hee University, Department of Physics, Seoul, Korea
[90]Sejong University, Seoul, Korea
[91]Seoul National University, Seoul, Korea
[92]University of Seoul, Seoul, Korea
[93]Yonsei University, Department of Physics, Seoul, Korea
[94]Sungkyunkwan University, Suwon, Korea
[95]College of Engineering and Technology, American University of the Middle East (AUM), Dasman, Kuwait
[96]Riga Technical University, Riga, Latvia
[97]University of Latvia (LU), Riga, Latvia
[98]Vilnius University, Vilnius, Lithuania
[99]National Centre for Particle Physics, Universiti Malaya, Kuala Lumpur, Malaysia
[100]Universidad de Sonora (UNISON), Hermosillo, Mexico
[101]Centro de Investigacion y de Estudios Avanzados del IPN, Mexico City, Mexico
[102]Universidad Iberoamericana, Mexico City, Mexico
[103]Benemerita Universidad Autonoma de Puebla, Puebla, Mexico
[104]University of Montenegro, Podgorica, Montenegro
[105]University of Canterbury, Christchurch, New Zealand
[106]National Centre for Physics, Quaid-I-Azam University, Islamabad, Pakistan
[107]AGH University of Krakow, Faculty of Computer Science, Electronics and Telecommunications, Krakow, Poland
[108]National Centre for Nuclear Research, Swierk, Poland
[109]Institute of Experimental Physics, Faculty of Physics, University of Warsaw, Warsaw, Poland
[110]Warsaw University of Technology, Warsaw, Poland
[111]Laboratório de Instrumentação e Física Experimental de Partículas, Lisboa, Portugal
[112]Faculty of Physics, University of Belgrade, Belgrade, Serbia
[113]VINCA Institute of Nuclear Sciences, University of Belgrade, Belgrade, Serbia
[114]Centro de Investigaciones Energéticas Medioambientales y Tecnológicas (CIEMAT), Madrid, Spain
[115]Universidad Autónoma de Madrid, Madrid, Spain

[116]*Universidad de Oviedo, Instituto Universitario de Ciencias y Tecnologías Espaciales de Asturias (ICTEA), Oviedo, Spain*
[117]*Instituto de Física de Cantabria (IFCA), CSIC-Universidad de Cantabria, Santander, Spain*
[118]*University of Colombo, Colombo, Sri Lanka*
[119]*University of Ruhuna, Department of Physics, Matara, Sri Lanka*
[120]*CERN, European Organization for Nuclear Research, Geneva, Switzerland*
[121]*Paul Scherrer Institut, Villigen, Switzerland*
[122]*ETH Zurich—Institute for Particle Physics and Astrophysics (IPA), Zurich, Switzerland*
[123]*Universität Zürich, Zurich, Switzerland*
[124]*National Central University, Chung-Li, Taiwan*
[125]*National Taiwan University (NTU), Taipei, Taiwan*
[126]*High Energy Physics Research Unit, Department of Physics, Faculty of Science, Chulalongkorn University, Bangkok, Thailand*
[127]*Çukurova University, Physics Department, Science and Art Faculty, Adana, Turkey*
[128]*Middle East Technical University, Physics Department, Ankara, Turkey*
[129]*Bogazici University, Istanbul, Turkey*
[130]*Istanbul Technical University, Istanbul, Turkey*
[131]*Istanbul University, Istanbul, Turkey*
[132]*Yildiz Technical University, Istanbul, Turkey*
[133]*Institute for Scintillation Materials of National Academy of Science of Ukraine, Kharkiv, Ukraine*
[134]*National Science Centre, Kharkiv Institute of Physics and Technology, Kharkiv, Ukraine*
[135]*University of Bristol, Bristol, United Kingdom*
[136]*Rutherford Appleton Laboratory, Didcot, United Kingdom*
[137]*Imperial College, London, United Kingdom*
[138]*Brunel University, Uxbridge, United Kingdom*
[139]*Baylor University, Waco, Texas, USA*
[140]*Catholic University of America, Washington, DC, USA*
[141]*The University of Alabama, Tuscaloosa, Alabama, USA*
[142]*Boston University, Boston, Massachusetts, USA*
[143]*Brown University, Providence, Rhode Island, USA*
[144]*University of California, Davis, Davis, California, USA*
[145]*University of California, Los Angeles, California, USA*
[146]*University of California, Riverside, Riverside, California, USA*
[147]*University of California, San Diego, La Jolla, California, USA*
[148]*University of California, Santa Barbara—Department of Physics, Santa Barbara, California, USA*
[149]*California Institute of Technology, Pasadena, California, USA*
[150]*Carnegie Mellon University, Pittsburgh, Pennsylvania, USA*
[151]*University of Colorado Boulder, Boulder, Colorado, USA*
[152]*Cornell University, Ithaca, New York, USA*
[153]*Fermi National Accelerator Laboratory, Batavia, Illinois, USA*
[154]*University of Florida, Gainesville, Florida, USA*
[155]*Florida State University, Tallahassee, Florida, USA*
[156]*Florida Institute of Technology, Melbourne, Florida, USA*
[157]*University of Illinois Chicago, Chicago, USA, Chicago, USA*
[158]*The University of Iowa, Iowa City, Iowa, USA*
[159]*Johns Hopkins University, Baltimore, Maryland, USA*
[160]*The University of Kansas, Lawrence, Kansas, USA*
[161]*Kansas State University, Manhattan, Kansas, USA*
[162]*Lawrence Livermore National Laboratory, Livermore, California, USA*
[163]*University of Maryland, College Park, Maryland, USA*
[164]*Massachusetts Institute of Technology, Cambridge, Massachusetts, USA*
[165]*University of Minnesota, Minneapolis, Minnesota, USA*
[166]*University of Mississippi, Oxford, Mississippi, USA*
[167]*University of Nebraska-Lincoln, Lincoln, Nebraska, USA*
[168]*State University of New York at Buffalo, Buffalo, New York, USA*
[169]*Northeastern University, Boston, Massachusetts, USA*
[170]*Northwestern University, Evanston, Illinois, USA*
[171]*University of Notre Dame, Notre Dame, Indiana, USA*
[172]*The Ohio State University, Columbus, Ohio, USA*
[173]*Princeton University, Princeton, New Jersey, USA*

[174]University of Puerto Rico, Mayaguez, Puerto Rico, USA
[175]Purdue University, West Lafayette, Indiana, USA
[176]Purdue University Northwest, Hammond, Indiana, USA
[177]Rice University, Houston, Texas, USA
[178]University of Rochester, Rochester, New York, USA
[179]The Rockefeller University, New York, New York, USA
[180]Rutgers, The State University of New Jersey, Piscataway, New Jersey, USA
[181]University of Tennessee, Knoxville, Tennessee, USA
[182]Texas A&M University, College Station, Texas, USA
[183]Texas Tech University, Lubbock, Texas, USA
[184]Vanderbilt University, Nashville, Tennessee, USA
[185]University of Virginia, Charlottesville, Virginia, USA
[186]Wayne State University, Detroit, Michigan, USA
[187]University of Wisconsin—Madison, Madison, Wisconsin, USA
[188]An institute or international laboratory covered by a cooperation agreement with CERN
[189a]University of West Bohemia, Plzeň, Czech Republic
[189b]Institute of Physics of the Academy of Sciences of the Czech Republic, Prague, Czech Republic
[189c]Czech Technical University, Prague, Czech Republic
[190]MATE Institute of Technology KRC, Gyöngyös, Hungary
[191a]Dipartimento Interateneo di Fisica di Bari, University of Bari
[191b]Dipartimento di Ingegneria Elettrica e dell'Informazione—Politecnico di Bari
[192]Università degli Studi di Siena and Gruppo Collegato INFN di Siena, Siena, Italy
[193]Department of Physics, Case Western Reserve University, Cleveland, Ohio, USA
[194]An institute or international laboratory covered by a cooperation agreement with CERN
[195]SLAC National Accelerator Laboratory, Menlo Park, California, USA

[a]Deceased.
[b]Also at Yerevan State University, Yerevan, Armenia.
[c]Also at TU Wien, Vienna, Austria.
[d]Also at Institute of Basic and Applied Sciences, Faculty of Engineering, Arab Academy for Science, Technology and Maritime Transport, Alexandria, Egypt.
[e]Also at Ghent University, Ghent, Belgium.
[f]Also at Universidade Estadual de Campinas, Campinas, Brazil.
[g]Also at Federal University of Rio Grande do Sul, Porto Alegre, Brazil.
[h]Also at UFMS, Nova Andradina, Brazil.
[i]Also at Nanjing Normal University, Nanjing, China.
[j]Also at The University of Iowa, Iowa City, Iowa, USA.
[k]Also at University of Chinese Academy of Sciences, Beijing, China.
[l]Also at China Center of Advanced Science and Technology, Beijing, China.
[m]Also at University of Chinese Academy of Sciences, Beijing, China.
[n]Also at China Spallation Neutron Source, Guangdong, China.
[o]Also at Henan Normal University, Xinxiang, China.
[p]Also at Université Libre de Bruxelles, Bruxelles, Belgium.
[q]Also at University of Latvia (LU), Riga, Latvia.
[r]Also at Another institute or international laboratory covered by a cooperation agreement with CERN.
[s]Also at Cairo University, Cairo, Egypt.
[t]Also at Suez University, Suez, Egypt.
[u]Also at British University in Egypt, Cairo, Egypt.
[v]Also at Purdue University, West Lafayette, Indiana, USA.
[w]Also at Université de Haute Alsace, Mulhouse, France.
[x]Also at Department of Physics, Tsinghua University, Beijing, China.
[y]Also at The University of the State of Amazonas, Manaus, Brazil.
[z]Also at Erzincan Binali Yildirim University, Erzincan, Turkey.
[aa]Also at University of Hamburg, Hamburg, Germany.
[bb]Also at RWTH Aachen University, III. Physikalisches Institut A, Aachen, Germany.
[cc]Also at Isfahan University of Technology, Isfahan, Iran.
[dd]Also at Bergische University Wuppertal (BUW), Wuppertal, Germany.
[ee]Also at Brandenburg University of Technology, Cottbus, Germany.
[ff]Also at Forschungszentrum Jülich, Juelich, Germany.
[gg]Also at CERN, European Organization for Nuclear Research, Geneva, Switzerland.

[hh]Also at Institute of Physics, University of Debrecen, Debrecen, Hungary.
[ii]Also at Institute of Nuclear Research ATOMKI, Debrecen, Hungary.
[jj]Also at Universitatea Babes-Bolyai—Facultatea de Fizica, Cluj-Napoca, Romania.
[kk]Also at Physics Department, Faculty of Science, Assiut University, Assiut, Egypt.
[ll]Also at HUN-REN Wigner Research Centre for Physics, Budapest, Hungary.
[mm]Also at Punjab Agricultural University, Ludhiana, India.
[nn]Also at University of Visva-Bharati, Santiniketan, India.
[oo]Also at Indian Institute of Science (IISc), Bangalore, India.
[pp]Also at Birla Institute of Technology, Mesra, Mesra, India.
[qq]Also at IIT Bhubaneswar, Bhubaneswar, India.
[rr]Also at Institute of Physics, Bhubaneswar, India.
[ss]Also at University of Hyderabad, Hyderabad, India.
[tt]Also at Deutsches Elektronen-Synchrotron, Hamburg, Germany.
[uu]Also at Department of Physics, Isfahan University of Technology, Isfahan, Iran.
[vv]Also at Sharif University of Technology, Tehran, Iran.
[ww]Also at Department of Physics, University of Science and Technology of Mazandaran, Behshahr, Iran.
[xx]Also at Helwan University, Cairo, Egypt.
[yy]Also at Italian National Agency for New Technologies, Energy and Sustainable Economic Development, Bologna, Italy.
[zz]Also at Centro Siciliano di Fisica Nucleare e di Struttura Della Materia, Catania, Italy.
[aaa]Also at Università degli Studi Guglielmo Marconi, Roma, Italy.
[bbb]Also at Scuola Superiore Meridionale, Università di Napoli 'Federico II', Napoli, Italy.
[ccc]Also at Fermi National Accelerator Laboratory, Batavia, Illinois, USA.
[ddd]Also at Ain Shams University, Cairo, Egypt.
[eee]Also at Consiglio Nazionale delle Ricerche—Istituto Officina dei Materiali, Perugia, Italy.
[fff]Also at Riga Technical University, Riga, Latvia.
[ggg]Also at Department of Applied Physics, Faculty of Science and Technology, Universiti Kebangsaan Malaysia, Bangi, Malaysia.
[hhh]Also at Consejo Nacional de Ciencia y Tecnología, Mexico City, Mexico.
[iii]Also at Trincomalee Campus, Eastern University, Sri Lanka, Nilaveli, Sri Lanka.
[jjj]Also at Saegis Campus, Nugegoda, Sri Lanka.
[kkk]Also at National and Kapodistrian University of Athens, Athens, Greece.
[lll]Also at Ecole Polytechnique Fédérale Lausanne, Lausanne, Switzerland.
[mmm]Also at Universität Zürich, Zurich, Switzerland.
[nnn]Also at Stefan Meyer Institute for Subatomic Physics, Vienna, Austria.
[ooo]Also at Laboratoire d'Annecy-le-Vieux de Physique des Particules, IN2P3-CNRS, Annecy-le-Vieux, France.
[ppp]Also at Near East University, Research Center of Experimental Health Science, Mersin, Turkey.
[qqq]Also at Konya Technical University, Konya, Turkey.
[rrr]Also at Izmir Bakircay University, Izmir, Turkey.
[sss]Also at Adiyaman University, Adiyaman, Turkey.
[ttt]Also at Bozok Universitetesi Rektörlügü, Yozgat, Turkey.
[uuu]Also at Marmara University, Istanbul, Turkey.
[vvv]Also at Milli Savunma University, Istanbul, Turkey.
[www]Also at Kafkas University, Kars, Turkey.
[xxx]Also at stanbul Okan University, Istanbul, Turkey.
[yyy]Also at Hacettepe University, Ankara, Turkey.
[zzz]Also at Istanbul University—Cerrahpasa, Faculty of Engineering, Istanbul, Turkey.
[aaaa]Also at Yildiz Technical University, Istanbul, Turkey.
[bbbb]Also at Vrije Universiteit Brussel, Brussel, Belgium.
[cccc]Also at School of Physics and Astronomy, University of Southampton, Southampton, United Kingdom.
[dddd]Also at University of Bristol, Bristol, United Kingdom.
[eeee]Also at IPPP Durham University, Durham, United Kingdom.
[ffff]Also at Monash University, Faculty of Science, Clayton, Australia.
[gggg]Also at Università di Torino, Torino, Italy.
[hhhh]Also at Bethel University, St. Paul, Minnesota, USA.
[iiii]Also at Karamanoğlu Mehmetbey University, Karaman, Turkey.
[jjjj]Also at California Institute of Technology, Pasadena, California, USA.
[kkkk]Also at United States Naval Academy, Annapolis, Maryland, USA.
[llll]Also at Bingol University, Bingol, Turkey.
[mmmm]Also at Georgian Technical University, Tbilisi, Georgia.
[nnnn]Also at Sinop University, Sinop, Turkey.
[oooo]Also at Erciyes University, Kayseri, Turkey.

[pppp]Also at Horia Hulubei National Institute of Physics and Nuclear Engineering (IFIN-HH), Bucharest, Romania.
[qqqq]Also at Texas A&M University at Qatar, Doha, Qatar.
[rrrr]Also at Kyungpook National University, Daegu, Korea.
[ssss]Also at Yerevan Physics Institute, Yerevan, Armenia.
[tttt]Also at Northeastern University, Boston, Massachusetts, USA.
[uuuu]Also at Imperial College, London, United Kingdom.
[vvvv]Also at Institute of Nuclear Physics of the Uzbekistan Academy of Sciences, Tashkent, Uzbekistan.